

# On the form of the human thoracolumbar spine and some aspects of its mechanical behaviour

**Citation for published version (APA):**

Snijders, C. J. (1970). *On the form of the human thoracolumbar spine and some aspects of its mechanical behaviour*. [Phd Thesis 1 (Research TU/e / Graduation TU/e), Mechanical Engineering]. Technische Hogeschool Eindhoven. <https://doi.org/10.6100/IR108907>

**DOI:**

[10.6100/IR108907](https://doi.org/10.6100/IR108907)

**Document status and date:**

Published: 01/01/1970

**Document Version:**

Publisher's PDF, also known as Version of Record (includes final page, issue and volume numbers)

**Please check the document version of this publication:**

- A submitted manuscript is the version of the article upon submission and before peer-review. There can be important differences between the submitted version and the official published version of record. People interested in the research are advised to contact the author for the final version of the publication, or visit the DOI to the publisher's website.
- The final author version and the galley proof are versions of the publication after peer review.
- The final published version features the final layout of the paper including the volume, issue and page numbers.

[Link to publication](#)

**General rights**

Copyright and moral rights for the publications made accessible in the public portal are retained by the authors and/or other copyright owners and it is a condition of accessing publications that users recognise and abide by the legal requirements associated with these rights.

- Users may download and print one copy of any publication from the public portal for the purpose of private study or research.
- You may not further distribute the material or use it for any profit-making activity or commercial gain
- You may freely distribute the URL identifying the publication in the public portal.

If the publication is distributed under the terms of Article 25fa of the Dutch Copyright Act, indicated by the "Taverne" license above, please follow below link for the End User Agreement:

[www.tue.nl/taverne](http://www.tue.nl/taverne)

**Take down policy**

If you believe that this document breaches copyright please contact us at:

[openaccess@tue.nl](mailto:openaccess@tue.nl)

providing details and we will investigate your claim.

ON THE FORM OF THE HUMAN  
THORACOLUMBAR SPINE  
and  
SOME ASPECTS OF ITS MECHANICAL  
BEHAVIOUR

PROEFSCHRIFT

TER VERKRIJGING VAN DE GRAAD VAN DOCTOR IN DE TECHNISCHE WETENSCHAPPEN AAN DE TECHNISCHE HOGESCHOOL EINDHOVEN, OP GEZAG VAN DE RECTOR MAGNIFICUS, PROF. DR. IR. A.A.Th.M. VAN TRIER, HOOGLEERAAR IN DE AFDELING DER ELECTROTECHNIEK, VOOR EEN COMMISSIE UIT DE SENAAAT TE VERDEDIGEN OP DINSDAG 22 DECEMBER 1970, DES NAMIDDAGS TE 4 UUR.

DOOR

CHRISTIAAN JOHANNES SNIJDERS

GEBOREN TE MALANG

Dit proefschrift is goedgekeurd door de promotoren  
prof. ir. A. Horowitz  
prof. dr. F. van Faassen

## Foreword

Inasmuch as the research concerned is engaged in the tangent plane of medical and engineering science this work is presented in two parts:

Part I is especially intended for medical scientists.

Part II is especially intended for the technically schooled reader and gives a description of apparatus developed along with the technical and mathematical backgrounds of Part I.

This work was supported by the following Institutions and Foundations:

The Eindhoven University of Technology,  
The Foundation Diaconessenhuis Hospital, Arnhem,  
The Research Division of the Foundation for Manual Medicine,  
Eindhoven,  
The Academic Radboud Hospital, Nijmegen,  
The Institute for Biomechanics and Rehabilitation, Free University at  
Amsterdam.

"I often say that when you can measure what you are speaking about and express it in numbers, you know something about it, but when you cannot measure it, when you cannot express it in numbers your knowledge is of a meagre and unsatisfactory kind".

Lord Kelvin

# Contents

## Part I

Chapter 1.	Description of the form of part of the human spine as visible in X-ray pictures by applying a mathematical formula with a small number of parameters	
1.1	Introduction	9
1.2	Method of characterizing the form of the kyphose-sacrum area by means of a few numbers	12
1.3	Statistical research on the kyphose-sacrum area	16
1.4	The load on the spine in natural standing posture	18
1.5	Description of the form of the spine in sitting posture	21
Chapter 2.	The dorsal contour of the spine	
2.1	Introduction	25
2.2	Recording of the dorsal contour	25
2.3	Mathematical description of the dorsal contour	26
2.4	Changes in form after some time	29
2.5	Click-clack phenomenon	38
Chapter 3.	Three-dimensional form of the human thoracolumbar spine	
3.1	Description of the form of the spine as visible in lateral and A-P X-ray pictures by applying a mathematical formula with a comparatively great number of parameters	41
3.2	Three-dimensional form of the human spine	44
3.3	Calculation of axial rotations	47
3.4	Measuring of axial rotations	47
3.5	Relation between force phenomena and spatial curve	52
3.6	Observations	58
Chapter 4.	Aspects of the mechanical behaviour of a vertebra-disc-vertebra segment	
4.1	Introduction	61
4.2	Schematic model of a motion segment	65
4.3	Load test on an autopsy specimen	70

4.4	Hypotheses about two wear-and-tear phenomena that manifest themselves in the case of angular rotation of two successive vertebrae	76
4.4.1	Wear and tear of the cartilaginous plate	76
4.4.2	Wear and tear of the annulus fibrosus	81
Conclusions		88
<b>Part II</b>	<b>Technical and mathematical backgrounds of Part I</b>	
Chapter 1.	Description of the form of a bent rod loaded at its extremities	
1.1	Origin of the formula with a minimum number of parameters	97
1.2	Load test on an elastic rod	102
1.3	Further research of the curvatures in the kyphose-sacrum area of the spine	109
Chapter 2.	Equipment for recording the dorsal contour of the spine	
2.1	Recording apparatus	115
2.1.1	Optical system	115
2.1.2	General information	117
2.2	Fixation of the person to be examined	119
2.3	Rotation measuring apparatus	120
Chapter 3.	Mathematical backgrounds with respect to the description of the three-dimensional form of the human thoracolumbar spine	
3.1	A formula with a comparatively great number of parameters	123
3.2	"Top view" of the human spine	123
3.3	Calculation of axial rotations	125
3.4	Relation between force phenomena and spatial curve	128
Chapter 4.	Mathematical backgrounds with respect to hypotheses about two wear-and-tear phenomena that manifest themselves in case of angular rotation of two successive vertebrae	
4.1	Determination of the straight part in the spatial curve	137
4.2	Wear and tear of the annulus fibrosus	137
References		143
List of symbols		149
Terminology		153
Summary		157
Curriculum vitae		159

To my Wife  
and my Parents

# Description of the form of part of the human spine as visible in X-ray pictures by applying a mathematical formula with a small number of parameters

## 1.1. Introduction

Although the spine is flexible, we are again and again struck by its typically individual form when the person concerned assumes a natural erect posture.

The description of this form, as also the determining of its dimensions and position in space, has been the work of many. Mostly the aim was to distinguish the pathological forms from the healthy ones.

The description of the form of the spine is an integrating part of the description of the posture and the constitution of the whole body.

Aspects such as the situation of the line running in the direction of gravitation through the centre of gravity of the whole body (1), the differences relative to the endomorphic, mesomorphic, and ectomorphic types (30) and the psychological relation of the individual to his surroundings (8) are involved in this procedure. With reference to the latter aspect a quotation from Cailliet (9): "The tall girl may stand slumped. In childhood she wished to be shorter as were her companions. She stooped "down to their height". Her counterpart, the short girl, stood "to her full height" to be taller, by standing on her toes, with her head erect, the chest protruding and her low back arched. All patterns of posture assumed in childhood for real or imagined results form a pattern that becomes deep seated. The pattern becomes not only a psychic pattern, but it gradually molds the tissues into somatic patterns that remain a structural monument to early psychic molding".

The side view of the spine has an undulatory aspect, the part regarded from the level of the shoulders down to the sacrum possesses the always recognizable basic form of an *S* and is called the thoracolumbar spine. The upper curve in the *S* is concave as seen from the ventral side and is called thoracal



kyphosis, the lower curve is convex as seen from the ventral side and is called lumbar lordosis.

Staffel (33) makes 5 differentiations in this S-shape: the normal, the round, the flat, the lordotic and the kypho-lordotic back. Broadly speaking, each category is characterized by a pronounced curved or flat kyphosis and/or pronounced curved or flat lordosis, with the exception of the category "normal" in which kyphosis and lordosis appear in an equivalent and not excessive degree.

These pronounced forms are accompanied by features of another nature. With the round back is seen an advanced position of the hip joints—it looks as if one is carrying something before him, to quote Staffel.

Accredited as a pathological form is the affection named after Scheuermann (5). Characteristic of the Scheuermann is the invigorated kyphosis, already introduced at an early age and manifesting itself through loss of elasticity of the discs intervertebrales and a wedge-formation at the ventral side of the vertebrae in the thoracal region of the spine.

These kyphotic deformities were found in those children who, after their elementary education, were schooled in some trade and had to do already rather hard work. In this connection the names "brick carriers' back" and "farmers' back" (Bauernrücken) point to a causal connection between the excessive mechanical demands made on the spinal column by the profession and the deformity of this part of the human system of support and motion. In a number of cases it is supposed that the origin of the Scheuermann is related to heredity.

In this respect scientific interest is aroused by the weak, round back of schoolchildren with defective posture (6).

Statistical research regarding the form of the human spine requires the recording of numerical geometrical data. The inquiries in this field are mainly based on the comparison of a practice-imposed limited number of data fixed by protractor or ruler. In 1956, Cramer (11) reported on a comparative study concerning the posture of the spine in 150 patients. In each investigated individual, standing upright, he measured what angle the 5th lumbar and the 12th thoracal vertebra made with the horizontal. The dorsal limit of the above vertebrae in the lateral X-ray pictures was taken as a standard. In an investigation carried out in 1960 by Bonne (6) the method indicated by Cramer was used also on 150 patients. In the cases of smaller gradients of the sacrum it was particularly the kypho-lordotic posture type that dominated.

Especially those cases with a flat lumbar profile (more extensive disc degenerations, cases of spondylolysis and spondylolisthesis, shortened hamstrings) were found in the group with a more erect sacrum.

In his monograph of 1959, Leger (20) considers measurements carried out on 30 healthy young men and an equal number of healthy young women who, in erect posture, were X-ray photographed in two directions. Leger distinguishes among this material eight form types of the spine. This difference is especially related to the place of the bending point in the S-shape and to the proportion between the length of the straight line, taken from the foremost and topmost point of the third lumbar vertebra up to the foremost and topmost point of the first thoracic vertebra and the greatest distance from this line to the thoracic spine. A conclusion based on these measuring results is that with the clinical and radiological investigation of young people the posture types of Staffel seldom occur. As a primal aim of this research is mentioned the renewed attack of the problem, not yet solved, of the normal, or rather the functionally most advantageous form of the spine in order to obtain a better basis for the appreciation of pathological situations.

As an ideal is posited that this most advantageous form may be determined by calculating, availing oneself of exact knowledge about loading and stiffness of the spine on all levels in static as well as in dynamic cases. This way is seen as not realisable inasmuch as the immense problems that may arise are lying in the extremely complicated loading situation, imposed by the force of gravitation and the muscular system together with the fact that the spine possesses 25 kinetic segments, shape and mechanical features of which are wonderful but varying from place to place and not to be determined mathematically in an accurate way. Even if under these circumstances one should agree to simplifications, a feeling of helplessness will arise, especially with regard to people accustomed to work with "technical material", after realizing that the living mechanism is not accessible for determining the many required data accurately and that these data will differ in respect of each individual.

Therefore, in the following we focus on what may be ascertained in the living individual in a simple way and with fair accuracy: *the geometry of the spine laid down in X-ray pictures.*

The aim is to describe the form of the spine by means of numbers for the sake of fundamental and statistical research and, by doing so, to obtain a better impression of the mechanical phenomena in the human spine.

We will confine ourselves in this to the individual in natural erect posture, because then the action of the dorsal muscles, as also the intra-abdominal pressure, may be considered minimal if not negligible.

## 1.2. Method of characterizing the form of the kyphose-sacrum area by means of a few numbers

Henceforth the form of the spine will be understood to be the smooth line on which lie the geometrical centres of the vertebrae and the intervertebral discs as visible in laterally taken X-ray pictures.

With regard to statistical aims the form of the spine will be described from the most dorsal point of the kyphosis down to the sacrum, because:

- (1) in that region the largest number of dorsal complaints occur, which is the reason that X-ray pictures are generally made of that region (Fig. 1.1 a);
- (2) the conditions at the extremities are salient (reference is made to the line in the direction of gravitation which is in the most dorsal point of the kyphosis the tangent to the smooth curve through the geometrical centres).

The X-ray pictures are made of individuals in a natural erect posture, because:

- (1) in this posture the individual form is expressed most clearly;
- (2) the action of the dorsal muscles and the intra-abdominal pressure may be considered small if not negligible.

In order to describe mathematically the kyphose-sacrum region the geometrical centres mentioned are defined in a system of coordinates.

The origin of the system of coordinates is located in the most dorsal geometrical centre, i.e. the hindmost point of the thoracal kyphosis.

The  $x$ -axis runs in the direction of gravitation, the  $y$ -axis is perpendicular to the  $x$ -axis (Fig.1.1 b).

Through the geometrical centres a curve can be drawn answering the function  $y = f(x)$ . By this general definition an unlimited number of functions can be covered that can all be adapted to the location of the centres measured. The adaptation becomes constantly better in proportion as the function comprises more adaptable parameters. However, in order to characterize the kyphose-sacrum region by only a few numbers, a formula has been attempted to find with *only two adaptable parameters*, by which an acceptable adaptation to the diverging forms of the spine is anyhow possible.

A simple formula which has turned out to answer our purpose is:

$$y = \frac{1}{L} \left( \frac{m}{6} \cdot \frac{A}{3} \right) x^3 + Ax^2 - L \left( \frac{m}{6} + \frac{2A}{3} \right) x + \frac{R}{L} x + \left( \frac{m}{6} + \frac{2A}{3} \right) \frac{L^2}{\pi} \sin \frac{\pi x}{L} - \frac{R}{\pi} \sin \frac{\pi x}{L} \quad (1.2.1.)$$

The parameter  $m$  is a measure of the curvature of the curve on the spot  $x = L$  (Fig. 1.2b). Changing  $m$  has no important influence on the form of the upper part of the curve. Changing parameter  $A$  does influence the height of the whole curve (Fig. 1.2a). The value of  $2A$  is a measure of the curvature of the curve on the spot  $x = 0$ .  $R$  is the  $y$  coordinate of the bottommost point (See also Part II, chapter I).

Figure 1.1b gives a result.

The coordinates of the geometrical centres of the vertebrae and the intervertebral discs were fed into a digital computer which, using the method of least squares, determined those values of  $A$  and  $m$  that produced a curve showing the optimum correspondence with the centres measured.

For this case  $A = 0.0034 \left( \frac{1}{\text{mm}} \right)$  and  $m = -0.0074 \left( \frac{1}{\text{mm}} \right)$ .

The differences between the values of  $y$  measured and those calculated were in this case smaller than 1.5 mm (0.06 in.), i.e. of the order of the inexactitude in the determination of the geometrical centres on the X-ray picture.

The method has been applied to 30 X-ray pictures of patients from various hospitals. However, this material must be regarded

Fig. 1.1a X-ray picture of the spine of a patient. Here and in the following illustrations the ventral side is at the right.

Fig. 1.1b Description of form of the area Kyphose-sacrum. Centres measured are marked  $x$ . The curve has been determined and drawn by a digital computer.

Fig. 1.1c Curvatures of the curve shown in Fig. 1.1b.



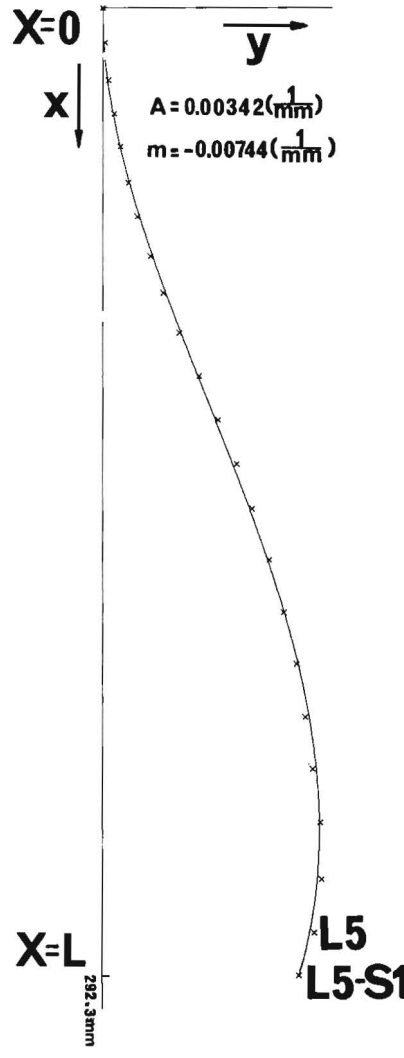
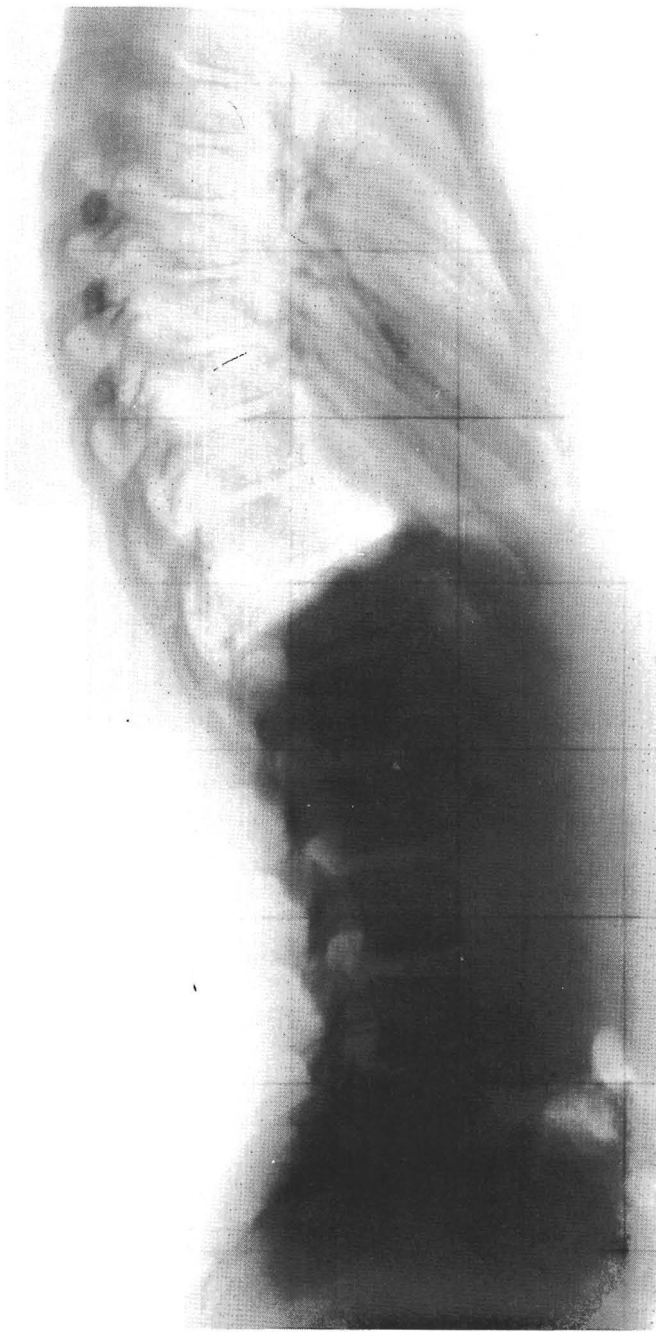


Fig. 1.1a

Fig. 1.1b

Curvature  $K$

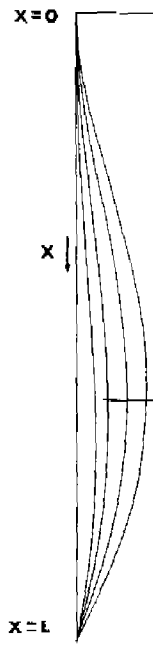
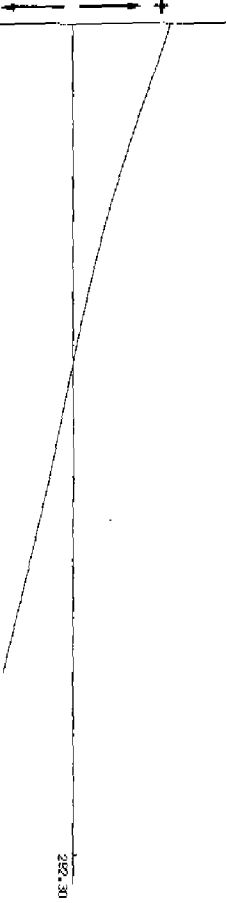


Fig. 1.2a  
Influence of  
parameter  $A$

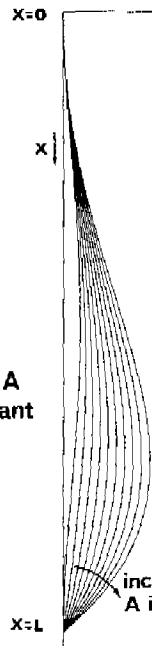


Fig. 1.2b  
Influence of  
parameter  $m$

Fig. 1.1c

comparatively small, we would mention that in this material the differences between measured and calculated values of  $y$  were:

in 17% smaller than 1 mm,

in 53% smaller than 1.5 mm,

in 87% smaller than 2.3 mm.

In the remaining relatively low number of cases we found a few centres lying locally at a distance of the magnitude of 3 mm from the curve calculated. We found a trend to less accurate results in cases of badly identifiable contours of the vertebrae, in cases with a certain discontinuity in the form, in cases with  $y$  values greater than 100 mm, and in cases with scoliosis with the consequence of optical distortion in the sagittal projection.

It is difficult to decide in which cases a sufficiently accurate description is given and in which cases this is not, since in our opinion also in the less accurate results the curve calculated represented the character of the form, at least to a degree sufficient for statistical research. We may remark that at the beginning we considered an accuracy as in Fig. 1.1b with only two parameters chosen freely by the computer, to be impossible.

After a six times repeated determination of the geometrical centres of one X-ray picture of subnormal quality we found the following standard deviations:

In the coordinates  $L$  0.9 mm and  $R$  0.6 mm, in  $A$   $2.10^{-5}$  ( $\frac{1}{\text{mm}}$ )

and in  $m$   $1.9.10^{-4}$  ( $\frac{1}{\text{mm}}$ ). Taking into account that in our

material we found values of  $A$  between  $0.3.10^{-3}$  ( $\frac{1}{\text{mm}}$ ) and

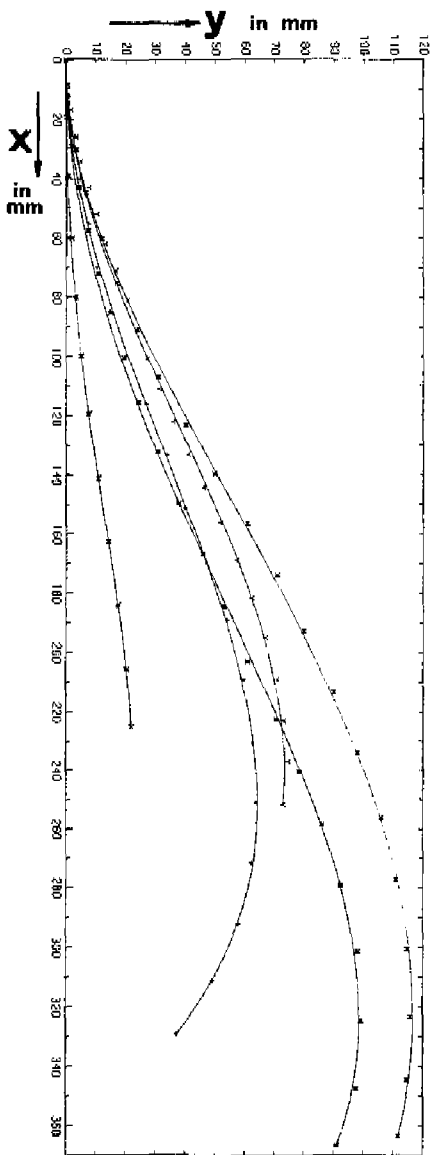
$5.10^{-3}$  ( $\frac{1}{\text{mm}}$ ), and values of  $m$  between  $0.5.10^{-3}$  ( $\frac{1}{\text{mm}}$ ) and

$15.10^{-3}$  ( $\frac{1}{\text{mm}}$ ) we may state that this method of description

of form is sufficiently accurate for the sake of making a differentiation in individual forms.

### 1.3 Statistical research on the kyphose-sacrum area

Only after investigating a great number of healthy persons as well as persons with dorsal complaints can an interpretation with reference to clinical pictures be given of the numerical values of the parameters or the data to be derived directly from them (e.g. curvatures). On the ground of the opinions quoted in the introduction and based on only the measurement of the inclination of the 5th lumbar vertebra, we pronounce



the expectation that an investigation according to our method which allows of obtaining with a few numbers a far more comprehensive characterization of kyphosis as well as of lumbar lordosis, will procure significant correlation coefficients between clinical picture and form. The X-ray pictures handled by us originate from various hospitals and have been made with unequal film-focus distances, etc. Our exclusive aim was to investigate whether the method practised was applicable with respect to very diverging forms (Fig. 1.3).

Fig. 1.3.  
Description of several diverging forms



#### 1.4. The load on the spine in natural standing posture

In the foregoing description of form has been exclusively dealt with. In order to draw conclusions from the forms found as to the load on the spine it is for simplicity plausible to compare the spine with an elastic rod of technical material. In the newborn baby the whole spine shows a slight kyphotic curvature which during standing and walking (after the period of raising the head from the prostrate position) assumes the always recognizable basic form of an S.

Consequently, it is justifiable to presume that the curved form of the spine is, among other causes, brought about by the influence of forces exerted on the spine and that particularly such a form is developed that corresponds to a certain degree with that of an elastic rod of "technical material", loaded under analogous conditions.

A first indication in this direction is found in what follows:

In a number of the X-ray pictures examined by us the area AC (Fig. 1.4a) (in C the tangent is parallel to the x-axis) has, with fair approximation, the property of the symmetrically loaded elastic rod of figure 1.4b: when this page is turned  $180^\circ$  on the bending point W, the same form of curvature returns.

Although this discovery enables us neither to replace in thought the spine simply by a continuous, homogeneous, isotropic elastic rod that becomes straight in unloaded condition, nor to define the exact position of the neutral line, we are convinced that certain features in the mechanical behaviour of the spine become comprehensible by comparison with an elastic rod.

That this conviction is not new is proved by the medical literature in which this comparison is repeatedly made. In this connection it was posited already by Meyer (1891) that the spine can bear independently its own weight together with the load suspended as does an S-shaped or goose-necked spring ("wie die sog. Schwanenhalsfeder die Schwere des Kutschkastens trägt").

This pronouncement, into which Strasser (1913) entered further, already gives the impression that with the load on the spine in standing posture a dominating influence must be ascribed to the load near the extremities. This will apply in a still higher degree to the lumbar region of the spine, regarded separately, where the ribs have not to be taken into consideration. On this ground we report the following, based

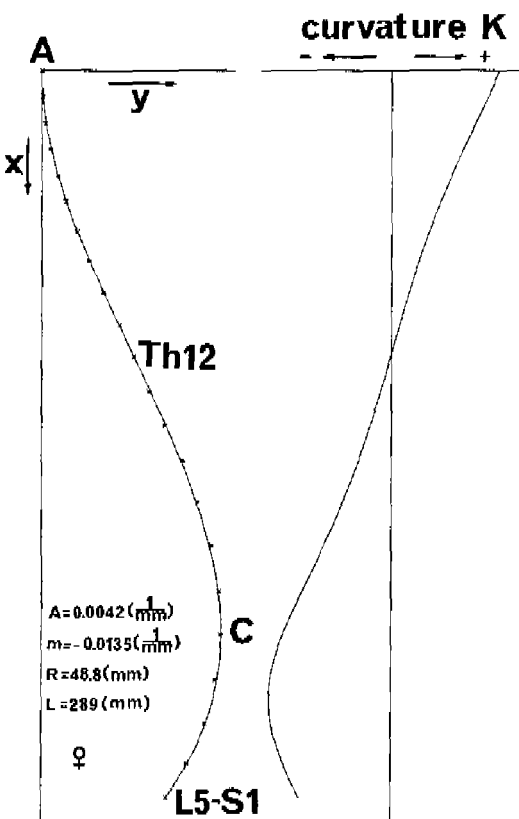


Fig. 1.4a

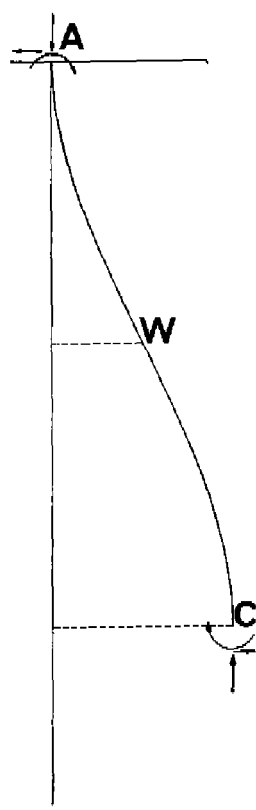


Fig. 1.4b

Fig. 1.4a The tangent in C is parallel to the x-axis

Fig. 1.4b Form of a symmetrically loaded elastic rod which is e.g. straight in unloaded position.

only on the fact that with an increasing bending moment the curvature in the spine will increase too.

For an elastic rod which in unloaded condition is straight,  $m = -0.0074$  (Fig. 1.1b) would mean that at point  $x = L$  a

clockwise moment would act (the sign (-) indicates the sense of rotation of the moment in the illustration concerned).

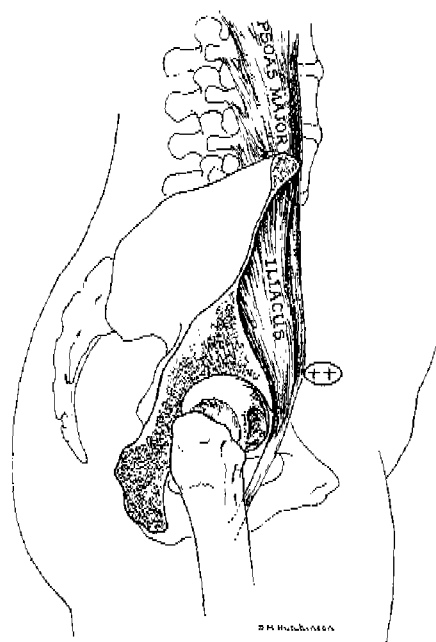


Fig. 1.5 *Basmajian, 1961.*

The fact that in all X-ray pictures examined by us this sign (-) appeared, raises the impression that the tension in the M. ilio-psoas puts its stamp on the curvatures in the lumbar part of the spine.

In fact:

- (1) The position of its spots of insertion allows the M. ilio-psoas to exert a clockwise moment with respect to the support of the spine.
- (2) Electromyographic investigations (Basmajian, 1961) have shown that ilio-psoas remains constantly active in the erect posture in contrast to the other large thigh muscles. It would appear that ilio-psoas functions as a ligament to

prevent hyperextension of the hip joint while standing" (Fig. 1.5).

The preceding statements are accentuated by Meyer (1889), Fick (1911) and Strasser (1913) who postulate that the vertical through the centre of gravity of the upper part of the body falls behind the axis connecting the centres of the heads of the femura.

Strasser states that there is no question of a labile position with the possibility of the upper part of the body overbalancing sometimes forward and sometimes back:

"the hip joint is held in position by the continuous tension of the anterior (ligaments and) muscles acting against the weight of the body".

An analogy of such a mechanism by which a moment around a joint axis is procured through tension in ligaments and muscles in erect posture, is to be found located in the ankle joints.

It is common knowledge that the vertical through the centre of gravity of the whole body intersects the supporting plane of the feet in front of the axis of the articular talocruralis (29). Equilibrium around this axis is procured, among other causes, through tension in the triceps surae and the plantar aponeurosis (17).

#### 1.5. Description of the form of the spine in sitting posture

The loose sitting posture and the unconstrained standing posture have in common that the action of the dorsal tensors may be considered minimal.

An X-ray picture has been made of one and the same person in standing and in sitting posture (Fig. 1.6). The sitting posture could also be described accurately (table 1.1).

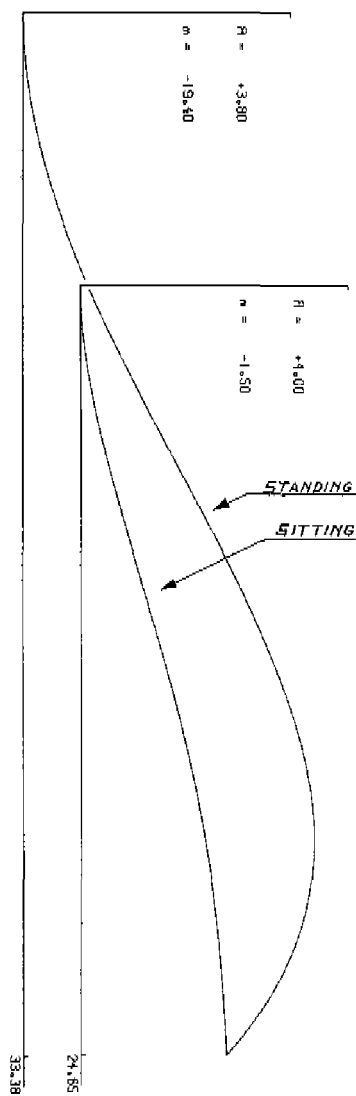


Fig. 1.6 Description of the form of the kyphose-sacrum area in standing and sitting posture of one person

$$L = 246.5 \text{ mm} \quad R = 54,4 \text{ mm} \quad A = 0.004 \left(\frac{1}{\text{mm}}\right) \quad m = -0.0016 \left(\frac{1}{\text{mm}}\right)$$

measured values of $x$ in mm	measured values of $y$ in mm	calculated values of $y$ in mm	difference between values measured and those calculated of $y$ in mm
0.0	0.0	0.00	0.00
15.2	0.9	0.86	- 0.04
30.7	3.3	3.26	- 0.04
47.6	7.2	7.23	0.03
64.7	12.3	12.24	- 0.06
82.5	18.1	18.09	- 0.01
100.0	23.5	24.05	0.55
118.3	30.3	30.17	- 0.13
136.5	36.3	35.83	- 0.47
155.0	41.0	40.93	- 0.07
175.3	45.5	45.63	0.13
194.8	48.9	49.17	0.27
215.4	52.0	51.93	- 0.07
234.2	53.8	53.64	- 0.16
246.5	54.4	54.40	0.00

table 1.1

*Description of form of the kyphose-sacrum area in sitting posture.  
This is illustrated in Fig. 1.6.*

## The dorsal contour of the spine

### 2.1. Introduction

The characteristic form of the spine seen as the flowing line through the geometrical centres of the vertebral bodies, manifests itself also in the contour of the back. Notwithstanding the upwards diminishing length of the processus spinosi and the upwards diminishing width of the vertebral bodies, the individual character at the back contour is preserved, taking into account some shifting in accent. This is mainly owing to the fact that the ply of tissue between the extremities of the processus spinosi and the skin is generally very thin.

Although the dorsal contour of the spine is not identifiable in the lateral aspect of the body because of its being hidden by the dorsal tensors, the protruding scapulae, and the nates, a great many descriptions have been made according to silhouette pictures (6). It is obvious that the form is especially applicable to ample statistical research inasmuch as in many cases making X-ray pictures is not indicated.

Research in this connection has been effectuated by Appleton (2). He measured the distance from the vertical through the hindmost point of the heels to the most dorsal point of the occiput and the kyphosis and to the uppermost point of the gluteal cleft. Charrière (10) effectuated a similar investigation and paid special attention to the position of *C7*, to the most dorsal point of the kyphosis, and to the foremost point of the lumbar lordosis. Both investigators draw conclusions from their observations in relation to pathological and normal forms. With the same intention regarding the description of X-ray pictures, as mentioned before, we tackled the form of the dorsal contour.

The first task was to reproduce the dorsal contour on a sheet of paper, without influencing the natural erect posture.

### 2.2. Recording of the dorsal contour

In what follows the dorsal contour of the spine will be understood to be the smooth line that passes through the points on

the skin that are considered to represent the most dorsal points of the processus spinosi. This form cannot be defined through lateral projection or through a picture taken from the side. Therefore, the skin has to be approached from behind. The methods of recording the dorsal contour by means of mechanical contact with the skin were rejected by us, inasmuch as touching the reflexogenous region would disturb the unconstrained posture. The solution chosen incorporates an optical system by which points on the skin can be represented on a recorder roll. The person whose spine is to be examined is standing with the heels against a wooden block (Fig. 2.1); the vertical through the hindmost limitation of the heels is in the recording the vertical line in the middle of the recording paper. Shoulders and pelvis are held with very little force in order to prevent the person from moving too much in the sagittal plane during the measuring period of about 45 seconds (See also Part II, Chapter 2).

The recording of the dorsal contour gives only a picture of the form of the spine in the sagittal plane. Since the form of the spine in the frontal plane is of importance as well, an apparatus has been developed for measuring also optically the axial rotation and the oblique position of the shoulders and the axial rotation of the pelvis with respect to the supporting plane of the feet. As to the posture of the shoulders we refer to the acromion. It is supposed that the rotations mentioned give an impression of the bending of the spine in the frontal plane.

### 2.3. Mathematical description of the dorsal contour

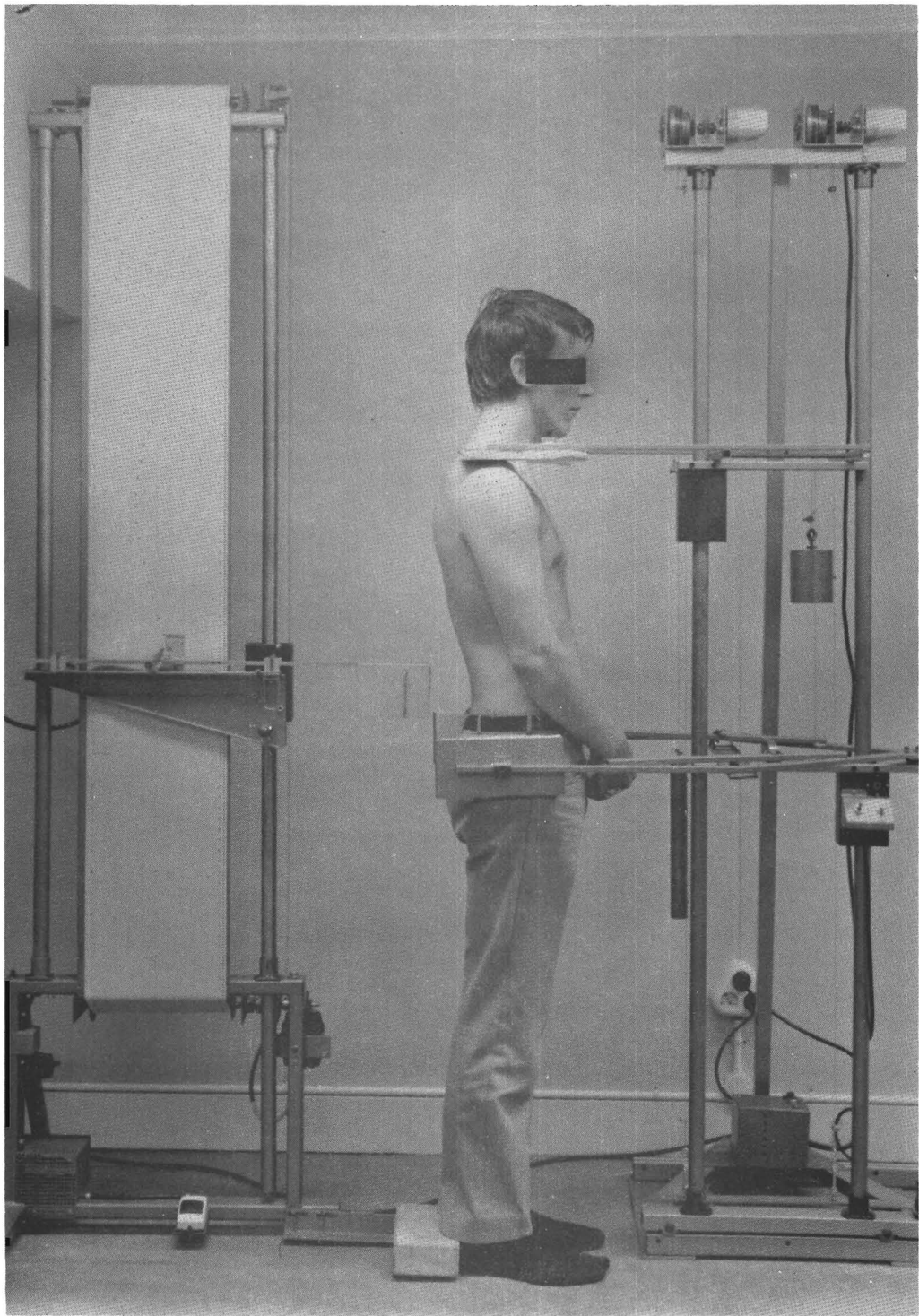
Notwithstanding the accuracy of the method of recording it is to be expected that a description of form with a small number of parameters will procure results of lower accuracy than obtained with X-ray pictures, because unevennesses and other irregularities of the back and movements of about 2 mm in the sagittal plane during the measuring period have an important influence on the measurement. However, it has become evident that it is possible to characterize the kyphose-sacrum region with the help of the formula (1.2.1.) already applied to the X-ray pictures. In Fig. 2.2. a region above the most dorsal point of the kyphosis has also been adjoined.

---

Fig. 2.1 *Recording of the dorsal contour.*







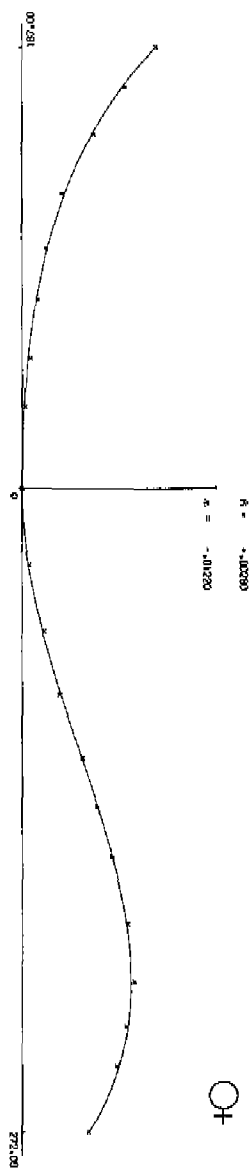


Fig. 2.2 Description of the dorsal contour of the spine

Inasmuch as our research of the dorsal contour is not restricted to the description of only part of the spine as it is generally X-ray photographed in medical practice, we prefer in this case the method of description of form as introduced in the following section.

#### 2.4. Changes in form after some time

It should be noted that here and in the case of X-ray pictures instantaneous records are concerned, and that even in the course of a day certain transformations may take place. The questions now arising are the following:

- (1) To what degree can be assumed the possibility of reproducing the position in space of the spine e.g. as seen with regard to the vertical through the backs of the heels.
- (2) To what degree can be assumed the possibility of reproducing the form of the spine, paying special attention to curvatures.
- (3) To what degree does the spine transform during a day or during a longer time.

The answers to these questions are not to be found in the literature, which is understandable because making a great number of total X-ray pictures of one and the same person is not indicated. Our accurate method of recording the dorsal contour of the spine allows us to give an answer to the preceding questions.


Answer to question 1:

Two healthy persons, among whom the author, and a person with dorsal complaints took up 3 postures, one accentuating shoulders brought forward, one accentuating shoulders brought backward and one intermediate posture. In all three postures

---

Fig. 2.3a. *Different positions of the dorsal contour of the spine of one person. One posture with shoulders brought forward, one posture with shoulders brought backward, and one intermediate posture. The straight line is the vertical through the backs of the heels. Here and in the following pictures the ventral side is at the right.*

Fig. 2.3b. *The form of the dorsal contour in the three postures of Fig. 2.3a.*

Fig. 2.3c. *Curvatures ( $K$ ) in the forms of Fig. 2.3b. Greatest difference in curvature at contour L5 is  $0.013 \left(\frac{1}{\text{mm}}\right)$ .* 

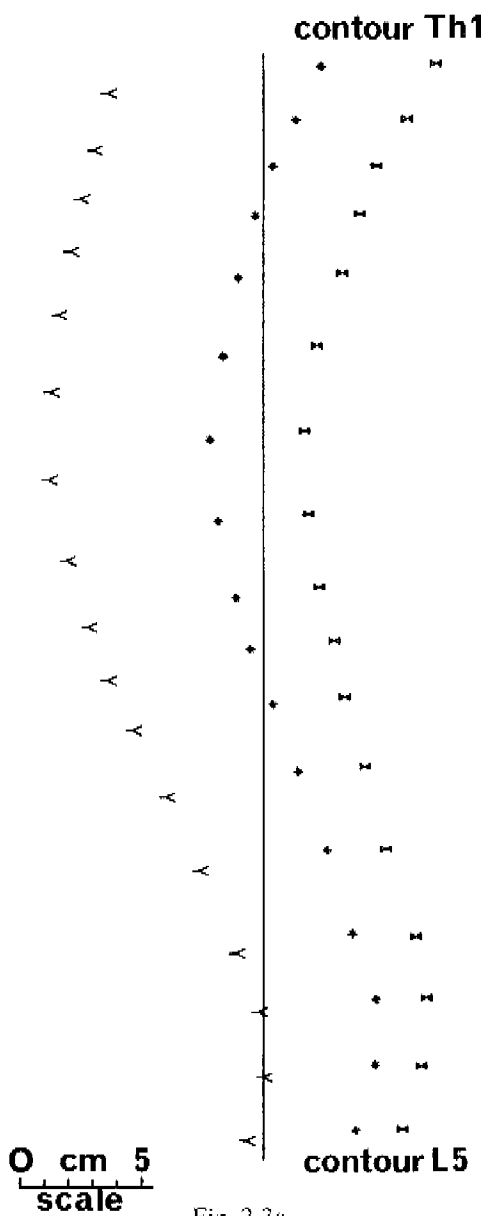


Fig. 2.3a

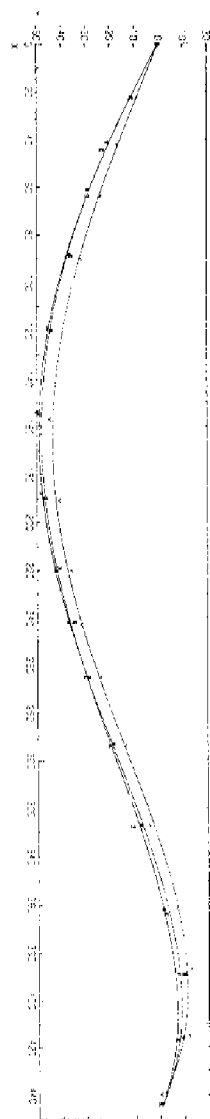


Fig. 2.3b

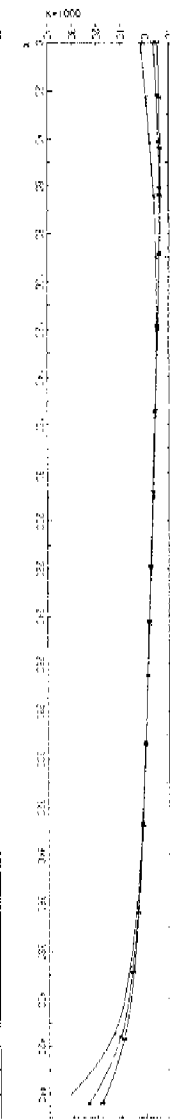


Fig. 2.3c

a certain stability and unconstraint was introduced; of course, the intermediate posture met these criteria best. The accuracy of the recording was increased by marking the extremities of the processus spinosi in ink on the skin.

Fig. 2.3a. represents the three postures taken up by the author. The largest displacement of the shoulders in horizontal direction is 135 mm and of the spinous process of L 5=65 mm. Other experimental persons too, showed this important shifting, interestingly related to the size of the supporting plane of the feet. It is remarkable that the curvature in the lumbar spine increases in proportion as a posture with a more advanced backward slope is taken up, as becomes evident from Fig. 2.3c. and which corresponds with 1.4. To what degree it may be assumed that the intermediate posture can be reproduced has been investigated in six adults. The measuring was repeated with an interval of a couple of minutes, with feet joined and hands crossed in front of the groin. Between the successive measurements the person walked around in the room containing the measuring apparatus. Fig. 2.4a. shows the observations on the person with the least reproducible posture. Although the largest shifting in horizontal direction is approximately 2 cm, the connecting line of Contour Th1 and Contour L 5 appears to rotate only approx. 30° with respect to the vertical.

---

Fig. 2.4a. *Reproducibility of the intermediate posture. The straight line is the vertical through the backs of the heels.*

Fig. 2.4b. *The form of the dorsal contour in the utmost right and the utmost left posture of Fig. 2.4a.*

Fig. 2.4c. *Curvatures (K) in the utmost right and the utmost left form of Fig. 2.4a.*

contour Th1

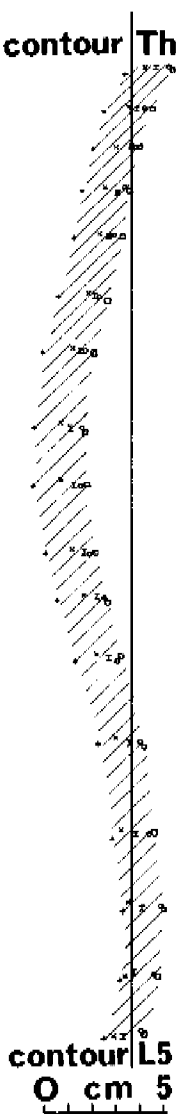


Fig. 2.4a

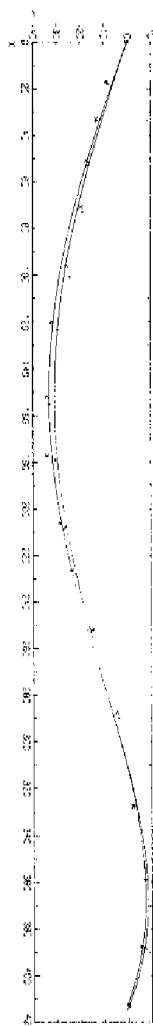


Fig. 2.4b

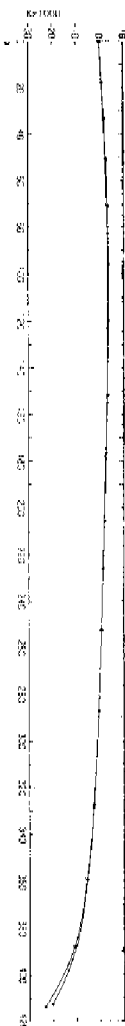


Fig. 2.4c

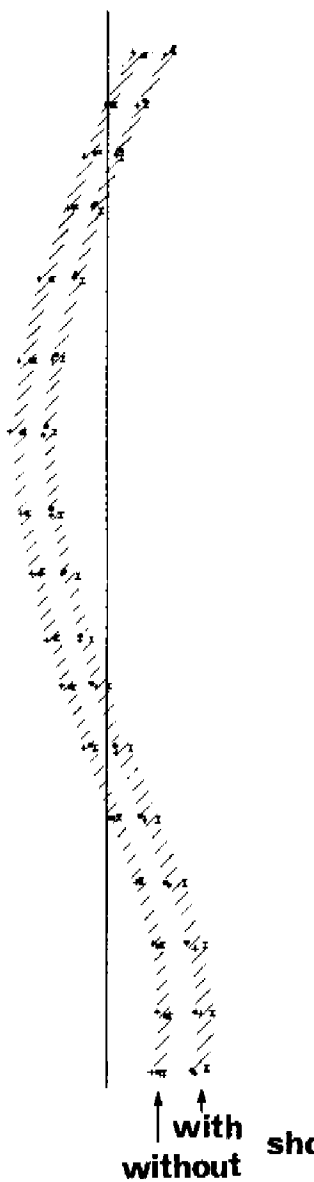


Fig. 2.5

As is evident from Fig. 2.5. the posture of the author is very reproducible. Here a comparison has been made between the posture with and without shoes. For clearness' sake the posture with shoes has been drawn on the same level as the posture without shoes. A correction has been made for the thickness of the counter.

Fig. 2.5 *The position of the dorsal contour with and without shoes. The straight line is the vertical through the backs of the heels.*

To what degree the intermediate posture relative to a human being can be reproduced will have to be explored on large groups of persons. In view of our first impressions our opinion is that the position of the spine, seen in the total image of the natural standing individual (this being an objective datum) can be rather well reproduced but that the distances in horizontal direction with regard to the vertical through the backs of the heels can show considerable variations.

Answer to question 2:

In order to determine especially the curvatures in the dorsal contour a system of coordinates has been composed that does not refer to the direction of gravitation but to the line connecting the points Contour Th 1 and Contour L 5. Description of the form with a formula with four parameters *A, B, C* and *D*, freely chosen by a computer, defined for the person mentioned before (Fig. 2.4a) the values in table 2.1 and in Fig. 2.4b and 2.4c. The formula used is:

$$y = Ax^3 + Bx^2 + Cx + D \sin \frac{\pi x}{L} \quad (2.4.1)$$

	<i>L</i> in mm	<i>A</i> in $\frac{1}{\text{mm}^2}$	<i>B</i> in $\frac{1}{\text{mm}}$	<i>C</i>	<i>D</i> in mm	curvature at $x = L$ (contour L 5) in $\frac{1}{\text{mm}}$	angle of connecting line from Contour Th 1 to Contour L 5 with the vertical
position utmost right	412,5	$-4.1 \cdot 10^{-6}$	$2.1 \cdot 10^{-5}$	0,68	-132	-0.020	1° 50'
position utmost left	413,5	$-4.4 \cdot 10^{-6}$	$4.8 \cdot 10^{-5}$	0,73	-141	-0.023	1° 20'
difference	1	$0.3 \cdot 10^{-6}$	$2.7 \cdot 10^{-5}$	0.05	9	0.003	30'

Table 2.1. *Numbers belonging to Fig. 2.4b and 2.4c.*

The curvature-shifting at  $x = L$  is considerably inferior to that in the case of Fig. 2.3, as is shown in Fig. 2.4c. It may be concluded that, paying special attention to curvatures, the form of the spine is well reproducible in the intermediate posture.

Answer to question 3:

The recording of the dorsal contour in the intermediate posture has been regularly repeated during a period of three weeks. Some results of one case, representative of the above investigation, are shown in Fig. 2.6a. and b, and table 2.2. Consequently, it is evident that with these adults the form of the spine remained remarkably constant during a longer period. The form of the author's spine appears not to have changed appreciably in so much as a period of two years.

	$L$ in mm	$A$ in $\frac{1}{\text{mm}^2}$	$B$ in $\frac{1}{\text{mm}}$	$C$	$D$ in mm	curvature at $x = L$ (contour L 5) in $\frac{1}{\text{mm}}$	angle of connecting line from Contour Th 1 to Contour L 5 with the vertical
March 1968 2.00 p.m.	437	$-4.6 \cdot 10^{-6}$	$6.5 \cdot 10^{-4}$	0.39	-151	-0.022	$-1^{\circ}10'$
April 9, 1970 10.00 a.m.	444*	$-4.6 \cdot 10^{-6}$	$6.0 \cdot 10^{-4}$	0.65	-165	-0.024	$-1^{\circ}50'$
April 9, 1970 3.00 p.m.	437*	$-4.4 \cdot 10^{-6}$	$5.2 \cdot 10^{-4}$	0.60	-151	-0.020	$-2^{\circ}10'$

Table 2.2

*Changes in form of the author's spine after a longer period of time (See Fig. 2.6)*

\* See page 36

Fig. 2.6a *Changes in form in the intermediate posture after a longer period of time.*

Fig. 2.6b *Curvatures according to Fig. 2.6a.*





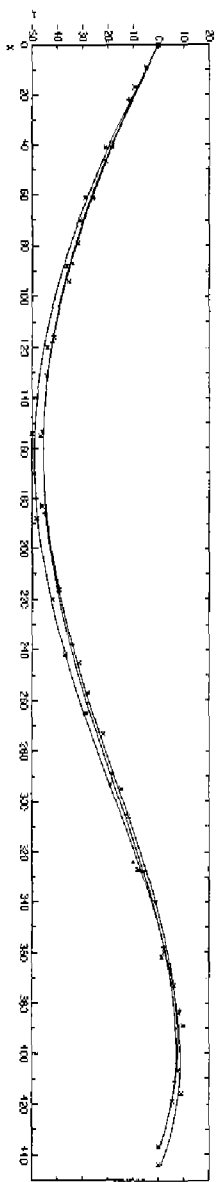


Fig. 2.6a

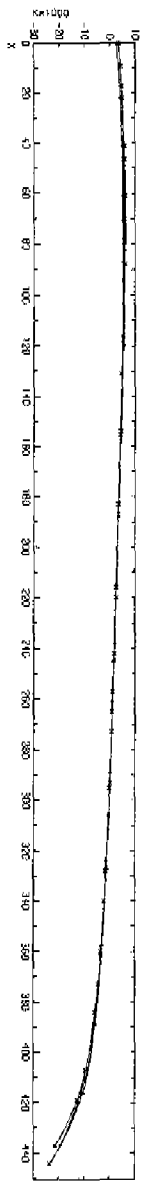


Fig. 2.6b

\* On behalf of comparison of both these lengths one to the other the following has to be taken into account:

In consequence of breathing contour Th1 may move approx. 3.5 mm in vertical direction. We further ascertained that the standard deviation in the recording and measuring of the  $x$ -coordinate amounted to approx. 0.4 mm. Because of these reasons we investigated separately on three healthy persons how much the spine shortens in the period between 9.00 a.m. and 1.00 p.m. For this sake recording of the distance  $L$  was repeated 6 times in two intermediate postures for each person. With the average values of  $L$  we obtained the following picture:

---

age	sex	shortening of $L$	shortening of $L$ in % of $L$
32	f	5.7 mm	1.4 %
34	m	5.4 mm	1.2 %
53	m	3.2 mm	0.7 %

---

#### *Conclusion:*

Our *first impression* is that the form of the spine can be reproduced well in the unconstraint standing posture with the appropriate position of the feet and the hands and the direction of looking.

However, the position of the spine with respect to the supporting plane of the feet will show rather noticeable variations. When composing a system of coordinates it will therefore be better, in view of statistical research, not to refer the coordinates to the direction of gravitation.

The consequence for statistical research of the kyphose-sacrum area, visible in X-ray pictures and described before, is that the reference in the direction of gravitation, chosen there, might be a less successful choice.

For obvious reasons, however, we have not been able to verify whether the variations in the values of the parameters to be found, resulting from posture alteration in the sagittal plane, are inadmissibly great.

On the ground of the above results we think we may bring forward the following perception.

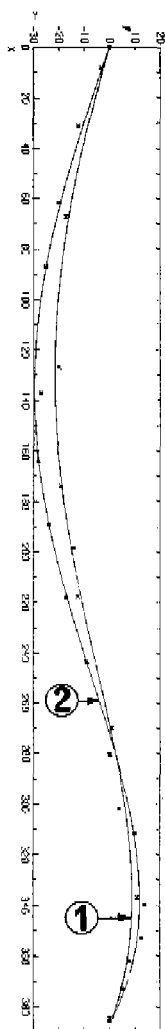


Fig. 2.7a

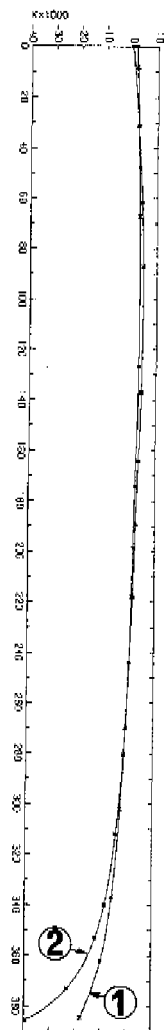


Fig. 2.7b

Fig. 2.7a shows the dorsal contour of the spine of a healthy woman. Curve 1 was determined a number of months before pregnancy, curve 2 three months after childbirth; in both cases the recordings were made about noon.

As can be seen in Fig. 2.7b, the curvature proves to have increased significantly in the lumbar region, viz.  $0.021 \left(\frac{1}{\text{mm}}\right)$  at contour L 5.

## 2.5. Click-clack phenomenon

In the following consideration we start from figure 2.8 which represents the form of a loaded elastic rod.

In position A the moment in the hinge situated at the bottom-most point is zero.

If in the plane of the diagram a moment is caused to act on the hinge in a counter-clockwise direction under the same load conditions, the rod will assume the form as shown in position B.

If this moment is increased, the rod will suddenly buckle, so as to assume the position represented by curve C, and will maintain this position even if the counter-clockwise moment is no longer exercised. If we want the rod to resume its original form, a clockwise moment must first be exerted.

This may be popularly called a click-clack phenomenon, resembling the clicking of a convex metal lid.

In analogy with the elastic rod one might expect also the spine to assume a natural posture resembling curve C.

This form appears in fact to occur in the case of the relaxed sitting posture and can be described by recording the dorsal contour. As an example, we give the case of a hypermobile girl aged 22 (Fig. 2.9a) who was supported at the shoulders in a loose sitting posture.

The greatest difference in the curvature (representative of the change in the bending moment) was found in the lumbar area (Fig. 2.9b).

---

Fig. 2.8. *Click-clack phenomenon of an elastic rod*

Fig. 2.9a. *Dorsal contour of the spine of a hypermobile girl aged 22 in standing and loose sitting posture (Not all of the contour of the thoracolumbar spine has been recorded).*

Fig. 2.9b. *The curvature changes its sign in the lumbar area.*

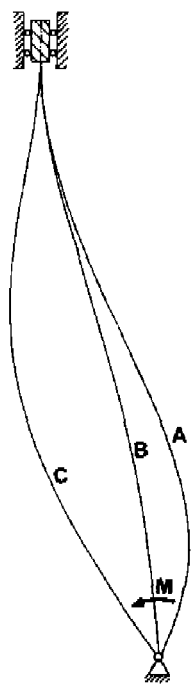


Fig. 2.8.

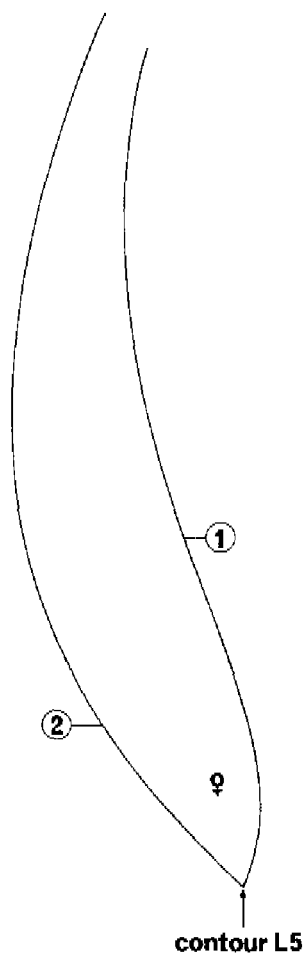


Fig. 2.9a.

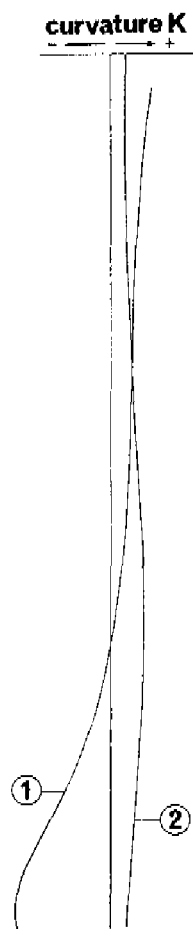


Fig. 2.9b.



## Three-dimensional form of the human thoracolumbar spine

- 3.1. Description of the form of the spine as visible in lateral and Anterior-Posterior (A-P) X-ray pictures by applying a mathematical formula with a comparatively great number of parameters.

In the lateral projection (Fig. 3.1a) the contours of the vertebral bodies in the upper thoracal area are generally hardly to be determined or not at all. Much information is lost on account of the depiction of the ribs and the shoulder girdle. Under these circumstances Fig. 3.1b was produced by means of a formula with four parameters to be chosen by the computer according to the method of least squares.

In the A-P projection only those cases are of interest to the description of form if a curvature in the frontal plane exists, the cases of scoliosis (Fig. 3.2a).

From a clinical point of view such pictures are unfavourable and in many severe cases surgery is resorted to in order to restore the column in a more straight position.

Fig. 3.1a *Laterally taken X-ray picture of a man, aged 43, a patient with dorsal complaints*



Fig. 3.1b *Description of form of the thoracolumbar spine by applying a formula with a comparatively great number of parameters* 

Fig. 3.2a *A-P X-ray picture of the same person as mentioned in Fig. 3.1. The A-P projection shown in Fig. 3.2a is perpendicular to the lateral projection in Fig. 3.1a and the proportion of projection is as well as possible the same.*

Fig. 3.2b *Description of form of the thoracolumbar spine from the A-P projection.* 

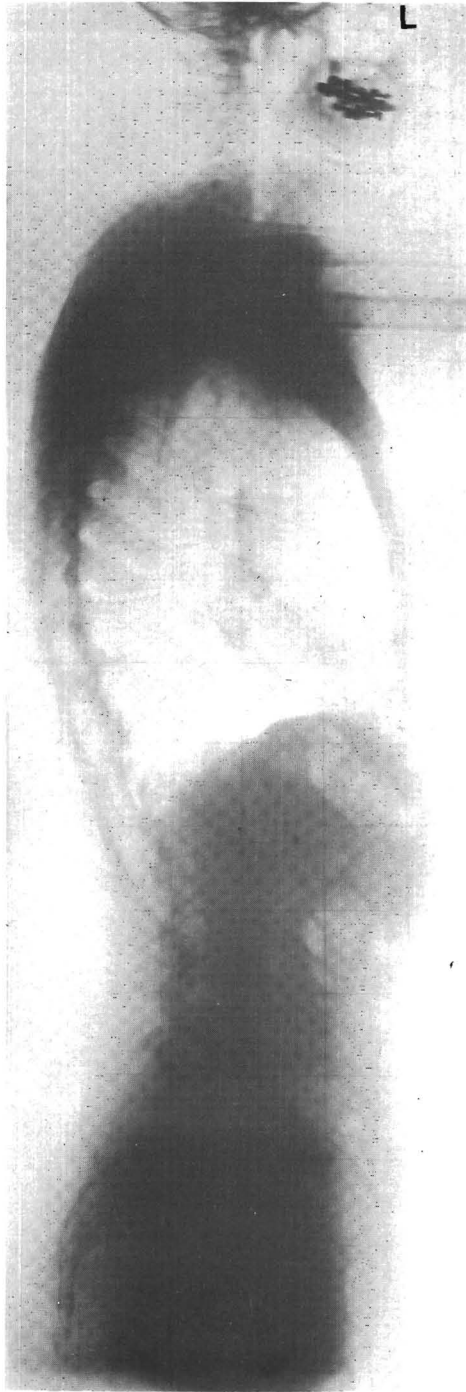


Fig. 3.1a

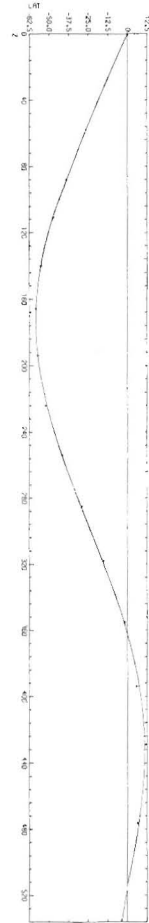


Fig. 3.1b



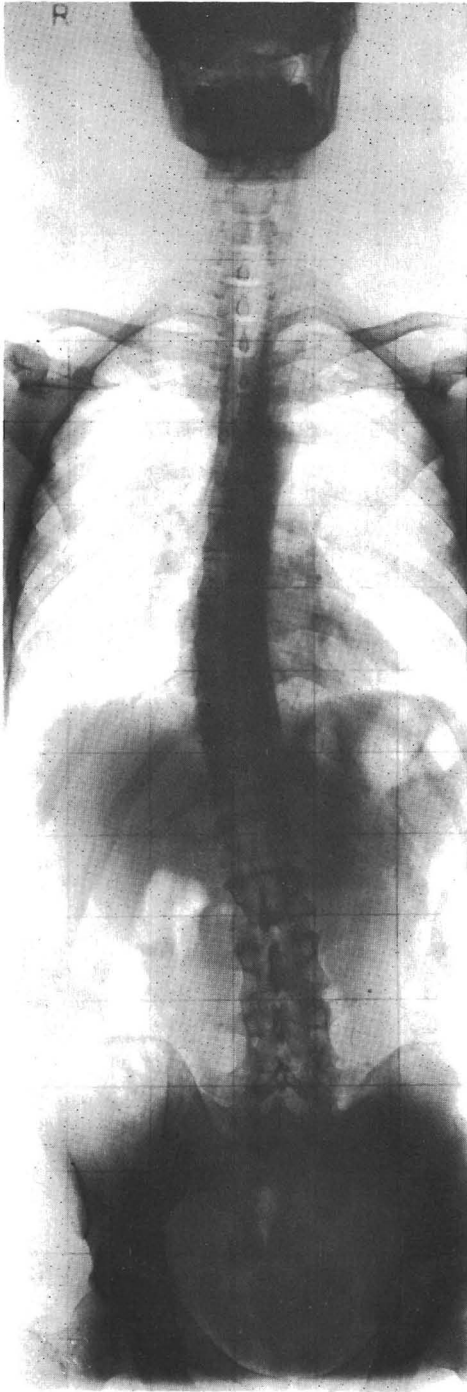


Fig. 3.2a



Fig. 3.2b

The more detailed numerical definition of this form was carried out by Reese (27) who measured all the coordinates of the geometrical centres as well as all the angles of inclination of the vertebral bodies. The position of the femoral heads, too, was involved in the research. A method is indicated by which the real length of the curved centre line of the vertebral bodies can be calculated. This method is based on an approximation of the curve by arcs of circles.

The method practised by us not only enables us to define mathematically the entire form by which the computer can calculate with the procured numerical values of the parameters the real length of the curve as well as the angles of inclination of the vertebral bodies and the curvatures directly, but also allows us to carry out the description of form in three dimensions.

### 3.2. Three-dimensional form of the human spine

The coordinate-axes used for the description of the lateral and A-P projections can be combined to a three-dimensional system of axes rotating to the right (Fig. 3.3). When making the X-ray pictures of the person in a natural standing posture with joined feet, care was taken that the A-P projection was to be perpendicular to the lateral projection and that the proportion of projecting was as well as possible the same. With the X-ray equipment available the two projections could not be made at the same time. It has to be assumed that the position of the spine was not the very same in the two projections.

By composing both projections fixed mathematically, which is done by the computer, the spatially curved form of the spine is obtained, i.e. the flowing line passing by approximation through the geometrical centres of the vertebral bodies. The top view, in fact the picture obtained by looking downward in the direction of the force of gravitation, can now be easily found (Fig. 3.4).

The projections of the various levels are indicated by +. For the location of these levels, reference is made to the  $z$ -coordinates of the centres of the vertebral bodies as visible in the lateral projection.

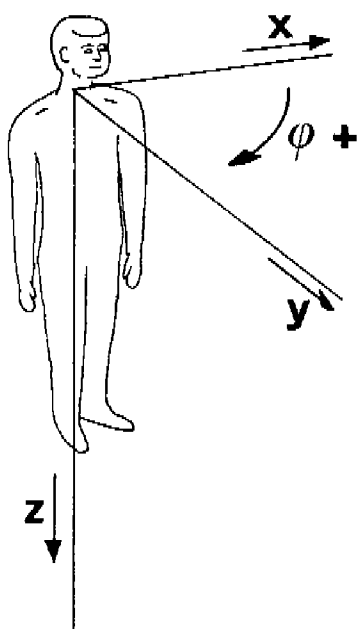


Fig. 3.3 *Coordinate-axes*

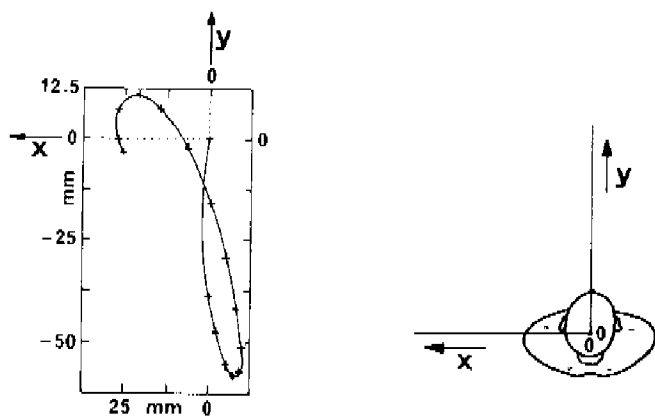


Fig. 3.4

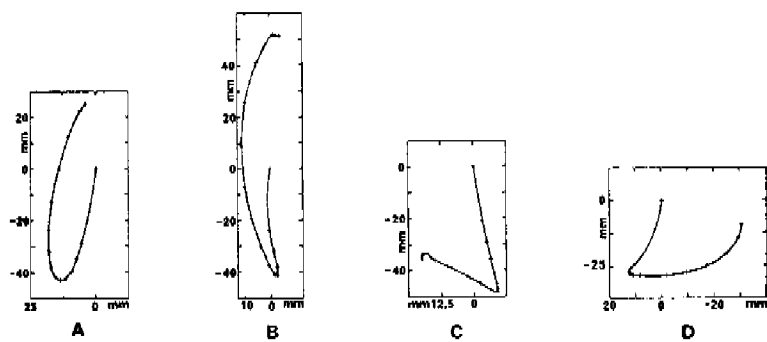


Fig. 3.5

### 3.3 Calculation of axial rotations

A measure of the axial rotations existing in the spatial curve of Fig. 3.4, bent in two directions can be computed mathematically (see Part II- 3.3). The rotations found in this way are entirely related to a spatially curved line and have as such nothing to do with the rotations in the human spine itself.

We have investigated whether, and if so to what degree, the mathematical measure of axial rotations gives an impression of the axial rotations in the spine concerned.

### 3.4 Measuring axial rotations

In the A-P projection, an axial rotation of a vertebral body with regard to the plane of projection manifests itself by an eccentric position of the projection of the processus spinosus with regard to the projection of the vertebral body.

The extent of this eccentricity is called by us  $e$  (Fig. 3.6.). If now the axis of the axial rotation, seen in the top view, passes through the point  $O$ , the distance  $d$  between  $O$  and the extremity of the processus spinosus will be known. The axial rotation

$\varphi$  can now be calculated with  $\tan\varphi = \frac{e}{d}$ .

The great problem that arises now is the measuring of  $d$ . The instantaneous point  $O$  is not marked in the X-ray pictures and cannot even be determined in the living mechanism. A certain hold is found in "Die Kyphose im Jugendalter" by Gütz (15) where it is said that the centre of rotation of a lumbar vertebra lies approximately in the third frontal part of the spinous process (Fig. 3.7a.). No further differentiation as to level is made. According to Davis (12) and White (36) it can be assumed that the centre of rotation at the level of the 5th thoracic vertebra lies in the anterior part of the vertebral body (Fig. 3.7b.). In our first trial to determine the rotations on the various levels we assumed that Fig. 3.7a. applies to L3-4, that Fig. 3.7b. applies to Th5-6, and that the distance between  $O$  and the centre line changes linearly along the spine.

The second problem in determining  $d$  is the measuring of the length of the spinous processes. On the lateral X-ray picture the spinous processes of the lumbar part are visible but they generally cannot be seen in the thoracic part on account of the projection of the ribs.

---

Fig. 3.4 Top view derived from Fig. 3.1b and Fig. 3.2b

Fig. 3.5 Top view of several diverging spines with scoliosis

In view of this part we made a combination of X-ray picture and dorsal contour of the spine, by which an impression as to the length of the spinous processes could be obtained. The dorsal contour being a 1 : 1 recording, in combining dorsal contour and X-ray picture we had to make allowance for the proportion of projection of the latter. Following the way as described before, paved with measuring errors and uncertainties, we found the rotations marked x in Fig. 3.8.

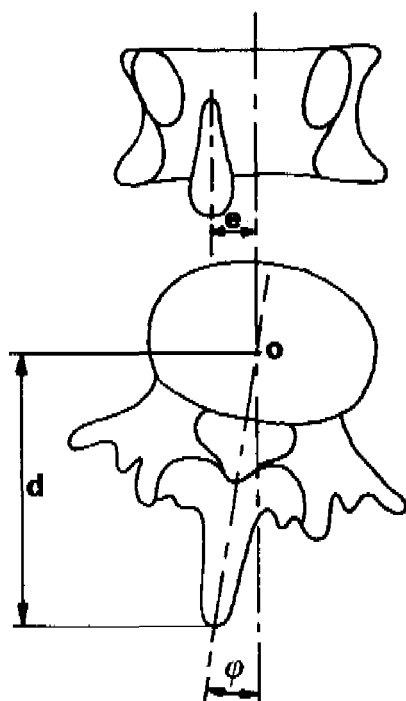


Fig. 3.6 *Axial rotation  $\phi$*

By multiplying the mathematical measure of axial rotations by a factor 41.89, we find the curve in Fig. 3.8 from which it may be concluded that the trend of the rotations measured corresponds remarkably well with that of the mathematical measure of axial rotations.

It has to be observed that the measuring errors in the thoracal part exceed those in the lumbar region. We further shifted here along an angle  $\varphi = 2.46^\circ$  the curve representing the mathematical measure of axial rotations in order to find a due correspondence with the axial rotations measured. We think the necessity of this acceptably inasmuch as the position of the spine of the person in the A-P projection has not to correspond completely with the theoretical system of axes. When reviewing the rotations with the help of an A-P X-ray picture it seems therefore more sensible to consider the rotations of the vertebral bodies with respect to each other and to attach less importance to the absolute values.

Total X-ray pictures of five cases of scoliosis were handled by us in the way mentioned above and identical results were found.

Fig. 3.8

*Mathematical measure of the axial rotations in the spatial curve of Fig. 3.4 compared with the measured axial rotations of the vertebrae*

Fig. 3.9

*Axial rotations in the spatial curves of Fig. 3.5 B and C*

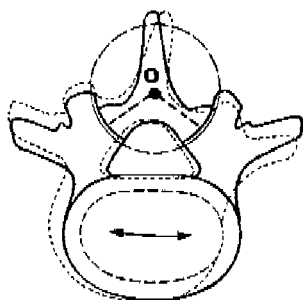


Fig. 3.7a

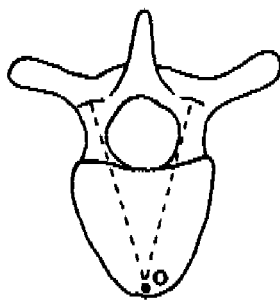


Fig. 3.7b

Fig. 3.7

*Centre of axial rotation on different levels*

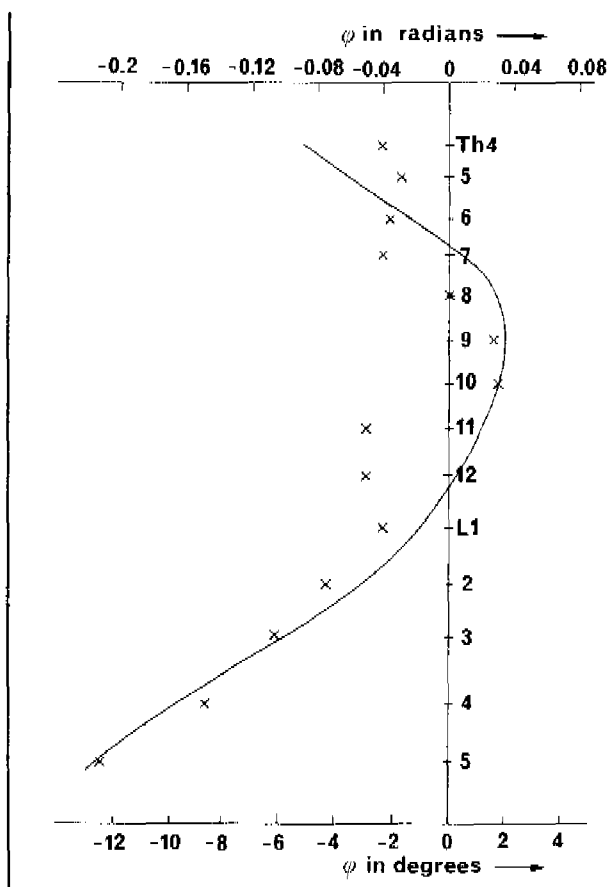


Fig. 3.8



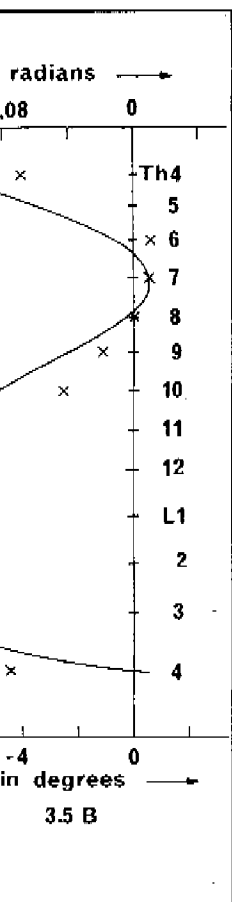


Fig. 3.9

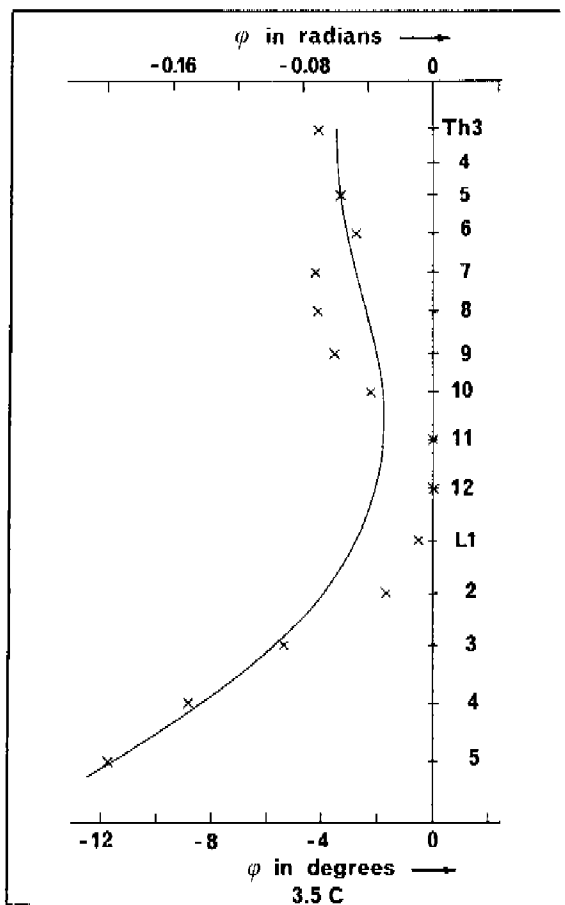


Fig. 3.9

That the top view already gives an impression of the trend of the axial rotations becomes apparent from the fact that the rotations of Fig. 3.5. C and D show an analogous but opposite trend. The rotations of Fig. 3.5. B and C are represented in Fig. 3.9, from which it appears that the rotations have a distinctly different trend from that in Fig. 3.8.

#### *Calculation of centres of axial rotation*

From the foregoing it has become evident that the correspondence between the values of the axial rotations calculated and those measured in the thoracal area is inferior to that in the lumbar area.

This has to be attributed to the fact that it was incorrect to assume arbitrarily a linear trend of the distance from the centres of axial rotation to the centre line. So, after calculating the multiplying factor by assuming the positions of the centres of axial rotation of Th5 and L4 as mentioned, we proceeded to adapt the centres of axial rotation of the other vertebrae to the further calculated axial rotations. By doing so we find, in the case of Fig. 3.5C., centres of axial rotation marked 0 in Fig. 3.10a. We compared the trend of the places of these points with the centres as they had been determined by Davis for exclusively the thoracal area. The correspondence with the centres of axial rotation calculated by us is remarkable. Notable is also the sharp change-over of the thoracal to the lumbar area. This, too, is a well-known datum of anatomy.

### **3.5 Relation between force phenomena and spatial curve**

The preceding part dealt with description of form together with calculation and measuring of axial rotations.

In the following part we will try to obtain a global impression of the force phenomena that play a dominating role in the origin of the spatial curve described before, thus relative to the natural standing posture.

---

Fig.3.10a *Positions of calculated centres of axial rotation (marked 0). Line A - A represents the anterior margins of the vertebral bodies, line B - B the posterior ones.*

Fig.3.10b *Positions of centres of axial rotation in the thoracal area defined by Davis on an autopsy specimen.*

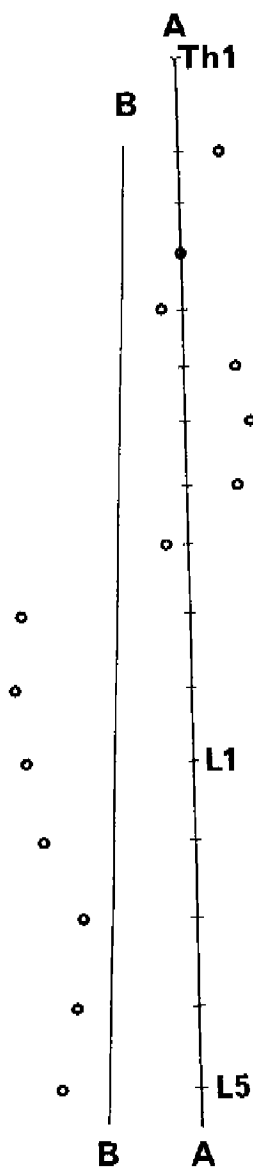


Fig. 3.10a

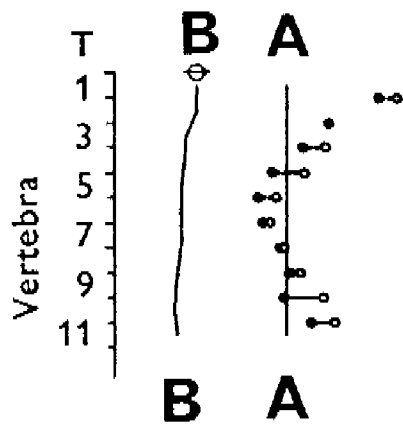


Fig. 3.10b

In case the spatial curve is considered to be the axis of a thin rod, straight when unloaded with the same mechanical properties over the whole length, there will be a linear connection, equal over the whole rod, between the axial rotation and the moment of torsion in the rod, the magnitude of the rotations being in direct proportion to the magnitude of the moments of torsion.

For a first orientation we imagine the rod to be only loaded at the extremities. In point Th 1 lying in the spine at the level of the shoulder-girdle (Fig. 3.11) are effected bending moments ( $M_x$  and  $M_y$ ), a moment of torsion ( $M_w$ ) and a force in the direction of gravitation ( $F$ ).

Fig. 3.12 shows the contribution of each force phenomenon, taken as a unit, to the moment of torsion in the bent rod at different levels. For the axis of this rod the spatial curve of the spine of Fig. 3.1 has been taken.

---

Fig. 3.12  
*Contribution of each force phenomenon, taken as a unit, to the moment of torsion in the bent rod*

---

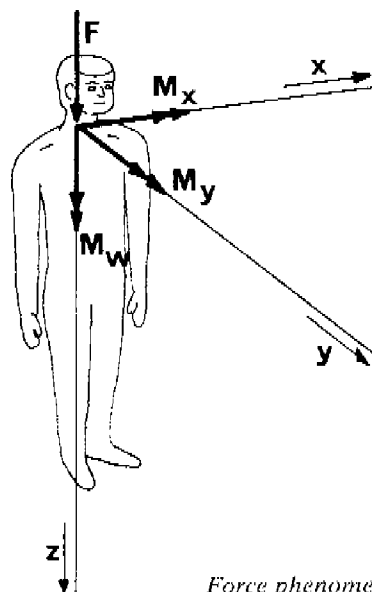


Fig. 3.11

*Force phenomena effected in point Th1*

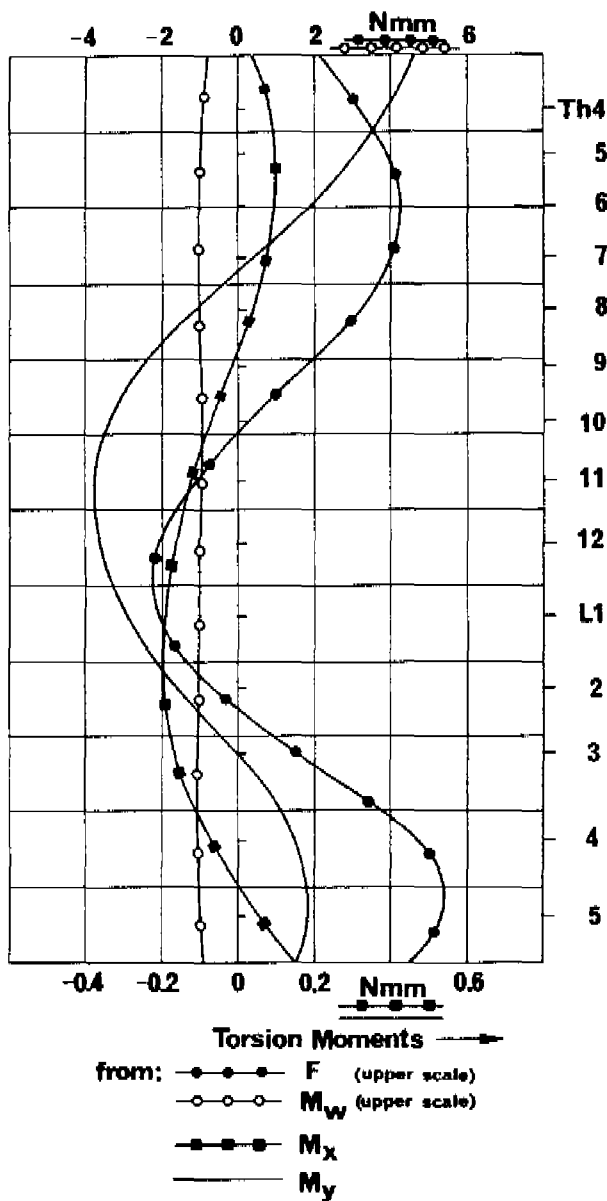


Fig. 3.12

If now we knew what rotations exist in the rod, we could make a choice as to the factors by which the force phenomena, taken as a unit, would have to be multiplied in order to obtain a line of torsion moments that, taking into consideration a multiplying factor, would correspond with the rotations existing in the rod.

We have at our disposal the following two important data, necessary to adapt this method to the spine, viz.,

1. We have at our disposal a mathematical measure giving us a good impression of the true axial rotations in the spine.
2. On the ground of data that White obtained from load experiments on autopsy specimens, we may assume that a linear connection exists between axial rotations and torsion moments at different levels of the spine, starting from axial rotations not exceeding physiological limits.

However, this way of calculating cannot simply be applied to the spine because we started from the very local application of the force phenomena, from the absence of rotations after unloading, and from the equality of the elastic resistance against axial rotation over the entire length of the rod.

Our knowledge being as yet insufficient to go a better way, we apply the abovementioned line of thought to the spine, in spite of the numerous objections that could be brought up against it. After all, we have to make a start somewhere.

If this method should appear to be auspicious, it is significant to introduce refinements.

We are aware that the following results will have to be interpreted with the necessary reserve.

According to (37), head, neck and arms represent 17.7% of the body's weight. The weight of the shoulder-girdle is estimated by us at 10% of the weight of the trunk, resulting in approximately 5.3% of the body weight. In this way force  $F$  is found to be 23% of the body weight. The weight of the person in consideration (Fig. 3.1) is 712 N so that we find for  $F$ : 164 N.

Assuming that the relation  $GI_p \cdot \eta = M_w$ , in which  $\eta$  represents the axial rotation per unit of spine length, and  $GI_p$  the resistance against axial rotation, applies to the spine, we find with  $F = 164$  N a value for  $GI_p = 2.4 \cdot 10^5$  Nmm<sup>2</sup>.

In White's book (36) on page 46 is given the remarkable linear connection between axial rotation and moment of torsion at various levels of the thoracic spine, determined on the spine of a cadaver.

With the help of these data we composed table 3.1. We ourselves had to adjoin an essential datum: the distance between the geometrical centres of the connecting vertebral bodies of the various discs. For this purpose we took the average values of the corresponding distances as could be measured from the X-ray pictures of the five cases of scoliosis examined by us. A correction has been made for the proportion of projection, which is 0.895.

disc	$\varphi$ axial rotation in degrees at $M_w = 2000 \text{ Nmm}$	$\varphi$ axial rotation in radians at $M_w = 2000 \text{ Nmm}$	distance between centres of con- necting vertebral bodies in mm	$\eta$ axial rotation per unit of spine length in rad. $\text{mm}^{-1}$	$GI_p$ resistance against axial rotation in $\text{Nmm}^2$
Th 1-2	13.1°	0.2286	19.9	0.01149	1.741.10 <sup>5</sup>
Th 3-4	7.2°	0.1257	19.7	0.006381	3.134.10 <sup>5</sup>
Th 5-6	6.5°	0.1134	23.2	0.004888	4.092.10 <sup>5</sup>
Th 7-8	7.2°	0.1257	23.6	0.005326	3.755.10 <sup>5</sup>
Th 9-10	4.3°	0.07505	24.8	0.003026	6.609.10 <sup>5</sup>
Th 11-12	1.0°	0.01745	27.4	0.000637	31.400.10 <sup>6</sup>

Table 3.1

Although measuring on autopsy specimens cannot give an exact image of the spine in the living body, we think we may say that from the values of  $GI_p$  in table 3.1. it should be concluded that there exist important differences at the various levels. According to the same source it may be concluded that  $GI_p$  in corresponding discs of various persons may differ a factor 4. At the same time, comparison as to age and as to the ratio disc height/disc diameter indicated no significant correlation coefficients.

We composed table 3.1 in order to prove that the values of the average  $GI_p$  of the thoracolumbar spine calculated by us and given in table 3.2., appear in the same order of magnitude.

person of Fig.:	best adaptation for $\lambda$ *	$\alpha$	$\alpha \cdot \lambda$	body weight in N	23% of body weight	$GI_p$ in $\text{Nmm}^2$
3.4	41.89	0.161.10 <sup>-4</sup>	6.74.10 <sup>-4</sup>	712	163.8	2.43.10 <sup>5</sup>
3.5 B	35.44	0.795.10 <sup>-5</sup>	2.78.10 <sup>-4</sup>	530	121.9	4.38.10 <sup>5</sup>
3.5 C	21.25	0.716.10 <sup>-5</sup>	1.52.10 <sup>-4</sup>	692	159.1	10.53.10 <sup>5</sup>

\* See Part II-3,4

Table 3.2

Starting from the value of  $GI_p$  given in table 3.2 for the case of Fig. 3.4 we found  $M_w = 382$  Nmm,  $M_x = -2290$  Nmm and  $M_y = -1040$  Nmm. These values are rather high, considering that 2000 Nmm equals about 2 kilogramforce on a lever arm of 10 centimetres. However, when the rotations are partially effected by the downward increasing influence of the self-weight of the spine, and of the weight of the muscles attached to it, etc., it may be expected that when neglecting this influence, in addition to a distorted picture too elevated values for the moments will be found on the spot (h l).

Part II - 3.4 explains basically how the self-weight of the spine and the parts of the trunk attached to it can be taken into the calculation. It also mentions why we have not proceeded to this calculation.

Consequently, we are aware that many more refinements will have to be made in the method and that even after this the certainty remains that factors having a casual character can never be taken into the calculations. When confining ourselves to the cases of scoliosis generated by purely mechanical phenomena, very local excessive nonsymmetric muscle tensions in the erect posture are to be expected in a number of cases.

On the ground of the preceding, as well as on the ground of the fact that it is to be expected that the postures of the persons investigated during the making of the lateral X-ray pictures may differ from those during the making of the A-P projections, it is not surprising that in two cases out of the five investigated by us the force phenomena calculated did not have the direction expected by us on the basis of our loading model. We further expect that in serious cases of scoliosis only the description of the three-dimensional form and the calculation of the trend in the axial rotations will be successful. Calculation of the true magnitude of the axial rotations as well as that of the torsional rigidity will then be no longer possible inasmuch as the divergencies of the assumptions will be out of all proportion. In such cases only differential methods may produce usable results.

### 3.6 Observations

It is common knowledge that lateral flexion and rotation of the spine never occur separately. A general explanation of this phenomenon is that the spinal movements are determined by the orientation of the planes of the articular facets.

Indeed, reasoning from this point of view, a correspondence is



found between orientation of facets and the rotations in case of lateral bending. On the ground of our assumption that the mechanical behaviour of the spine roughly shows analogy with that of an elastic rod, and of our related findings we prefer what could be considered as a converted proposition. We posit that the spine behaves according to the laws of mechanics and that the orientation of the joint facets fits in with the axial rotation provoked by the lateral bending in the spine.

As a fact, in applied mechanics it is known that in case a flexible rod is bent first in one plane and then, when held in this bent position, is bent in a plane perpendicular to the first, torsion moments arise in the rod, and consequently it will at the same time always rotate on its longitudinal axis (25). The resultant of the bending moments, which are perpendicular to each other, has in fact a component in the direction of the axis of the rod.

Although the mathematical measure of the axial rotations was presented primarily in order to make it possible to indicate the trend of these rotations on the entire thoracolumbar spine by calculation, we mention here that the measure chosen appears to be connected with the degree of bending in the frontal plane (See Part II - 3.3).

Where, in the foregoing, starting from the spatial curve of the spine, we tried to find the forcephenomena that play a dominating part in the origin of the spatial curve, we were entering upon a sector where we are obstructed by too numerous unknown factors, which, having a casual character, can never be discounted. However, because the values of  $G/I_p$  calculated (Table 3.2) in spite of the many uncertainties and approximations appear to be of the order of magnitude of the values found in literature, we think we may say that after introducing further refinements in the method, a calculating tool may be achieved that may contribute to a better understanding and the treatment of scoliosis.

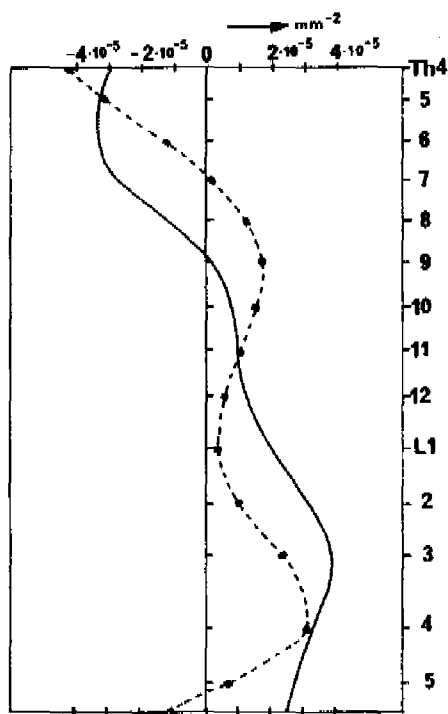


Fig. 3.13. Adaptation of torsion moments (dotted line) to the mathematical measure of axial rotations per unit of spine length for the case of Fig. 3.12. (See also Part II - chapter 3.4.).

# 4

## Aspects of the mechanical behaviour of a vertebra-disc-vertebra segment

### 4.1 Introduction

The vertebral bodies of a lumbar segment shown in Fig. 4.1 possess an elliptical form in top view. In the kyphotic part of the spine this aspect, regarded in upward direction, obtains more and more the accent of a circle. From the vertebral body arises an arc providing space for the spinal cord. The arc has two processes directed sideways, the processus transversi, and one process directed backward, the processus spinosus.

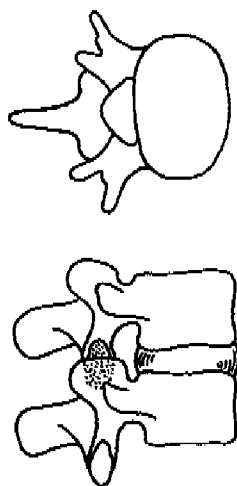


Fig. 4.1 *Vertebra-disc-vertebra segment (motion segment)*

Between two successive vertebral bodies is found a joint also shaped by processus arising from the arc, the two directed downward, the processus caudales, being encircled by the two processus directed upward and belonging to the underlying vertebra, the processus craniales,

In the thoracic part of the spine the vertebrae bear two costal facets on each side of the vertebral bodies; the transverse process directed laterally and backward bears a facet for articulation on its anterior aspect, close to its extremity. The facets of two successive vertebrae together with the facets of one rib form one joint (4).

In addition to the influence of the articular intervertebralis the movement with regard to each other of two successive vertebrae is governed by several ligaments, on the one hand connecting the vertebrae firmly to each other and on the other allowing ample movements through a relatively high elasticity with respect to the bone (motion segment).

Between the successive vertebral bodies is found the intervertebral disc. Each intervertebral disc consists of three portions (7), viz. the superior and inferior cartilaginous end-plates of the adjacent vertebrae, the annulus fibrosus consisting of concentric lamellae of fibro-elastic tissue, and the gelatinous central portion of the disc - the nucleus pulposus

The annulus fibrosus is attached above and below to the cartilaginous plates in its more central portions, to the bone of the peripheral portion of the end-plate at the site of the epiphyseal ring, at the extreme periphery, to the sides of the vertebral bodies. This peripheral portion fuses to and is inseparable from the anterior and posterior longitudinal ligaments. These ligaments are vertical bands of fibrous tissue which run over the whole length of the spinal column. The anterior ligament is of uniform width and is very strong, being firmly attached to the whole anterior surface of each vertebral body. The posterior ligament, on the other hand, has a calloped appearance and is attached only to the discs and the superior and inferior margins of the vertebral bodies. Along the posterior surfaces of the vertebral bodies, it narrows to a thin strip with but a tenuous attachment to the posterior aspect of the centra.

The mechanical behaviour of the motion segment has been approached by many investigators. From an engineering point of view the results of load-experiments on autopsy specimens are of great interest, because in the mechanical modelling of the human system one should have access to the relative biomechanical data before the modelling process can be significant. In the literature at our disposal the measuring results are frequently given in a sense not directly applicable to calculating, and if they are, the data essential from our point of view often fail.

In the following is given a global impression of the mechanical behaviour of a motion segment with reference to investigations by Nachemson (23), Rolander (28), White (36), and Galante (13).

#### *Axial load*

With axial load on a motion segment the height of the disc diminishes. When the compression increases, normal lumbar discs show an increasing resistance against deformation; at a load of approx. 500 N the relation between compression and deformation becomes fairly linear.

In a case where the reduction of altitude of the disc at approx. 3000 N was 1 mm, relatively small to be sure, the reduction of altitude of the connecting vertebral body appeared amply an order of magnitude smaller.

Residual deformations in the latter order of magnitude were observed after complete load series.

The connection between pressure in the nucleus pulposus and axial compression is linear. It has been demonstrated that the pressure in the nucleus is omnilateral and evenly spread, the nucleus itself being hypothetically incompressible, also in moderately degenerated discs.

Comparison of specimens before and after removing the posterior elements showed that the latter carry roughly 20% of the axial load. In specimens without posterior elements and with approximately equal surfaces of annulus and nucleus in the cross-section, 1/4 of the axial load was carried by the annulus and 3/4 by the nucleus.

#### *Bending moment*

Under a constant axial load as well as under an axial load increasing proportionally with the bending moment, the connection between angular rotation and bending moment is linear in both the sagittal and the frontal plane. The flexural rigidity of a motion segment in the case of dorso-flexion is higher than that in the case of ventro-flexion.

Removal of the posterior elements from thoracal vertebrae has no influence worth mentioning on the resistance against bending in the frontal plane.

However, the effect in the sagittal plane is important. In fact, the rigidity in the case of dorso-flexion diminishes approximately 55%, in the case of ventro-flexion approximately 35%. A similar trend is observed in the lumbar area where the

intersection of the ligamentum flavum effectuated the most important decrease of rigidity.

*Remark:*

The above mentioned conclusions are based on observations in relation to which we found no indication whether the load had been corrected with respect to the inclination of the tangent-plane of the ball bearings that have an essential function in the loading equipment concerned.

With increasing bending moment in various directions the pressure in the nucleus pulposus also increases.

Determination of the instantaneous centres of rotation of successive lumbar vertebrae showed a very important spread in spite of which the following trends were observed: In case of ventro-flexion the centre of rotation turns towards dorsal, in case of dorso-flexion towards ventral.

In the frontal plane, too, the centre of rotation moves in the direction opposite to the direction of bending. In the study concerning thoracic vertebrae the centres of rotation have been determined with the help of X-ray pictures. A much smaller spread was found and at the same time a correspondence with lumbar segments in case of bending in the frontal and the sagittal plane: the centre of rotation moves in the direction opposite to the direction of bending.

*Transverse forces*

Transverse forces effectuating shear go with bending. Shear can be investigated separately by taking care that in a loading equipment the endplates are kept parallel. Whether such investigation has been carried out is unknown to us.

*Torsion moments*

The connection between axial rotation and moment of torsion in the thoracic spine is remarkably linear. Removal of the posterior elements effectuated a decrease of resistance against torque of approx. 35%. The instantaneous centres of axial rotation were positioned at the levels of Th5 and Th6 in the anterior part of the vertebral body, at the levels of Th9 and Th12 in the posterior part, and at the levels of Th7 and Th8 in the space of the spinal cord. Looking in the frontal plane these centres of axial rotation were located rather centrally.

In the foregoing only a small portion of the literature has been referred to. It is of great importance to us that the quoted trends in the mechanical behaviour point remarkably well to what has been said by White: "It can be stated that in this series for the forces employed, in relation to some gross estimates of the loads imposed by gravity, the specimens behaved in a manner that can be analysed in mechanical terms of a spring constant".

#### 4.2 Schematic model of a motion segment

It has been proved experimentally that a vertebral segment can transfer the abovementioned force phenomena. A schematic model of a motion segment without posterior elements (Fig. 4.2) is very useful to indicate outlines. The vertebrae will be supposed to be rigid with respect to the intervertebral disc and fibrous system.

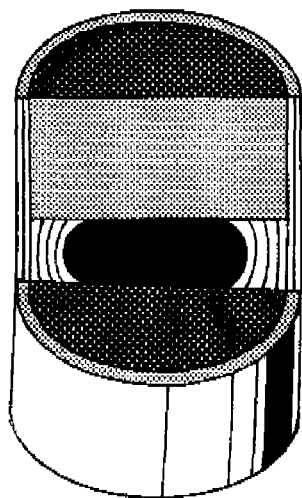


Fig. 4.2

*Motion segment without posterior elements*

### *Axial load*

As a result of axial compression, an overpressure ( $p$ ) with respect to the space located outside the fibrous layer enclosing the nucleus will be generated in the nucleus. This layer has been considered by Nachemson as a thin-walled tube. It has been calculated that the tangential stress in the anterior part of the annulus is  $2.1 p$  and in the thinner posterior part of the annulus  $3.7 p$ . Sonnerup (32) considers a thin circular disc representing a central slice of the intervertebral disc. He regards the material as inhomogeneous because the rigidity of the annulus increases from the inner towards the outer part according to measurements made by Galante. In spite of the annulus material being non-linear, as measured from the relaxed state, linear elasticity is assumed, because a preload always exists on a disc in situ, so that the influence of non-linearity is of minor importance to the incremental stressfield developed by an additional axial load. After applying representative material constants a remarkable evenly distributed tangential stress will be found. This provision is exceptionally favourable because in the cross-section of a thick-walled tube of homogeneous technical material, inwardly loaded by pressure below elastic limits, the tangential stress on the inside far exceeds that on the outside.

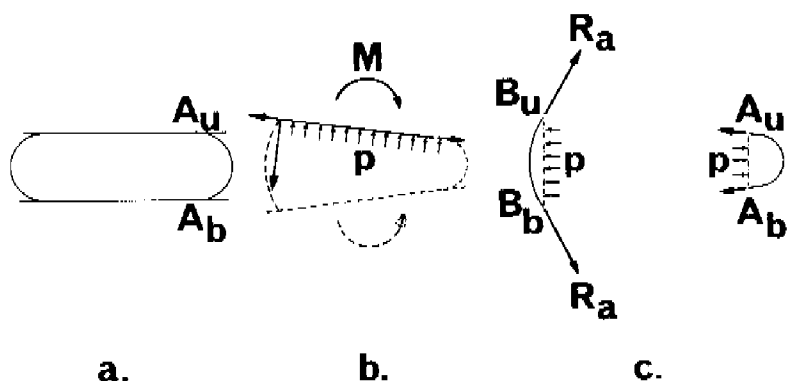


Fig. 4.3 Schematic representation of equilibrium in case of a pure bending moment



### *Bending moment*

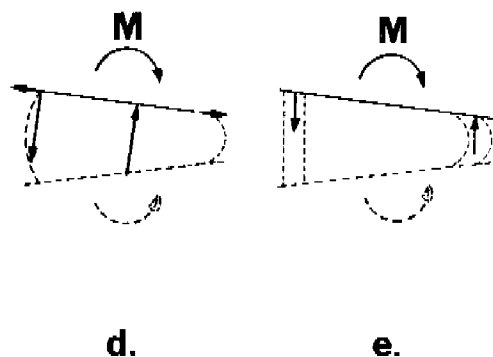
In a first approach we only consider the nucleus and its directly adjoining annulus fibres.

Supposing that the annulus fibres can only carry tensile forces, it seems at first sight that a moment ( $M$ ) could not be carried unless  $A_u$  and  $A_b$  (Fig. 4.3a) touch, i.e. make bone-to-bone contact.

Bone-to-bone contact may be avoided:

- (a) If the provision of overpressure is made in the space limited by the netting and the vertebral bodies (Fig. 4.3b).

This overpressure may be thought to be effectuated by geometrical reduction of the space within the annulus in case of angular rotation. However, when the nucleus is thought incompressible, this reduction will cause overpressure in the nucleus which effectuates expansion of the annulus. The geometrical reduction should exceed the augmentation of space effected by elongation of the tension-loaded fibres that have to procure the force resultant  $R_a$ . In the unloaded state a reasonable flexural rigidity is plausible, if an overpressure is already present. This is in reality the case, because the nucleus has a considerable inclination towards swelling (imbibition). As a consequence, the annulus fibres are preloaded, which entails the addition-



*for explanation.*

al advantage that in this way the fibres are loaded up to a steeper area of the load extension curve.

Remark:

By considering very schematically the equilibrium of an annulus fibre imagined to be a thread (Fig. 4.3c) it will appear, already because  $p \cdot B_u B_b$  is greater than  $p \cdot A_u A_b$ , that the left fibres are more heavily loaded and that the force in longitudinal direction of the spine in the point of fixation to the vertebral body will in any case be greater on the left side than on the right. Starting from the fact that by bending forward the disc shows the wedge form sketched in Fig. 4.3, it is obvious that radial fissures will be found in the annulus fibres at the dorsal and dorso-lateral side (35, cit. Lindblom). It may also be expected that ruptures will occur sooner at  $B_u$  and  $B_b$  than at  $A_u$  and  $A_b$ . If such ruptures cause disc-prolaps or protrusion (Hernia nuclei pulposi) it might be said that, starting from the foregoing reasoning, this phenomenon occurs predominantly on those spots in the spine where:

- (1) parallelism between the vertebrae in natural standing posture is greatest (straight spine);
- (2) angular rotation between the vertebrae while bending forward is greatest (lumbar area);
- (3) the product of pressure and disc-height is greatest in the bent position (we expect this to be the case in the lumbar area in relatively long spines).

Although the problem with regard to hernia nuclei pulposi is far more complicated than suggested above, the gross indication where and especially in what spines it occurs, and that it arises while bending forward, corresponds with the experience of orthopaedic surgeons consulted on the point.

In the above consideration the hernia attributed to the "concealed disc" according to Dandy (35): the weak intervertebral disc, has not been incorporated.

- (b) If a sufficiently hard and disc-shaped body is present between the vertebrae and, while bending, is pushed towards the narrow side of the space, or at least stays in the proximity of its original position (Fig. 4.3d).
- (c) If the annulus fibres can carry compressive forces (Fig. 4.3e). It has been determined experimentally (Nachemson) that

the layer composed of concentric lamellae can carry compressive forces: We think it interesting to compare experimentally the flexural rigidity before and after removal of the gelatinous nucleus pulposus.

#### *Transverse forces acting on the vertebrae*

For simplicity, it has been assumed in Fig. 4.4 that after applying the transverse forces  $P$  the distance between the vertebrae has remained the same and that the vertebrae have remained parallel to each other.

For considering this force phenomenon those fibres of the annulus fibrosus situated towards the interior of the disc, represented by a netting of crossed fibres, are predominant. (See also Fig. 4.4.3).

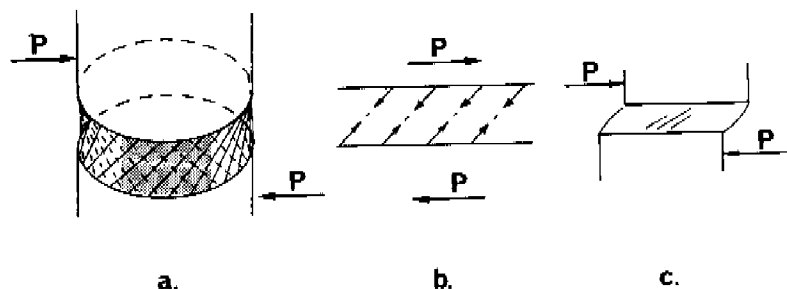


Fig. 4.4 *Transverse forces*

From Fig. 4.4 the following may be seen:

- (1) In the dark-coloured area only half of the fibres present can share the mechanism of forces.
- (2) Fibres lying outside the dark-coloured area partake of the equilibrium of forces in only a small measure.
- (3) Interior equilibrium with a larger transverse force can only be established after the vertebrae are shifted with respect to each other (Fig. 4.4c) (Spondylolisthesis).

These three points are attended with drawbacks. For a satisfactory description of the transfer of great transverse forces the help of the intervertebral joints must therefore be added.

### *Torsion moments acting on the vertebrae*

True torque can also be transferred by half of the fibres as sketched in Fig. 4.4. As soon as the centre of motion turns towards a position outside the centre of the vertebral bodies, true rotations will be coupled with radial shear (influence of the posterior elements).

In the foregoing a model has been described which is in principle capable of transferring elementary force phenomena. By piling up a number of such-like motion segments the sketch in Fig. 4.5 will be produced. It represents a continuous very elastic thin-walled tube, reinforced internally by means of discs constantly kept at a certain distance from each other by a medium, indicated in black, surrounded by a strong layer. The mechanical behaviour of such a system, constructed of technical material, is in principle accessible to mathematical description. It must be admitted that after such a description a very long way still has to be gone before the human spine will be mapped out in detail in mechanical respect.

#### 4.3 Load test on an autopsy specimen

The autopsy specimen shown in Fig. 4.6 in unloaded state has been loaded in ventro-flexion as well as in dorso-flexion. The load equipment has been described in Part II - 1.1. The bending moment was obtained by applying an accurately horizontal force on the uppermost vertebra. No axial load was applied. In order to measure accurately the angular rotation ( $\Psi$ ) of the vertebral bodies in the X-ray pictures, nails were driven into the vertebral bodies to serve as references during the measuring. The angle measuring was done from a tenfold optical enlargement of the X-ray picture with an accuracy indicated by the standard deviation of 2.5'. In Fig. 4.7a is given the relation found between angular rotation ( $\Psi$ ) and moment in ventro-flexion, recorded at the various levels. The moments have been calculated with respect to the geometrical centres of the discs; the error in the determination of these centres resulted in a standard deviation

---

Fig. 4.5 *See text for explanation*

Fig. 4.6 *Autopsy specimen in unloaded state. Male, aged 43. Completely visible are the discs L3-4- up to Th10-11. Note the straightness.*

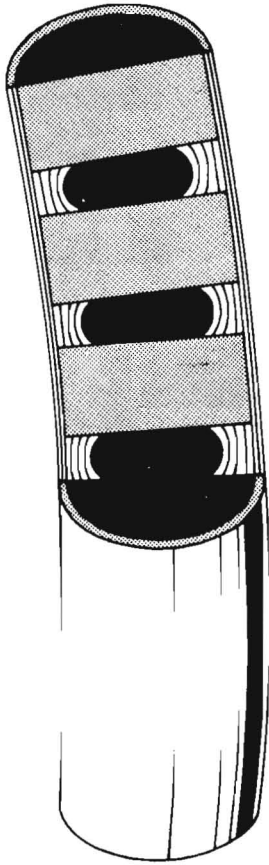


Fig. 4.5

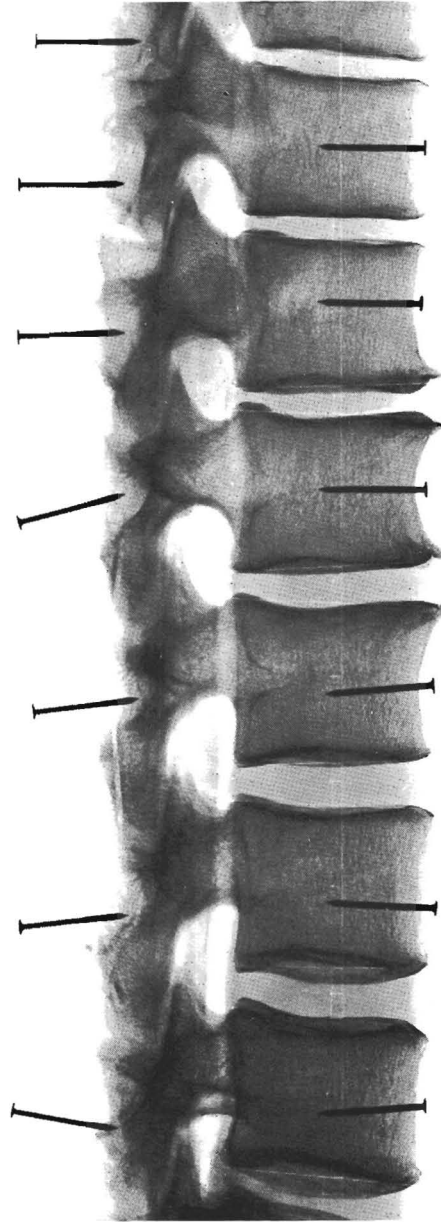


Fig. 4.6

of 0.4 mm in the values of the distance between horizontal force and centres. Fig. 4.7b shows the observations in dorso-flexion.

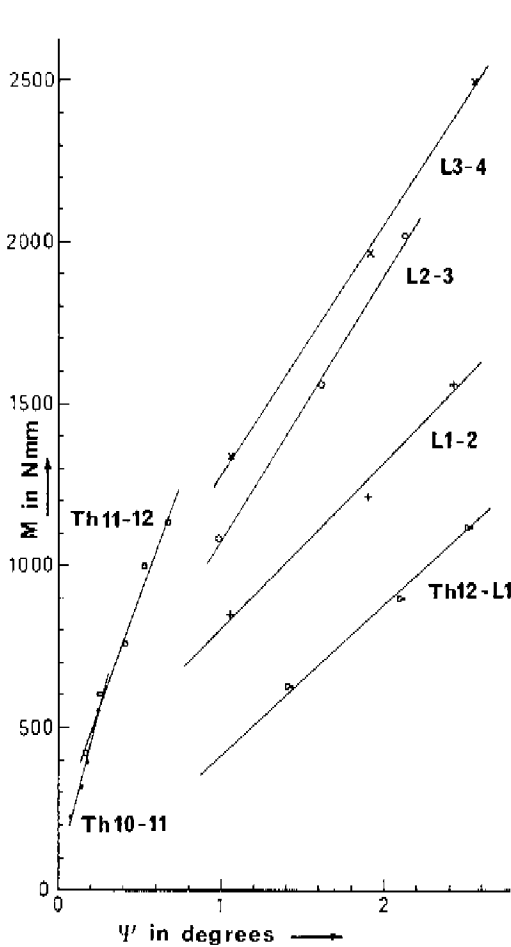


Fig. 4.7a *ventro-flexion*

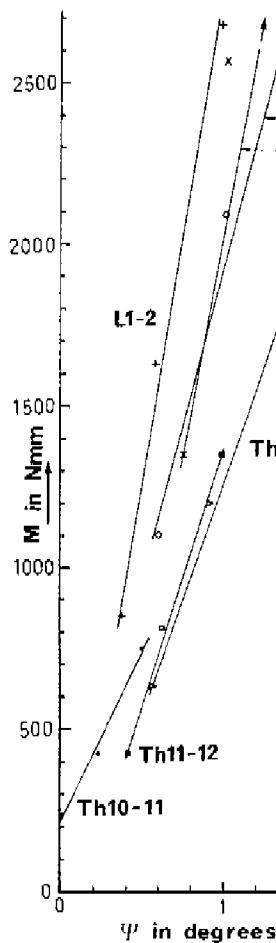


Fig. 4.7b *dorso-flexion*

Remarks to Fig. 4.7.

- (1) The angular rotations are indicated to a maximum of 2.6 degrees inasmuch as we think that in this region one can speak of an initial flexural rigidity for every disc considered.
- (2) The lines of regression are not passing through  $M = 0, \Psi = 0$ , from which it becomes evident that the absolutely unloaded state is a position hardly to be realised.

Since the connection for the given load series is virtually linear, the factor  $EI$ , measure of the flexural rigidity, has been calculated by a regression line according to the formula

$$EI = \frac{ML}{\Psi} \quad (4.3.1)$$

In Fig. 4.8a are given the results with respect to ventro-flexion. The average heights of the discs in unloaded state stand in line

1 for  $L$  in (4.3.1). In line 2  $L$  in (4.3.1) has been replaced by the distances between the geometrical centres of the connecting vertebral bodies in the unloaded state and is given in this way the flexural rigidity related to the spine length.

---

Fig. 4.8a Line 1 represents the flexural rigidity related to disc height in ventro-flexion.

Line 2 represents the flexural rigidity related to spine length in ventro-flexion.

Fig. 4.8b This figure represents geometrical data of the autopsy specimen in unloaded state. A correction has been made in accordance with the proportion of the X-ray projection. Line 3 represents the average heights of the discs. Line 4 represents the maximum width of the vertebral bodies. Off the vertical scale the distances between the geometrical centres of the discs can be read.

Fig. 4.8c In this figure a comparison can be made between the flexural rigidity related to the spine length in ventro-flexion (line 5) and the flexural rigidity related to spine length in dorso-flexion (line 6).

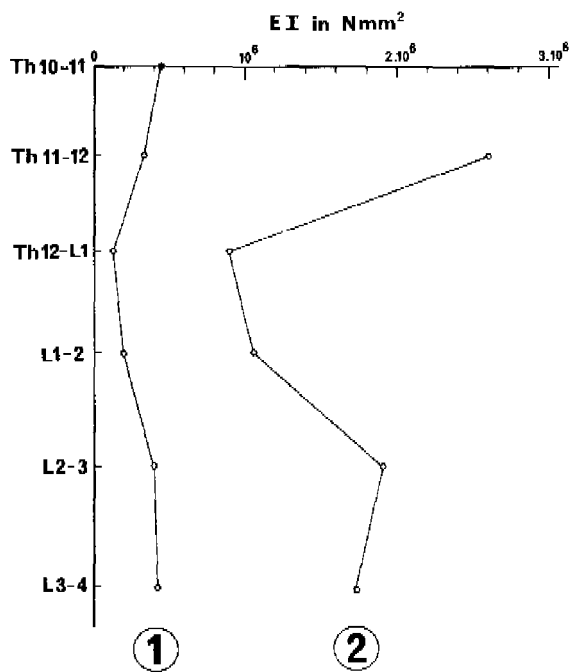


Fig. 4.8a



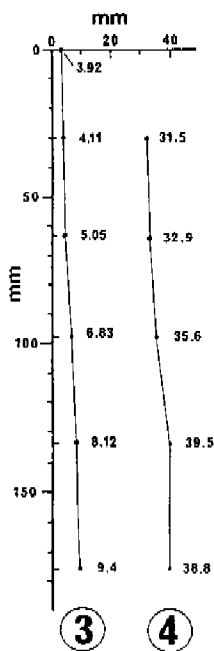


Fig. 4.8b

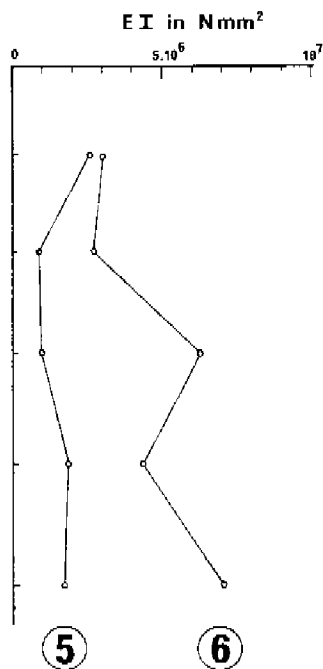


Fig. 4.8c

Commentary on Fig. 4.8 - Spondylosis deformans.

The most striking point here is that the initial flexural rigidity of the discs Th12 - L1 and L1 - L2 is far less than that of the surrounding discs. On the ventral side, both discs showed very distinctly *spondylosis deformans* contrary to the other discs, which are perfectly sound in this respect.

This deviation is attributed to slackening of the disc by loss of turgor in the nucleus (15), which fits in with our observation (See also 4.2, bending moment). From the trend of the average height of the discs determined in the unloaded specimen it cannot be concluded that the discs with spondylosis deformans are notably lower than the other ones.

#### *Average flexural rigidity related to spine length*

Neglecting the influence of the discs affected, the average initial flexural rigidity related to spine length of this specimen in ventroflexion is  $EI_a = 2.1 \cdot 10^6$  (Nmm<sup>2</sup>).

For comparison: a solid steel rod the round cross-section of which has a diameter of 3.8 mm, possesses an equal degree of flexural rigidity.

For dorso-flexion we found  $EI = 4.8 \cdot 10^6$  (Nmm<sup>2</sup>).

Lucas and Bressler (21) determined in an analogous way the average flexural rigidity of the whole thoracolumbar spine of an autopsy specimen while bending it in the frontal plane. They found  $EI = 3.2 \cdot 10^6$  (Nmm<sup>2</sup>) for the area of the spine related to our study.

#### **4.4 Hypotheses about two wear-and-tear phenomena that manifest themselves in the case of angular rotation of two successive vertebrae**

##### **4.4.1 Wear and tear of the cartilaginous plate**

Starting from the netting adjoining the nucleus being convex, the schematic representation of Fig. 4.4.1 can make it clear to us that in the case of angular rotation the nucleus material on the left of the line  $B_u - B_b$  in position *a* has moved to the right of the line  $B_u - B_b$  in position *b*. For simplicity's sake the fibres on the left are thought to be perfectly stretched in this position. The deformation of form of the cross-section will also cause displacement of material across the line  $A_u - A_b$ . In proportion as the structure of the nucleus becomes more compact in the sense that resistance against deformation increases, the influence of the

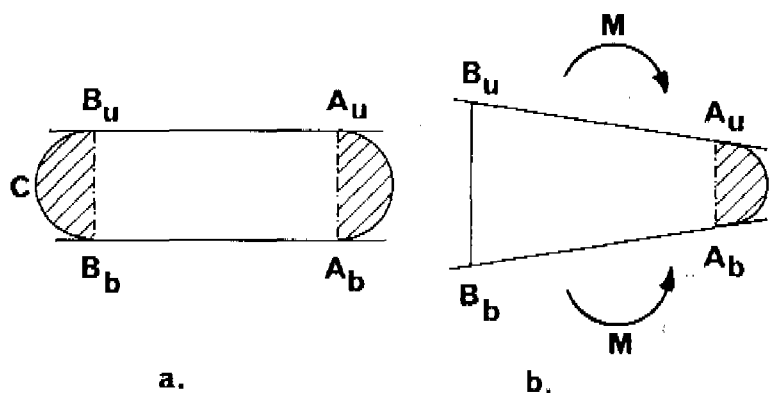


Fig. 4.4.1 See text for explanation

active shear-stresses in the nucleus material, generated by the displacement of this material, will manifest itself more and more in the form of friction, and possibly in a certain degree of sliding, in the plane where contact is made with the cartilaginous plates. Our first assumption is that this occurs in reality, which leads to our next assumption that the phenomenon results in wear and tear of the endplates. In the latter last sentence "wear and tear" might be better replaced by: "a certain reaction of the subchondral bone".

In the hip-joint wear and tear leads in the long run to sclerosis of the subchondral joint tissue. Sclerotic tissue has a better absorption capacity for X-rays which manifests itself in X-ray pictures in spots shaded distinctly lighter than the reproductions of nearly equal masses of similar tissue.

Our third assumption is now that intensive friction and possible sliding of the nucleus along the cartilaginous plates induces sclerosis.

The discs in which this phenomenon has its strongest effect are:

- (1) The discs of which the cartilaginous plates are most parallel. In fact, the diminution of the section  $B_u - C - B_b$  of the cross-section is maximum at the beginning of the rotation (Fig. 4.4.1).
- (2) The discs in which the moment to be transferred alters its sign most frequently (e.g. while walking), in other words, where from a certain aspect the curve is alternatively convex and concave. It could be said that on such spots the

nucleus material *shoots hither and thither* ("Der Nucleus rollt und quillt in dem Faserwerk der Zwischenwirbelscheibe hin und her" (15)).

In order to give ground to our hypothesis we have investigated total X-ray pictures as to "lightshaded spots".

The files of a certain clinic contained 28 laterally taken X-ray pictures of the thoracolumbar spine of as many patients in natural standing posture.

In each of three of these *only one* disc showed lightshaded spots by the cartilaginous plates, and that on the spot where the nucleus pulposus may be expected. We especially ascertained that the spots had not been caused by the projection of ribs. The spots were found in the discs Th 9-10, Th 10-11 and Th 11-12, which, after description of form of the line through the geometrical centres of the vertebrae and intervertebral discs, appeared to be the first, second or third disc above the bending point in the centre line of the lateral projection (table 4.4.1).

age	sex	disc with sclerosis	bending point in centre line of lateral X-ray picture	nearest bending point(s) in centre line of A-P X-ray picture	straightest point in three dim. curve
40	m	Th 10 - 11	Th 11 - 12	Th 11 - 12	Th 11 - 12
43	m	Th 10 - 11	Th 12 - L1	Th 12 - L1	Th 10 - 11
56	m	Th 9 - 10	Th 12 - L1	Th 7 - 8 Th 9 - 10 Th 12 - L1	Th 12 - L1

Table 4.4.1

*Three cases with ONLY ONE disc showing lightshaded spots at the cartilaginous plates. The fact that only men are concerned here is a coincidence, because we selected X-ray-pictures with only one disc showing the phenomenon.*

The phenomenon being basically omnilateral, three dimensional descriptions of form were made, because in all cases a slight curvature was shown in the available A-P projections, which is normal. In all cases investigated the disc with the lightshaded spot was situated in the straight part of the spatial curve. In addition of this, it was observed that the spots occur more in the upper part of the area which may be considered almost straight. As a consequence, the new aspect arose that the axial

rotations also have some influence on the phenomenon. According to Gregerson (14) the maximum axial rotations between successive vertebrae during walking were indeed found at the level of Th7.

The fact that the phenomenon is ascribed by us mainly to movements during walking indicates that the consideration about the straight part of the spine in natural erect posture is not entirely correct. However, we assume that the form of the spine in natural erect posture does not differ essentially from that during walking.

Although the above observations fit remarkably well in with our reasoning, it should be noted that the lightshaded spots are coupled with local undulations in the cartilaginous plates, which increases the number of unknown factors. However, in the following observation this need not be taken into account.

Fig. 4.4.2 shows the X-ray picture of an autopsy specimen, male, aged 31. All the discs are perfectly sound and possess straight cartilaginous plates. Only with the cartilaginous plates of the discs Th 8-9, Th9-10, Th10-11 and Th11-12, appear very distinctly lightshaded stains by the spots where there is contact with the nucleus pulposus.

Here investigation of microscopic slides showed indeed a highly increased compactness of bony tissue adjoining the cartilaginous plates. Only the bottommost cartilaginous plate of Th8 showed a small local undulation (Schmorl's Node). (Verified by the Division of Pathological Anatomy of the Academic Radboud Hospital at Nijmegen).

On the ground of our descriptions of form we may assume that during life also in this spine the above discs were positioned near or in the straightest part of the spine.

An important point in our reasoning is that the discs predisposed to this phenomenon are those in which the moment to be transferred changes its sign most frequently, i.e. what is called unstable equilibrium is concerned. An analogy of such instability is found with those hip-joints where the vertical through the centre of gravity intersects the axis through the centres of the heads of the femura. Exactly and exclusively in these cases Gutmann (16) found coxarthrosis (cases with a horizontal

---

Fig. 4.4.2 *Autopsy specimen, male, aged 31.*  
*Visible are the discs L3-4 up to Th7-8.*





Fig. 4.4.2

pelvis, defined by an angle of inclination between the border-line of the first and the second sacral vertebra and the horizontal smaller than 30 degrees).

We think that with the preceding observations we have furnished a foundation for our hypothesis, though, indeed, we have only broadly described it. We admit that this foundation was born from circumstantial evidence, which from a scientific point of view does not supply a rigid proof.

Remark: If this wear-and-tear mechanism is a reality, we may conclude that it refers to any human spine. In this connection we mention that Fig. 4.4.2 shows one of the only two autopsy specimens investigated by us.

#### 4.4.2. Wear and tear of the annulus fibrosus

Cailliet (1962) and Galante (1967) give a simple schematic representation of the annulus fibrosus in order to indicate the play of forces in this system of fibres in the case of varying loads exerted on the adjoining vertebral bodies.

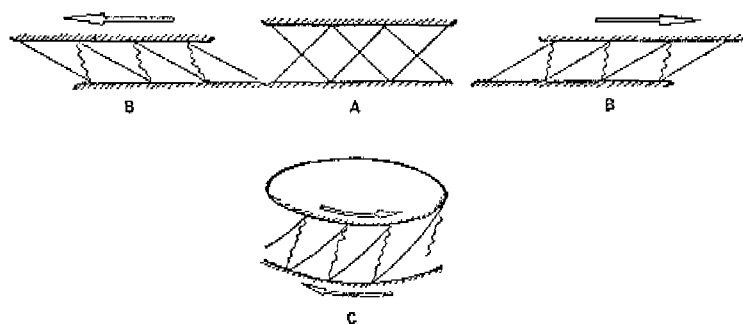
Fig. 4.4.3 represents the model designed by Cailliet; Galante's model is fundamentally identical. The annulus fibrosus is represented by a layer of crossed fibres.

In the following we make use of the above schematic representations in order to make an effort to offer an explanation of a result of loading tests on vertebral bodies carried out by Brown, Hansen and Yorra (1957). They describe in what way a vertebral segment is subjected to an alternative bending-moment, while a slight axial force was exerted on the vertebral bodies (Fig. 4.4.4).

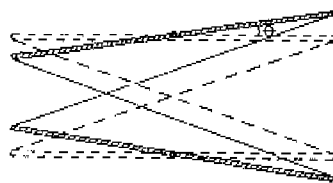
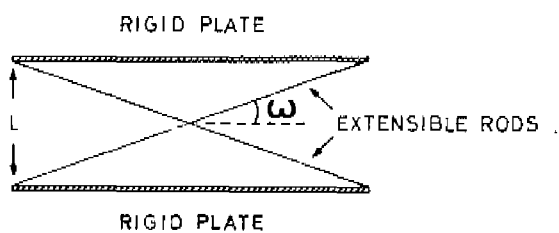
The angular rotation of the vertebral bodies was 5 degrees, the frequency 1100 cycles per minute.

It is reported that after 1000 cycles the disc broke in a plane parallel with and positioned in about the centre of the distance between the cartilaginous plates. After studying sagittal sections (Fig. 4.4.5) it appeared that all annulus fibres were broken. Only the peripheral layer fusing with the periosteum at the sides of the vertebral bodies and with the ligamentum anterior and posterior, a layer thinner than 0.32 mm remained intact. (It should be noted that the fibres of the ligamentum longitudinalis posterior and of the ligamentum longitudinalis anterior run longitudinally; consequently, the model sketched in Fig. 4.4.3 is *not applicable* to these fibres).

Grossly this tear appeared to be fresh although with respect to



Cailliet's model



ROTATION OF THE TRUSS

Galante's model

Fig. 4.4.3 Schematic model of the fibres of the annulus fibrosus



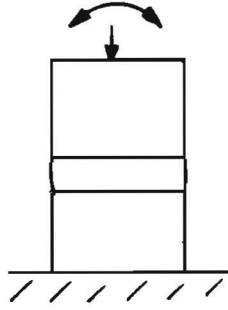


Fig. 4.4.4 *Alternative bending-moment in the case of a slight axial force*

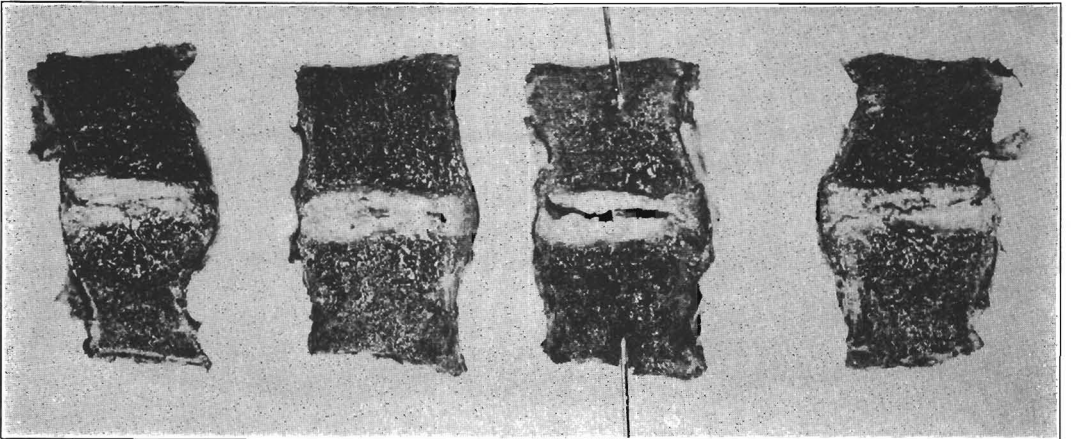


FIG. 46

Sagittal sections of specimen after failure in fatigue test. Note grossly normal appearance of annulus and nucleus pulposus except for the tear approximately midway between the plates. Grossly this tear appeared to be fresh although with respect to its locations and extent it resembled the tears seen in some extensively degenerated discs.

Fig. 4.4.5 *Sagittal sections of a specimen after failure in load-test. Brown, Hansen and Yorra (1957).*

its location and extent it resembled the tears observed in some extensively degenerated discs (Fig. 4.4.6, Güntz). It was said that no explanation of this phenomenon could be offered.

In order to frame a possible explanation of the above phenomenon we consider first Fig. 4.4.7. In state of rest the two crossing fibres have a small common tangent plane.

*b) Zerreiung*



Fig. 4.4.6

*Tears in degenerated disc  
Güntz (15)*

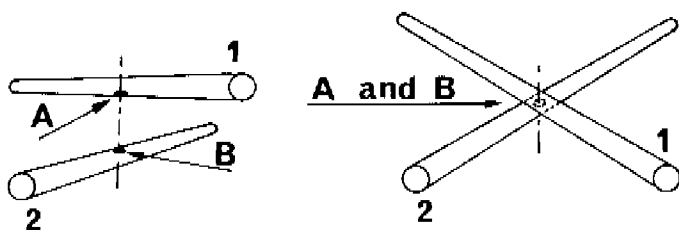


Fig. 4.4.7

*Crossed fibres of the annulus fibrosus with tangent planes A and B*

The small area A of fibre 1 touches the small area B of fibre 2. If we rotate the two adjoining vertebral bodies with respect to each other according to Fig. 4.4.4, A and B will not stay together. That means that the fibres slide along each other in a, in our opinion unfavourable direction because in case the fibres are pressed together as a result of overpressure in the nucleus pulposus, a relatively high surface stress will be created in the (instantaneous) small tangent plane.

It is reasonable to expect that wear arises then in these tangent planes. Furthermore, we start from the thought that such a form of wear and tear will be intensest in those areas of the fibrous layer where the planes comparable with A and B diverge widest in case of angle rotation. At least, the sliding speed will always be maximum there.

The divergency of these planes after angle rotation is taken by us as a measure of wear and tear in what follows.

In Part II - 4.2 the magnitude of the divergency has been described mathematically.

With a mathematical derivation, which is merely based on geometry, we can show that, making allowance for the unit elongation of each part of each fibre separately,

- (1) wear and tear is the same in points of intersection lying on a horizontal line and equidistant from the two vertebrae;
- (2) wear and tear in the netting is heaviest in areas in the middle of the distance between the two vertebrae;
- (3) wear and tear increases approximately linearly as the rotation of the two vertebrae increases;
- (4) wear and tear is greatest in the highest discs;
- (5) wear and tear is greatest where the angle ( $\omega$  in Fig. 4.4.3) between fibres and cartilaginous plate is smallest. In longitudinally arranged fibres this angle is great, viz.  $\omega = 90^\circ$  and here the expression describing this phenomenon becomes zero, which leads to the conclusion that there will be no wear and tear.

Starting from the foregoing reasoning, one can say that this form of wear and tear, if it occurs under physiological circumstances, will be greatest in places in the spine where:

- (1) the angular rotation between adjacent vertebrae is greatest (lumbar area);
- (2) the rotating movements are most frequent;
- (3) the pressure in the space bounded by the netting is heaviest;
- (4) the discs are highest (lumbar area).

Although from Fig. 4.4.6, borrowed from Guntz, it becomes evident that this phenomenon manifests itself under physiolo-

gical circumstances, we repeated the loading test as described before on the discs L3 - 4, Th9 - 10, Th10 - 11 and Th11 - 12 from a fresh autopsy specimen, male, aged 31, with a view to verify this phenomenon at a lower frequency. The angular rotation of the disc L3 - 4 was  $8^{\circ}$  and for the discs Th9 - 10, Th10 - 11 and Th11 - 12 it was  $5^{\circ}$ . For all discs the axial load was 200 N and the frequency 50 cycles per minute.

After 2000 alternations the tests were stopped. Externally nothing remarkable was to be observed. The study of sagittal sections showed that the fibres of the annulus fibrosus situated predominantly inward had given way in accordance with the design described.

The most striking indication was that the fibres heaviest traction loaded, those of the ligamentum longitudinalis Posterior and Anterior and the adjoining parts of the annulus fibrosus did not break but that exactly the annulus fibres in the lateral planes had given way.

Sections of the non-tested disc L1 - 2 of the same spine showed a perfectly sound netting of fibres (Verified by the Division of Pathological Anatomy of the Academic Radboud Hospital at Nijmegen).

#### *Fastening an autopsy specimen*

In order to generate the wear-and-tear phenomenon in an intervertebral disc described before, a simple loading instrument has been developed. In this instrument the bottommost vertebral body of an autopsy specimen is fastened to the earth. The uppermost vertebral body is given an alternating angular rotation, the angle being adjustable with respect to the bottommost vertebral body. The necessary bending moment is effected by a comparatively small transverse force on a long lever.

Moreover a constant axial load can be applied, directed towards approximately the centre of the intervertebral disc in any rotated position of the uppermost vertebral body.

An important provision, also necessary in other loading tests, is the solid fastening of a vertebral body. Fig. 4.4.8 represents a clamp realising a fastening with the property that the angular rotation of the clamp with respect to the cartilaginous plate is amply an order of magnitude smaller than the angular rotation of the cartilaginous plates of the successive vertebral bodies. A quick fastening is realised as follows (see Fig. 4.4.8):

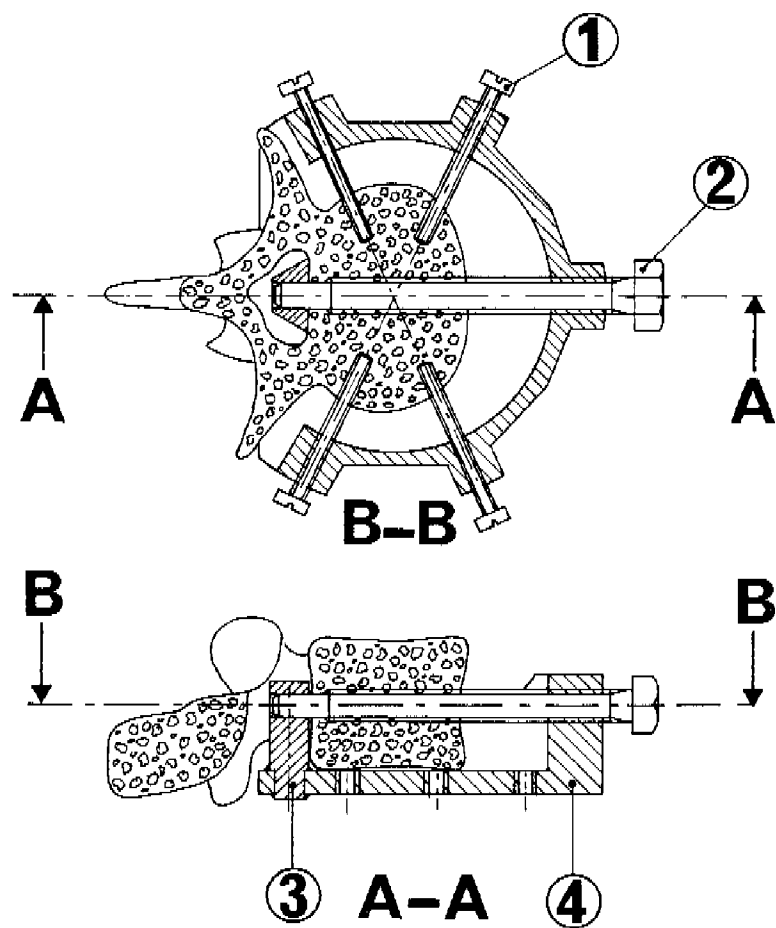


Fig. 4.4.8

4 is a block with a circular recess with a radius of 35 mm to receive a lumbar vertebra. The vertebral body is placed in this recess in such a way that part 3, attached to the block, fits in with the spinal canal. By means of the screws 1 (M3) driven by a pneumatic screw driver, the vertebral body is pressed against 3 and brought in a central position. Before applying bolt 2, a hole has to be drilled in the vertebral body with the help of a twist drill. While doing so, the screw thread in the block (M8) is protected against damage by a small thin-walled bush of hardened steel. After drilling the hole and removing the small bush, bolt 2 is driven on until the end has entered the hole in 3 with a close fitting.

All the parts are of steel and they are chromium-plated in view of thorough cleaning and sterilisation.

## CONCLUSIONS

The subject of the present thesis was inspired by medical scientists. The aim was to find and to describe codifications relative to the mechanical behaviour of the human spine. This object required fundamental research to be carried out. Because it was posited at the same time that the results of the research should constitute a contribution of practical value to medical science, the research was given a distinct direction: It was necessary to head for the development of "tools" in the sense of mathematical expedients as well as in the sense of apparatus. A further requirement was that in further research these tools could be manipulated by medical scientists in relation to problems which the nature of the profession would mainly place in the field of pathology.

In the thesis the form of the spine is the centre of attention. In view of the definition of what has to be understood to be the form of the human spine reference has been made to medical literature. The form of the spine is understood to be the fluent line on which lie the geometrical centres of the vertebral bodies and the intervertebral discs. This definition is sensible because it fits in with the human imaginative faculty and is also practical because the geometrical centres can be determined fairly accurately in X-ray pictures.

A far-reaching restriction is made by considering exclusively that situation which is characterized by a tension in the dorsal muscles and an intra-abdominal pressure, both of which may be considered small if not negligible. Of all the extremely compli-

cated loading situations this is the least complicated. Moreover a dominating influence may now be ascribed to the load originating from the force of gravitation.

The natural erect posture and the relaxed sitting posture occurring frequently in everyday life, comply with these criteria. It should be remarked that these postures occupy an important place in diagnosis of dorsal complaints. It may even be expected that faults in statics resulting from the modern pattern of life, are becoming more and more important factors in the generation of vertebranic diseases.

Chapter I shows that it is possible to characterize the form of the kyphose-sacrum area by means of a comparatively small number of parameters by applying a mathematical formula with the help of a digital computer. This area was chosen because in the case of dorsal complaints X-ray pictures are generally made of this region.

The intention is to carry out statistical research with the "tool" thus obtained aiming at finding a relation between form and clinical picture. Only after investigating a great number of persons will it appear whether this is realisable. However, for several reasons we cherish good hopes:

- (1) Various investigations based on geometrical data characterizing only the form of the spine to a very restricted limit procured positive results. The motive for these investigations was the conviction that an unfavourable form, seen as being inherent to an unfavourable loading situation, will lead to complaints sooner.
- (2) In addition to the fact that the method applied by us determines numerically the form of a great part of the spine, we can simply calculate the curvatures in the form of the spine. The two parameters handled for description of form, adapted to the individual, are already a measure of the curvatures at the extremities of the kyphose-sacrum area. Because in most cases it suffices in applied mechanics to judge the strength and the stiffness of a relatively long rod exclusively by the bending moment, it is plausible that exactly this judgement is of great importance to the spine. The want of a method enabling the calculation of curvatures has been expressed several times in medical literature (5) (20) (34), because it is known that also in the spine the curvature increases with increasing bending moment.

On the ground of this relation we give an exposition regarding the loading of the spine in natural standing posture, attributing special significance to the M.ilio-*psaos*.

In chapter 1.3 of Part II we go further into the analogy between the spine and a rod of technical material in order to indicate next in what way we expect to obtain further information on load and flexural rigidity of the kyphose-sacrum area in the living. Since the human body is highly inaccessible to a direct and accurate determination of the manifold information required, we will have to be satisfied with more or less rough approximations. Nevertheless, we do not consider it impossible that on the ground of the results of the first few steps taken in this direction practically manageable data may be obtained in spite of the approximations.

Chapter 2 discusses the dorsal contour of the spine. That its form is characterized by the centre line of the vertebral bodies is obvious. To what degree a systematic and at the same time mathematically definable connection exists between these two lines is an object of further research. Consequently, for the time being we consider the research of the dorsal contour as an individual research.

The first "tool" developed for this purpose is a recorder with which the dorsal contour of the spine can be recorded on a strip of paper in an optical way. Accuracy is satisfactory. In this connection special attention has been paid to the steadying of the person to be examined during the measuring time.

The apparatus is specially suitable for the investigation of healthy persons as well as of patients, because in many cases the making of X-ray pictures is not indicated. The number of records to be made of one and the same person is in principle unlimited, so that it is possible to record the contour in various postures and at regularly repeated points of time.

With this "tool" a number of problems were attacked that have the character of movement studies. Three adults in a more or less stable and unconstrained standing posture demonstrated that there can be a considerable distance between the positions of the shoulder when leaning forward and backward respectively.

Determination of the curvatures in the lumbar part of the dorsal contour confirmed what already had been posited in Chapter 1, viz. that the moment exerted around the axis of the hip-joints for equilibrium in standing posture, above all originating from the Ilio-psoas, puts its mark upon the curvatures in the lumbar part of the spine.

The posture lying between that directed extremely forward and that directed extremely backward, the intermediate posture, complies best with the criterion of unconstraint.



With the cooperation of six adults it was investigated to what degree this posture is reproducible, paying special attention to curvatures in the dorsal contour. It proved that the form of the dorsal contour, with special attention to curvatures, can be well reproduced. This conclusion was based on description of form of the entire thoracolumbar area. The formula handled in this connection included four parameters to be adapted by the computer. For the system of coordinates we refer to the connecting line of the points on the skin at the level of Th1 and L5. After ascertaining the reproducibility it was possible to investigate to what degree the form of the spine, weighed against the degree of reproducibility, alters with time. The conclusion with respect to the six adults examined was that during a prolonged period of time no significant alteration was observed.

A third conclusion arising from the research of the intermediate posture is that with a well reproducible form of the dorsal contour the distance between the spine and the vertical through the backs of the heels can show considerable variations.

When it had been ascertained that under normal circumstances the form of the adult spine does not alter appreciably in two years, one record of a healthy woman made before pregnancy and one made after childbirth were compared. The impression is that during pregnancy a strengthening of the lumbar lordosis occurs and that this does not vanish entirely after childbirth. From the comparison made between natural standing postures and loose sitting postures, which also lies in the field of differential diagnosis, has been selected the case of a hypermobile individual, inasmuch as in this case the inversion of the sign of the curvatures in the lumbar area was expressed extremely distinctly. This symptom is called the click-clack phenomenon, because in it is seen an analogy with what occurs while pressing a convex metal lid.

Chapter 3 deals with the three-dimensional form of the human thoracolumbar spine.

Description of the form of the spine in three dimensions is only significant if it concerns scoliosis. The three-dimensional form of the spine is understood to be the fluent line passing through the geometrical centres of the vertebral bodies.

This line is determined mathematically by combining the centre lines as these have been defined on the basis of a lateral and an A-P total X-ray picture. Of this line can be made a top-view by which is obtained a distinct impression of the form of the spine when looking in the direction of gravitation. We give a top-view of five spines in which highly interesting patterns can be per-

ceived. As it is common knowledge that in a spatially curved spine axial rotations occur, we tried, starting from nothing else but the spatial curve, to realise a "tool" with which the trend of the axial rotations could be calculated.

The mathematical measure wanted for this was based on the curvatures in the spatial centre line of the spine complying with the condition that the mathematical measure receives the magnitude zero when in the frontal projection the spine is perfectly straight. On the ground of five essentially different cases it has been proved that not only the trend calculated corresponds well with the one that could be measured in the A-P X-ray picture, but that even the mathematical measure, multiplied by a factor to be adapted to each individual, gives a good impression of the real magnitude of the axial rotations in the spine. When determining the real rotations occurring in the spine, we were handicapped by the incertitude as to the position of the centres of axial rotation. In the literature we found similar data about the positions at the level Th5-6 and in the lumbar area. After adapting the multiplying factor for the mathematical measure to these two levels, it appeared that the remarkable trend of the position of the remaining centres of axial rotation, calculated with this multiplying factor, corresponded remarkably well with those indicated for the thoracal area in the literature.

After obtaining a good mathematical measure of the axial rotations in the spine, we were able to try to get an impression of the force phenomena that play a dominating role in the formation of the axial rotations, i.e. in the origin of the spatial curve. We started from the fact given in literature that a linear connection exists between axial rotation and moment of torsion. For an impression of the great number of unknown factors that handicapped us, we refer the reader to chapter 3.4. In spite of this impediment it became evident that after estimating the force derived from the weight of head, neck, arms and shoulder girdle, in three cases the values of the average torsional rigidity of the thoracolumbar spine calculated appeared to be of the same order of magnitude, and that these values also appeared to be of the order of magnitude of the torsional rigidity determined on autopsy specimens as are to be found in the literature. On account of these results we believe that after introducing refinements in this method - we would suggest differential methods - a calculating tool may be obtained which will contribute to a better understanding of scoliosis and its treatment.

Chapter 4 concerns the essential component in our mechanical model of the entire spine: a segment disc-vertebra-disc.

Knowledge of the mechanical behaviour of such a segment is essential for a sensible modelling process of the whole spine. From the data in the literature it appears that the rigidity of a vertebral body exceeds that of a disc by an order of magnitude and that the reduction of altitude of the disc in case of axial load is very minute. On the ground of this a dominating role may be ascribed to the bending moment and the torsion moment when studying the alteration of form of the spine, which is also common when considering an elastic rod in Applied Mechanics. The linear connection between bending moment and rotation, determined on an autopsy specimen, as well as the linear connection between torsion moment and axial rotation induced us to apply it also to our calculations. Although this linear connection led to a considerable simplification, it should be remarked that a non-linear connection, provided it is fixed mathematically, may be taken into the same calculations. As to the position of the (instantaneous) centres of rotation during bending, no corresponding data were found. However, on the ground of the works of several authors it may be assumed that the distance from these centres of rotation to the centre line of the vertebral bodies and of the intervertebral discs will not exceed more than 20% of the diameter of the vertebral body, so that calculations based on the centre line may be considered fair approximations. Because of observation of trends in the displacement of the centres of rotation when bending autopsy specimens, we further assume that the calculations derived from the centre line will show deviations of a systematical nature. On the ground of the literature and of our own observations it may be expected that the centres of axial rotation could be remote from the centre line and that for this reason the torsional rigidity may be very different at various levels of the spine. A certain system may also be observed in the positioning of these centres of rotation. No data were found by us concerning the influence of the transverse force on the alteration of form of a vertebral segment. However, we assume that when considering the alteration of form of the spine, the influence of the transverse force is a secondary consideration inasmuch as the transverse force can be intercepted to a high degree by the bony tissue of the intervertebral joints.

In view of a mathematical description (not yet achieved) of the mechanical behaviour of a vertebra-disc-vertebra segment, a schematic model of such a motion segment has been introduced. Greatly interested in the bending moment, we did not, for sim-

plicity, include the posterior elements in this model because we consider the function of the intervertebral disc dominating and most interesting. With the help of the model an exposition is given concerning hernia nuclei pulposi.

In this chapter the results are given of a loading test on an autopsy specimen. On the basis of these results it could be ascertained that a loss of initial flexural rigidity is to be observed with spondylosis deformans. The aim of the loading test was, in fact, to get an impression of the flexural rigidity of the spine with respect to the spine length. In ventro-flexion the initial flexural rigidity appeared to be comparable with that of a solid steel rod the round cross-section of which has a diameter of approx. 4 mm. Since the consequences of the bending moment will not be expressed only in static loading but also in dynamic loading, we searched for a wear-and-tear mechanism resulting from frequent alteration of the bending moment. We believe we have succeeded in finding two wear-and-tear mechanisms.

According to our hypothesis the first manifests itself in sclerosis at the cartilaginous plates. We expect this to occur in the straightmost part of the spine. The phenomenon is seen by us mainly as a consequence of walking.

The second wear-and-tear mechanism, manifesting itself by rupture of annulus fibres, is especially expected by us to take place in the lumbar part of the spine.

The hypotheses of both wear-and-tear phenomena are supported mathematically.

## PART II

### TECHNICAL AND MATHEMATICAL BACKGROUNDS OF PART I

## Description of the form of a bent rod loaded at its extremities

### 1.1 Origin of the formula with a minimum number of parameters

Starting from a certain analogy in mechanical behaviour between spine and an elastic rod of technical material, the highly simplified model of load shown in Fig. 1.1. has been arranged to find a formula with a minimum number of parameters in view of the kyphose-sacrum area.

On the spot  $x = 0$ , which with reference to the spine is the most dorsal point of the kyphosis, the rod is clamped in such a way that the  $x$ -axis is there tangent to the axis of the rod.

On the spot  $x = L$  a hinge is thought in which can be introduced a moment. With regard to the spine, rotation around the hinge is thought to be effected by the tilting of the pelvis in combination with movement in the ilio-sacral joint, the provocative moment arising by tension in ligaments and muscles, generating a moment around the hip joints. Regarding, furthermore, the spine in unconstrained erect posture exclusively loaded by the force of gravitation, no horizontal forces will have to be incorporated in the model. After assuming that the self-weight of this part of the spine is of secondary importance, the equilibrium of the model is determined by  $F_A = F_L$  and  $M_A + M_L = F_A \cdot R$ . With increasing  $R$  the moments and, consequently, the curvatures of the axis of the rod will increase too. This trend was already encountered when studying contour pictures of one and the same person (See Part I, Fig. 2.3).

With this model in view a method from Applied Mechanics has been applied by which the bent form of a rod loaded in an analogous way is approximated by what are called "trial functions", satisfying the conditions at the extremities.

This procedure is used in the method of Rayleigh (38) and is intended to calculate by approximation the critical load of buckling.

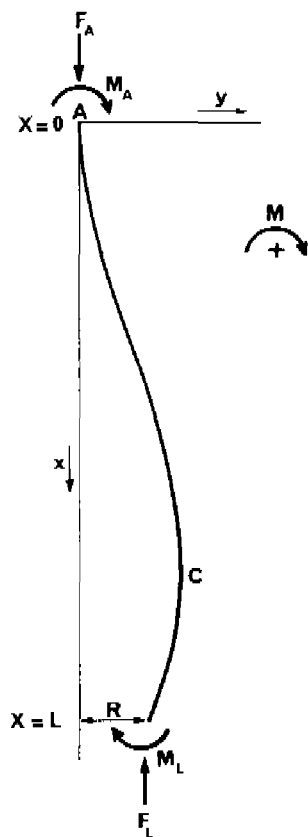


Fig. 1.1 *The axis of a rod loaded at its extremities*

Relative to our model the conditions at the extremities are:

$$(1) \quad x = 0 \quad y = 0$$

$$(2) \quad x = 0 \quad \frac{dy}{dx} = 0$$

$$(3) \quad x = L \quad y = R$$

with neglect of  $\frac{dy}{dx}$ : (4)  $x = L \quad \frac{d^2y}{dx^2} = -\frac{M}{EI} = m$

$E$  = modulus of elasticity of the material of the rod

$I$  = second moment of area about the axis of bending

The quotient  $EI$  is measure of the flexural rigidity of the rod.

By taking as a "trial function" the expression:

$$y = Cx^3 + Ax^2 + Bx + D + E \sin \frac{\pi x}{L}$$

the formula (Part. I - 1.2.1) will be found after substitution of the boundary conditions.

This formula is one of eight formulae of equal simplicity in

which have been used combinations of  $\sin \frac{\pi x}{L}$ ,  $\cos \frac{\pi x}{L}$ ,  $\sin \frac{2\pi x}{L}$ ,  $\cos \frac{2\pi x}{L}$ ,

and terms of a polynomial. These formulae have been applied separately to the form of the spine as visible in X-ray pictures and recordings of the dorsal contour of the spine.

It appeared that formula (Part I - 1.2.1.) met the requirements best, which was determined by comparing with each other the sums of the squares of the deviations of the measured and of the calculated values of  $y$ . A trial has been made to select from a function having a large number of terms and applied to forms of all categories, those terms with the most important part in the description of form. This trial has been stopped because the computer, now having a great number of possibilities, procured an adaptation to the points measured, which was an order of magnitude smaller than the measuring error. But the forms obtained through this adaptation showed more undulations than was expected, which excluded a sensible description.



The same phenomenon appeared when applying the function derived from the differential equation of the elastic line (see (44), page 51). In this function the term  $\sin \sqrt{\frac{F}{EI}} x = \sin kx$  appears to which the parameter  $k$ , de facto measure of the argument of sinus, could be adapted by the computer to the points measured, but which produced far too small arguments and, consequently, fluctuations in the forms procured.

The "trial function" itself procures only a play with forms and in doing so the parameters possess only geometrical significance. However, when an elastic rod of technical material is concerned, it can be simply derived from the known relation between bending moment and curvature that the parameter  $m$  is a measure of the moment exerted on the bottommost point of the rod.

It is also applicable to the chosen formula that  $\frac{d^2y}{dx^2} = 2A$  at  $x=0$ , so that  $2A$  is measure of the bending moment at  $x=0$ . If we posit  $m=0$  and  $R=0$ , the "trial function" becomes:

$$y = -\frac{A}{3L}x^3 + Ax^2 - \frac{2AL}{3}x + \frac{2AL^2}{3\pi} \sin \frac{\pi x}{L} \quad (1.1.1.) \text{ of which}$$

$$\frac{dy}{dx} = -\frac{A}{L}x^2 + 2Ax - \frac{2AL}{3} + \frac{2AL}{3} \cos \frac{\pi x}{L} \quad (1.1.2.) \text{ and}$$

$$\frac{d^2y}{dx^2} = -\frac{2A}{L}x + 2A - \frac{2A\pi}{3} \sin \frac{\pi x}{L} \quad (1.1.3.)$$

*Formula (1.1.1.) applied to the calculation of the critical force of buckling.*

According to Rayleigh's approximation method the critical force of buckling ( $F_c$ ) is calculated with Rayleigh's quotient:

$$F_c = EI \frac{\int_0^L \left(\frac{d^2y}{dx^2}\right)^2 dx}{\int_0^L \left(\frac{dy}{dx}\right)^2 dx} \quad (1.1.4.)$$

After substituting (1.1.2.) and (1.1.3.) in (1.1.4.) and after elaborating the integrals we find

$$F_C = \frac{\left(\frac{2\pi^2}{9} - \frac{4}{3}\right) A^2 L}{\left(\frac{14}{45} - \frac{8}{3\pi^2}\right) A^2 L^3} EI = 21.0137 \frac{EI}{L^2} \quad (1.1.6.)$$

For the loading situation under consideration Euler's Column Formula gives:

$$F_C = \frac{9\pi^2}{4} \cdot \frac{EI}{L^2} = 22.206 \frac{EI}{L^2} \quad (1.1.7.)$$

The difference between (1.1.6.) and (1.1.7.) is 5.37% of (1.1.7.).

Formula (1.1.1.) possesses with good approximation the feature that the area AC shows the symmetry around the bending point previously described in Part I - 1.4., which is determined as follows:

On the spot  $x_W$  holds  $\frac{d^2y}{dx^2} = 0$ , on the spots  $x_A$  and  $x_C$  holds  $\frac{dy}{dx} = 0$ .

By substituting  $\frac{dy}{dx} = 0$  in (1.1.2.) and after writing  $\cos \frac{\pi x}{L}$  in the form of a progression, we find:

$$-\frac{A}{L}x^2 + 2Ax - \frac{2AL}{3} + \frac{2AL}{3} \left(1 - \frac{\pi^2 x^2}{2L^2} + \dots\right) = 0$$

Elaborated furthermore this results in:

$$\left(\frac{1}{2L} + \frac{\pi^2}{6L}\right)x^2 - x = 0$$

which yields that  $\frac{dy}{dx} = 0$  with

$$x = 0 \quad \text{and} \quad x = \frac{2}{\frac{1}{L} + \frac{\pi^2}{3L}} \quad (\text{independent of } A) \quad (1.1.8.)$$

Substituting  $\frac{d^2y}{dx^2} = 0$  in (1.1.3.) and writing  $\sin \frac{\pi x}{L}$  in the form of a progression, we find:

$$-\frac{2A}{L}x + 2A - \frac{2A\pi}{3} \left(\frac{\pi x}{L} - \dots\right) = 0$$

Further elaboration results in

$$\left(\frac{1}{L} + \frac{\pi^2}{3L}\right) x - 1 = 0$$

from which it follows that  $\frac{d^2 y}{dx^2} = 0$  at

$$x = \frac{1}{\left(\frac{1}{L} + \frac{\pi^2}{3L}\right)} \quad (1.1.9.)$$

Comparison of (1.1.8.) and (1.1.9.) shows that when neglecting higher terms in the progressions  $x_C = 2 x_W$ .

After substituting (1.1.8.) and (1.1.9.) in (1.1.1.), to which primarily  $\sin \frac{\pi x}{L}$  has been written as a progression, we find that also is valid  $y_C = 2 y_W$ .

If  $m$  and  $R$  are not zero, it can for the entire formula Part I - 1.2.1. be proved in the same approximative way that  $x_C = 2 x_W$  and  $y_C = 2 y_W$  in the case of the combination of the parameters being such that

$$\frac{2A}{3} + \frac{m}{6} - \frac{R}{L^2} = 0$$

## 1.2. Load test on an elastic rod.

In connection with the bent rod shown in Fig. 1.3 an accurate measuring instrument has been designed with which a rod of technical material as well as an autopsy specimen of the spine can be loaded in an analogous way.

The assembly drawing of this instrument is shown in Fig. 1.4. and the principle is described with the help of Fig. 1.2. At A the rod is clamped perpendicularly to the horizontal beam B. The vertical steel strips D, 0.2 mm in thickness, are attached at the extremities  $C_1$  and  $C_r$  of the beam. At E the rod is attached to a hinge that on the one hand can be moved in the horizontal direction in respect of support S in order to reach a distance  $R$  to the vertical through A, and in which, on the other hand, a bending moment ( $M_L$ ) can be exerted on the rod. By displacing the hinge upward in respect of the earth (shaded thus: //) by means of a screwed spindle, the rod will receive a heavier load because the horizontal beam B is attached to the earth by the strips D, supported in G, in which pure tractive forces are generated.

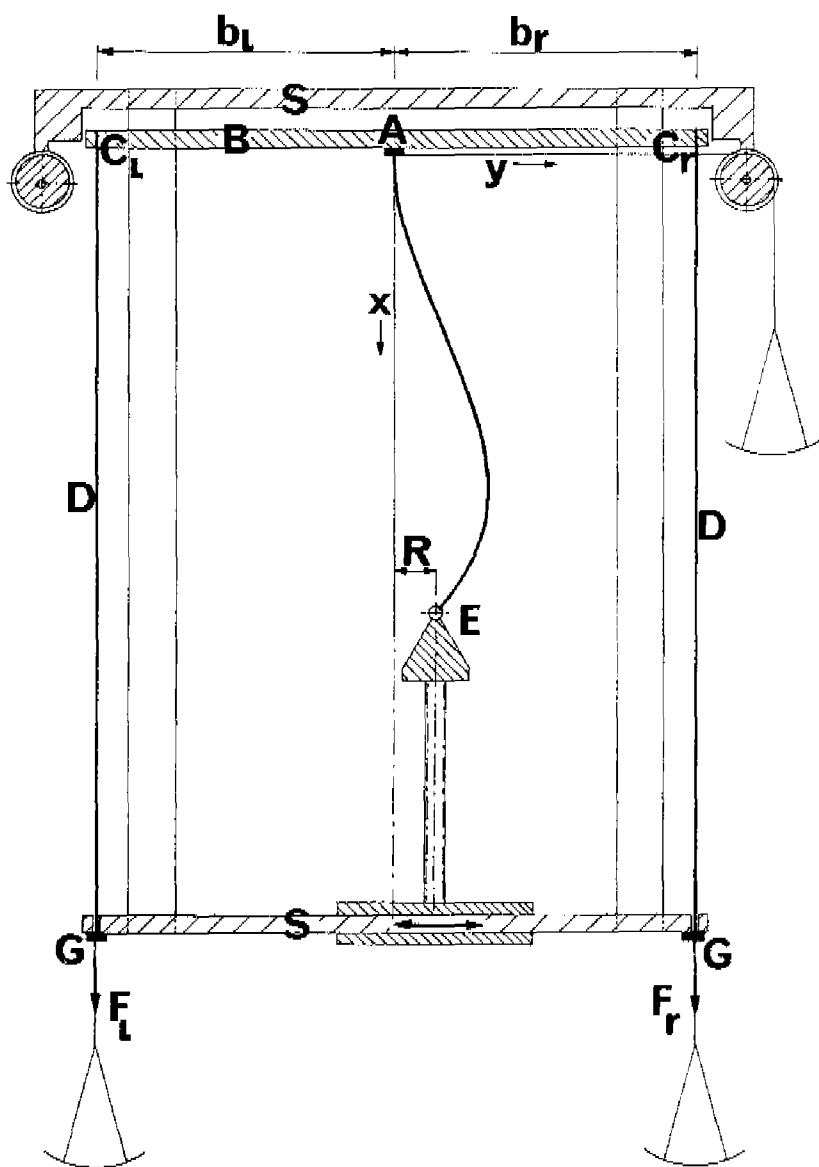


Fig. 1.2.

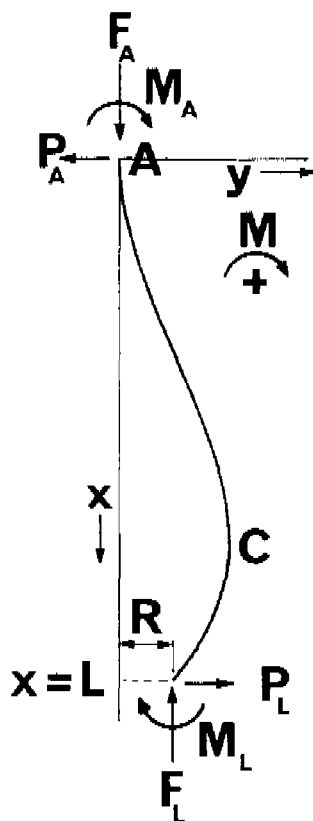


Fig. 1.3.

In any load condition (Fig. 1.3) the equilibrium of the rod in the plane of the drawing is given by:

$$P_A = P_L, F_A = F_L \text{ and } M_A + M_L - F_A R - P_A L = 0$$

The solution to these three equations with eight unknowns requires the measurement of five quantities. Measuring  $L$  and  $R$  is simple.

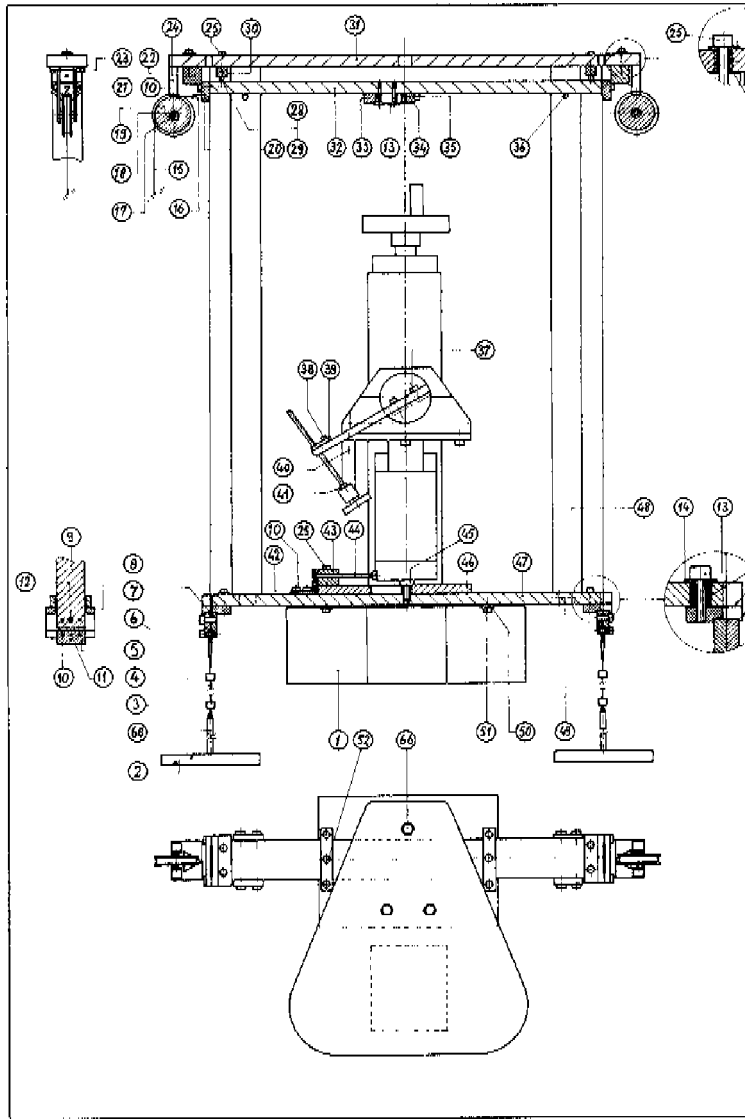
By measuring  $F_L$  and  $F_R$  both  $F_A$  and  $M_A$  will be known, since  $b_L$  and  $b_R$  are accurately determined. The measuring of  $M_L$  being rather complicated because, among other reasons, the hinge has to be designed friction free in this case, preference was given to measuring  $P_A$ . The forces  $F_L$ ,  $F_R$  and  $P_A$  can be measured simply with the help of force meters. In this respect force meters provided with strain gauges should be preferred in order that only small displacements appear under the influence of the load. However, in view of the static nature of this measurement, force measuring with the help of weights was chosen on account of the ease of transportability, simple attendance, constant availability of the measuring instrument, costs and accuracy.

When  $C_L$  touches the earth by a force  $P_A$  this force can be determined as follows:

to the wire fixed at  $A$ , which runs over a pulley with negligible friction in the bearings, is attached a pan on which weights can be placed.

By the adding of weights the moment arises at which the beam will be released at  $C_L$  and will touch at  $C_R$ . Whether the beam touches or not can be ascertained by designing  $C_L$  and  $C_R$  as electrical contacts to which a low voltage is applied. It appeared satisfactory when the beam  $B$  moved over a clearance of 0.19 mm. In the central position, when no contact is made on either side,  $P_A$  is known (the disadvantage of the method is that the force has to be determined by iteration). The above provision makes it possible to adjust  $P_A$  at the magnitude zero by increasing the moment  $M_L$  by means of a screw until neither contact is closed. The forces  $F_L$  and  $F_R$  are determined in an analogous way by means of weights. The rigidity of the entire construction is such that the elastic deformations are negligibly small with respect to those present in the loaded specimen.

Returning to the formula (Part I - 1.2.1) we tried to demonstrate that, in addition to correct adaptation of the formula to the coordinates of a bent rod, according to Fig. 1.3., it is also possible to draw conclusions with respect to the bending moments existing in the rod, starting from the curvatures calculated by the







computer. To this effect a load test has been carried out on a calibrated strip of springsteel,  $1.97 \pm 0.005$  mm in thickness and  $7.70 \pm 0.005$  mm in width, straight without load, by means of which even fairly great curvatures beneath the limit of elasticity could be obtained (43). With the modulus of elasticity indicated for this material, viz.

$E = 2.059 \cdot 10^5$  N/mm<sup>2</sup>, and the second moment of area about the axis of bending  $I = 4.91 \pm 0.05$  mm<sup>4</sup>, the flexural rigidity  $EI = 10.1 \cdot 10^5$  N mm<sup>2</sup>.

The following data of the instrument were determined:

$b_l = 198.2 \pm 0.1$  mm

$b_r = 201.9 \pm 0.1$  mm

The beam B is balanced around A and its weight is  $16.9973 \pm 6 \cdot 10^{-4}$  N.

The pan belonging to  $F_l$  has a weight of  $6.5535 \pm 2 \cdot 10^{-4}$  N.

The pan belonging to  $F_r$  has a weight of  $6.4848 \pm 2 \cdot 10^{-4}$  N.

The force measurements in view of which  $P_A$  has been *adjusted at zero*, produced the values of  $F_A$  and  $M_A$  given in table 1.1. The inexactitude in  $F_l$  and  $F_r$  has mainly to be attributed to hysteresis, which, however, did not exceed 0.2 N in the load conditions concerned, so that the inexactitude in  $F_A$  may be evaluated at  $\pm 0.4$  N.

For the description of form the coordinates of a number of points lying on the axis of the bent strip were measured with the help of an optical system. The  $x$ -coordinates were measured with a ruler with  $\frac{1}{20}$  vernier which produced a standard deviation in  $x$  of 0.025 mm. The  $y$ -coordinate was composed of two optical measurements, the one referring on the right side and the other on the left side of the strip. A ten times repeated measurement at the same level of  $x$  procured a standard deviation in  $y$  of 0.01 mm.

For each loading situation the curvature  $K$  was calculated at four levels the middle two of which were situated near the bending point in the bent strip:

$$K = \frac{M_A - F_A y}{EI} \quad (1.1.10)$$

After the description of form was carried out by means of formula (Part I - 1.2.1.), the differences between the values of  $y$  measured and those calculated appeared not to exceed 0.07 mm with an average of 0.025 mm, for all 9 points measured.

The curvatures of the curves obtained in this way were calculated and the results for the levels where the difference between the measured and the calculated value of  $y$  was smaller than three times the standard deviation in  $y$  are given in table 1.1. Comparing  $K$  obtained by (1.1.10) with  $K$  obtained by description of form, we can conclude that the differences between the values are in the order of magnitude of the error of measurement. Arrived at this point we may state that the formula used for the description of the kyphose-sacrum area of the human spine can also describe the form of a bent strip in the given load conditions with fair accuracy.

	$F_A$ in N $\pm$ 0.4 N	$M_A$ in Nmm $\pm$ 58 Nmm	$x$	$y$	$K$	$K$
			in mm $\sigma_x = 0.025$ mm	in mm $\sigma_y = 0.01$ mm	obtained with (1.1.10) in $\frac{1}{\text{mm}}$	obtained with description of form in $\frac{1}{\text{mm}}$
load 1	149.16	2716	48.05	3.39	+221.10 <sup>-2</sup>	+219.10 <sup>-2</sup>
			123.05	17.91	+007.10 <sup>-2</sup>	+013.10 <sup>-2</sup>
			148.05	23.56	-076.10 <sup>-2</sup>	-069.10 <sup>-2</sup>
			173.05	28.75	-153.10 <sup>-2</sup>	-162.10 <sup>-2</sup>
load 2	184.75	2746	48.5	3.58	-217.10 <sup>-2</sup>	-225.10 <sup>-2</sup>
			98.5	12.44	-050.10 <sup>-2</sup>	-033.10 <sup>-2</sup>
			123.5	17.63	+044.10 <sup>-2</sup>	+051.10 <sup>-2</sup>
			173.5	26.73	+206.10 <sup>-2</sup>	+207.10 <sup>-2</sup>

Table 1.1

### 1.3. Further research of the curvatures in the kyphose-sacrum area of the spine

Formula Part I - 1.2.1 can be manipulated in the present stage of the research exclusively for description of form, and if it is expected to find significant correlation-coefficients between form and clinical picture, this will suffice. However, a further important significance could be given to these forms, if we could estimate the load and the flexural rigidity which in our opinion have together the greatest influence on the creation of the bent form of the spine. Determining the flexural rigidity is in principle possible by considering the deformations effected by a known additional load. It is premised that the deformation as well as the additional load has to be of sufficient magnitude and that care is taken that the situation does not become unfavourably more complex as, for example, is the case when a relatively great tension in the dorsal muscles arises as a consequence of

reflex mechanisms. We expect that such a differential method can only procure accurate results when all muscle-action has been eliminated artificially. Inasmuch as this cannot be incorporated in the routine of medical practice, we consider it ideal that the estimating of the flexural rigidity as well as of the load situation can be confined to one X-ray picture of the kyphose-sacrum area, made in natural standing posture, and to additional data, such as body weight. Such an estimation then need not have the sence of absolute value for diagnostics, but has to be available for purposes of qualitative comparison. In the following we trace out a way that may lead to the result desired. Starting from the model in Fig. 1.3, in which  $P_A$  is taken zero and the self-weight of the rod is thought to be of a second order, we can draw up the following equation for the equilibrium of moments of the area A - C as indicated in Part I - Fig. 1.4:

$$M_A + M_C - F_A \cdot y_C = 0 \quad (1.1.11)$$

Assuming a linear connection between curvature  $K$  and bending moment, a perfect straightness after unloading, and an equal flexural rigidity for this area in first rough approximation, we obtain with (1.1.11):

$$K_A - K_C - \frac{F_A}{EI} \cdot y_C = 0 \quad (1.1.12)$$

After a description of form which is exact within three times the standard deviation of the measurement of the coordinates,  $K_A$  and  $K_C$  can be calculated (for that matter, for this purpose a formula with more parameters can be taken). With a known  $y_C$ ,  $\frac{F_A}{EI}$  can be calculated.

In Fig. 1.5  $K_A - K_C$  has been plotted against  $y_C$  for 16 X-ray pictures, originating from one clinical hospital and made with a proportion of projection as equal as possible in natural standing posture of patients aged between 10 and 57 years. Already a trend can be seen from which may be derived a certain relation between  $F_A$  and  $EI$ . That the deviations from the regression line are not insignificant is obvious since in our schematic representation  $F_A$  is mainly related to the body-weight and  $EI$  can show important individual differences simply as a result of difference in stage of degeneration of the spine.

Even with the exceptional simple representation of things given in (1.1.12) we still have three unknown magnitudes:  $F_A$ ,  $E$  and  $I$ .

With respect to the magnitude  $E$  it has to be determined what influence on the value of  $E$  is caused by the spine not becoming perfectly straight after unloading. The two autopsy specimens investigated by us showed curvatures that were 2.5 to amply 10 times smaller than found by us on an average on corresponding spots in the area A - C in the persons under consideration. Provisionally we shall assume that this factor exercises a systematic influence on our calculations.

Assuming that on the ground of (37) a connection exists between  $F_A$  and body-weight, a geometrical measure has to be found determining the magnitude of  $I$ . In our opinion we get a

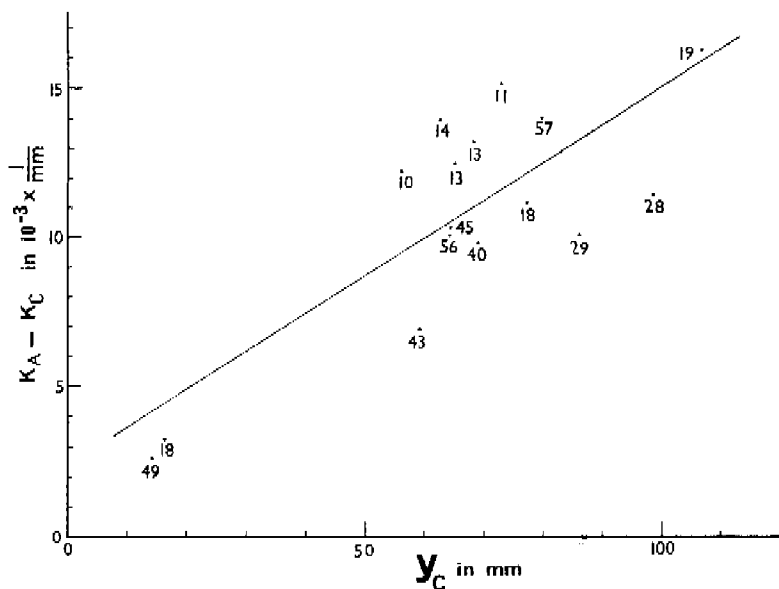


Fig. 1.5 Sum of curvatures at the extremities of the area A - C plotted against the  $y$ -values of C for 16 lateral X-ray pictures. The ages of the persons concerned are indicated near the dots. The straight line is the regression line.

rough impression of  $I$  from the magnitude of  $d^4$ , in which  $d$  is the width of the vertebral body in the sagittal plane. In Fig. 1.6 the measure of  $I$  calculated in this way is plotted against the body-weight, taking  $d_a$  as an average over the area A - C.

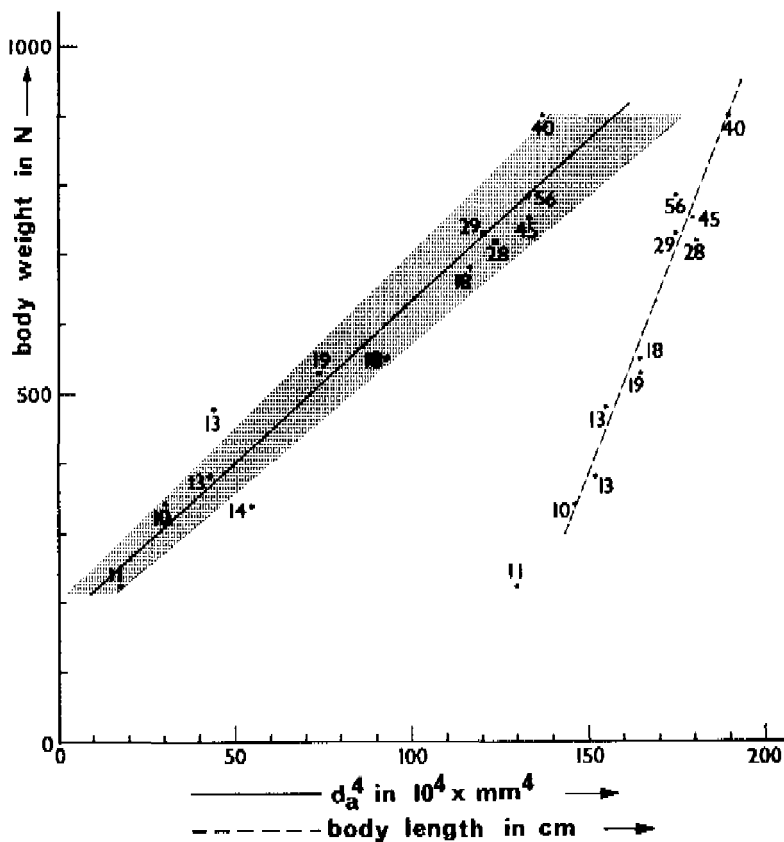


Fig. 1.6 Body weight plotted against the measure of  $I$ ,  $d_a^4$ , the straight line representing the line of regression. The shaded area indicates an error of  $\pm 1$  mm in the determination of  $d_a$  together with a measuring error in the body weight of  $\pm 10$  N ( $\pm 1$  kgf).

For comparison the body weight has been plotted against the body length in the same diagram. Here the dotted line is the line of regression. The ages of the persons concerned are indicated near the dots.

The shaded area around the regression line indicates an estimated error in  $d_a$  of  $\pm 1$  mm caused by distortion resulting from the X-ray projection and an error of measurement on the X-ray picture along with an estimated error in the body weight of  $\pm 10$  N. When taking this into account a remarkable linear trend can be observed, even enabling us to make a rough estimation of the body weight after calculation of  $d_a^4$ .

Remark: When the X-ray pictures were made the body weight and the body length were not measured of all the 16 persons mentioned before.

In order to obtain a rough impression of the order of magnitude of  $F_A$  we calculated the product of  $\frac{F_A}{EI}$  according to (1.1.12) and the average flexural rigidity  $EI_a$  of an autopsy specimen according to Part I - 4.3:

$$F_A = \frac{F_A}{EI} \cdot EI_a \quad (1.1.13)$$

Two persons out of the 16 mentioned above were about the same age, and their corresponding vertebral bodies had about the same diameter, taking into account the proportion of projection. In table 1.2  $F_A$  has been calculated according to (1.1.13) compared to the body weight of the persons involved. The order of magnitude is already as expected when compared with the values of  $F$  in Part I - 3.5 estimated at 23% of the body weight. The fact that the values exceeded 23% is attributed to the consideration that point A is positioned lower than Th1 and that the spine is not perfectly straight in unloaded position, etc.

sex	age	body length	body weight	$F_A$ (1.1.13)	$F_A$ in % of body weight
m	40	189 cm	907 N	288 N	32%
m	45	180 cm	754 N	320 N	43%

Table 1.2

We accentuate that the preceding consideration is only meant to show a way by which it may possibly be determined with the help of one single X-ray picture with additional data as body weight, whether a spine is stiffer or more flexible than the average. Before this is possible, it will be necessary to do a great deal of research and to introduce refinements into the method of calculation.

## Equipment for recording the dorsal contour of the spine

### 2.1. Recording apparatus

#### 2.1.1. Optical system (Fig. 2.1)

The light of a strong lamp (5.5 V - 35 W) is only partially transmitted by a diaphragm in which have been made two slits (height 0,4 mm).

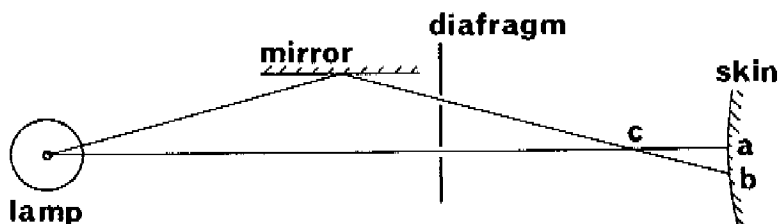


Fig. 2.1 *Optical system*

The portion of light in the horizontal plane hits the skin at "a". Another portion strikes the mirror and after refraction passes through the upper slit so as to hit the skin at "b". The two light beams intersect at "c".

By moving the optical system in the horizontal direction to the right "b" will approach "a". "a" and "b" coincide when "c" hits the surface of the skin. At this moment (to be determined visually) a pencil attached at a fixed distance from point "c" places a dot on the vertically fitted roll of paper (Fig. 2.2.). In actual fact, there are not two slits but two sets of slits, each comprising 7 slits in a row. As a consequence, in Fig. 2.2. "a" and "b" show horizontal dotted lines. This provision is necessary since in cases of scoliosis or oblique posture the measuring must take place over a wide area.

The optical system is transportable on a support in the horizontal direction.



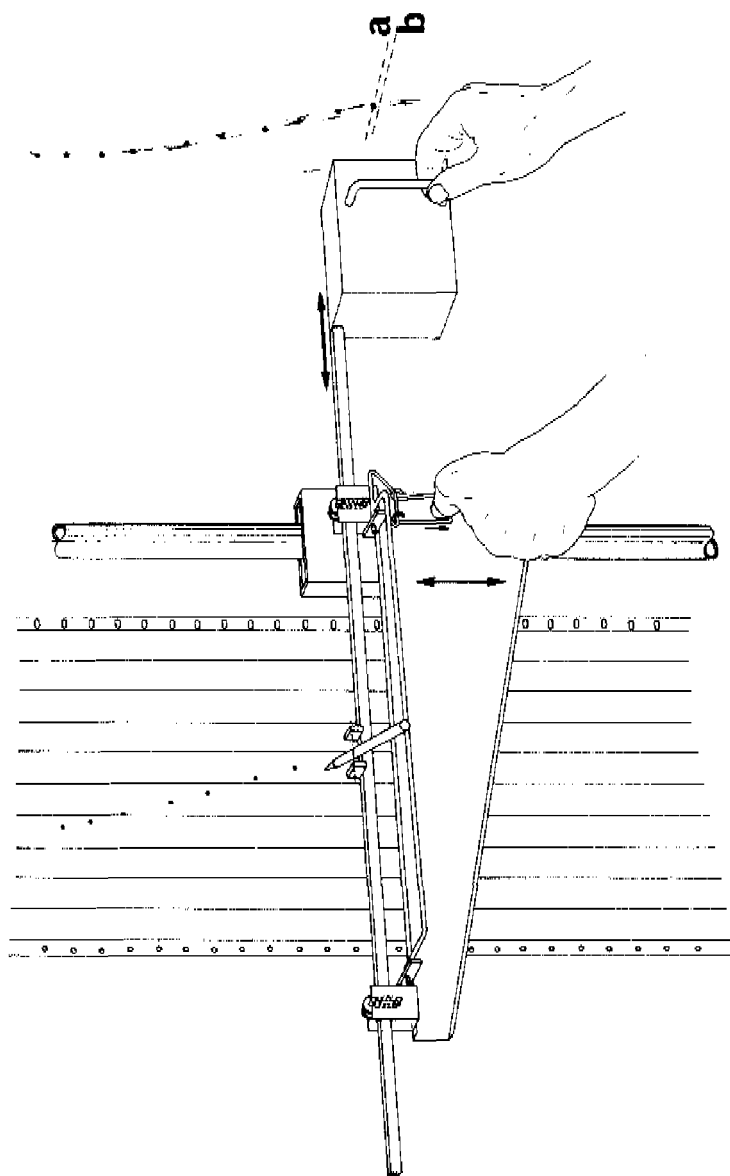


Fig. 2.2. Optical system in horizontal direction transportable on a support

It has been investigated with what degree of accuracy a person could bring the two dotted lines "a" and "b" into one line. By means of a ruler with  $\frac{1}{20}$  vernier the standard deviation with regard to a fixed plane was determined. Series of 10 adjustments each were carried out.

The most inaccurate series gave a standard deviation of 0.1 mm. In view of the purpose aimed at, the optical system may be considered satisfactorily accurate. In order to avoid distortion in width of the dotted lines care has been taken that the surface of the mirror, the two rows of slits in the diaphragm, and the straight thin filament of the lamp run parallel to each other and are perpendicular to the sagittal plane.

### 2.1.2. General information

The lamp of the optical system is connected to a foot operated switch. The optical system is moved in the horizontal direction (Fig. 2.2.) by the right hand. A smooth straight guidance free from slackness and over-indication has been obtained by having the rectangular pipe to which the optical system is fitted, sliding between dust-proof roller bearings, the upper ones of which are pressed by spring force.

The pencil is moved by means of a light lever system operated by the thumb of the left hand. The left hand also transports the support along a vertically mounted pipe, by means of which it is possible to make recordings on various levels. The vertical guidance is also free from slackness and over-indication owing to the provision of two grooved rollers, the grooves being V-shaped (Fig. 2.3.). The centre of gravity of the support lying left from these rollers, the support will be pressed constantly against the pipe. The support is in vertical equilibrium through the tractive force  $G$  in the string originating from a counter weight in the vertical pipe.

The strip of recording paper passes over electrically driven commercially available recorder guiding rollers.

The frame rests on three chocks adjustable in height. It has been designed in such a way that sufficient space is available for the movements of the operator.

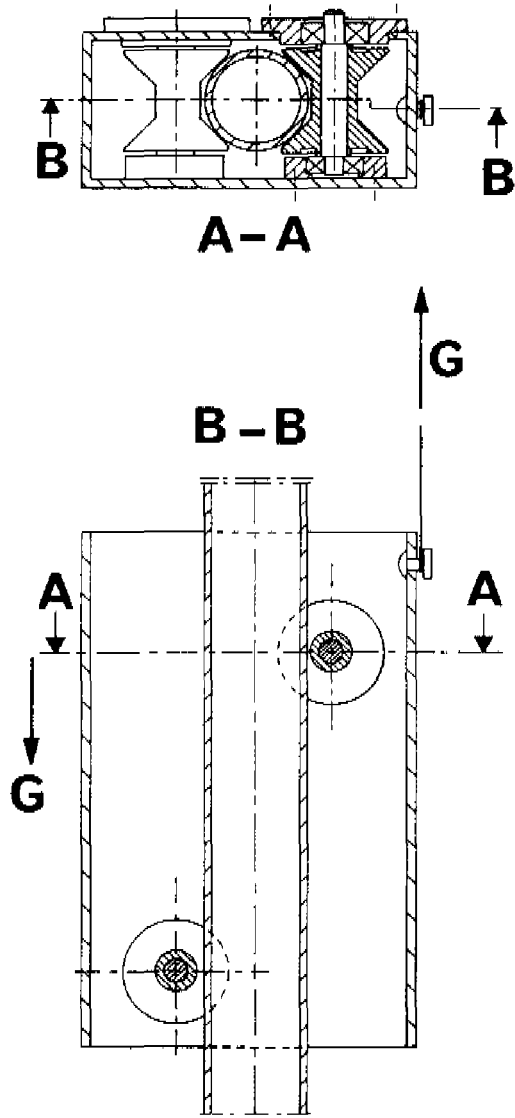


Fig. 2.3 *Guidance of the support*

## 2.2. Fixation of the person to be examined

In order to ensure that the person to be examined does not make undue movements in the sagittal plane during the measuring period, shoulders and pelvis are steadied with gentle force. The manner of steadying must be well reproducible and may not affect the unconstrained posture of the person taken up at the beginning. The procedure is the following:

After the person has taken up his place in front of the recording apparatus (Part I - Fig. 2.1.), the steadying apparatus in front of him has to be moved on rails to the left until the shoulder-support is positioned right above the shoulders. By means of a brake the steadying machine is blocked on the rails in this position. The pelvis clamp is then still entirely open. Shoulder-support and pelvis clamp are adjustable in height along vertical pipes. The guidance is free from slackness and has the design described above (Fig. 2.3.). Adjustment is by means of a two direction electric motor driving a grooved disc on which runs the string, at one end of which is attached the support and at the other the counterweight (Fig. 2.4.).

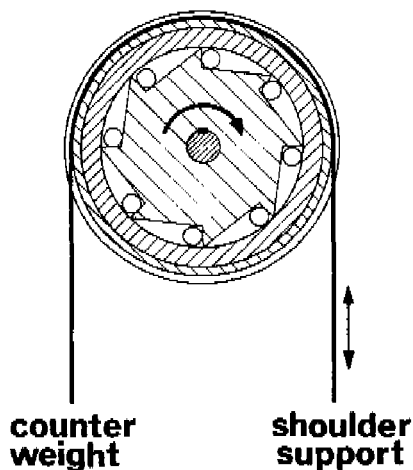


Fig. 2.4.

The steadying of the person in sagittal direction is now arranged by lowering the shoulder-support on to the shoulders. The support, clad with a thin cover of rubberfoam rests on the shoulders with a force of 2 N and adapts itself to any oblique posture of the shoulders. In order not to hinder the slight movements of respiration, the disc (Fig. 2.4.) is attached to a freewheel coupling. When the motor rotates clockwise it does not drive the disc, so that the shoulder-support may move freely up and down.

As soon as the shoulder-support has been positioned the pelvis clamp is closed. Both arms of the clamp, with coinciding centres of rotation in the horizontal plane, are pulled together by a constant force spring (negator) (45), by which a pinching force of 5 N on the pelvis is obtained.

In consequence of the free rotation in the horizontal plane the arms will not hinder the movements in the frontal plane.

In order to get an impression about the degree of fixation in the sagittal plane the movement during one minute on the various levels of the spine has been checked in a number of persons. It appeared not to extend 2.1 mm. Likewise the adjustment of the supports had no influence on the posture of the person.

General remarks:

When designing the recording device with apurtenances as described, laid down in 87 workshop drawings with a total of about 1600 dimension notations, many considerations played a part, the most salient of which being: satisfactory accuracy; 1 : 1 measuring results at once available, readily elaborated in a simple way, and to be easily related to the vertical through the backs of the heels which is already indicated on the recording roll; simple and quick attendance, even by unskilled people; rigid and at the same time light construction in view of easy transport; reduced costs; reliable and no or only few costs of up-keep.

### 2.3. Rotation measuring apparatus

The recording of the dorsal contour and the measuring of the rotation of the shoulders and the pelvis with respect to the supporting plane of the feet, are carried out in one investigation. The rotation of the shoulders is measured in order to get an impression of the curvatures of the spine in the frontal plane. The principle of measuring the shoulder rotation is described with the help of Fig. 2.5.

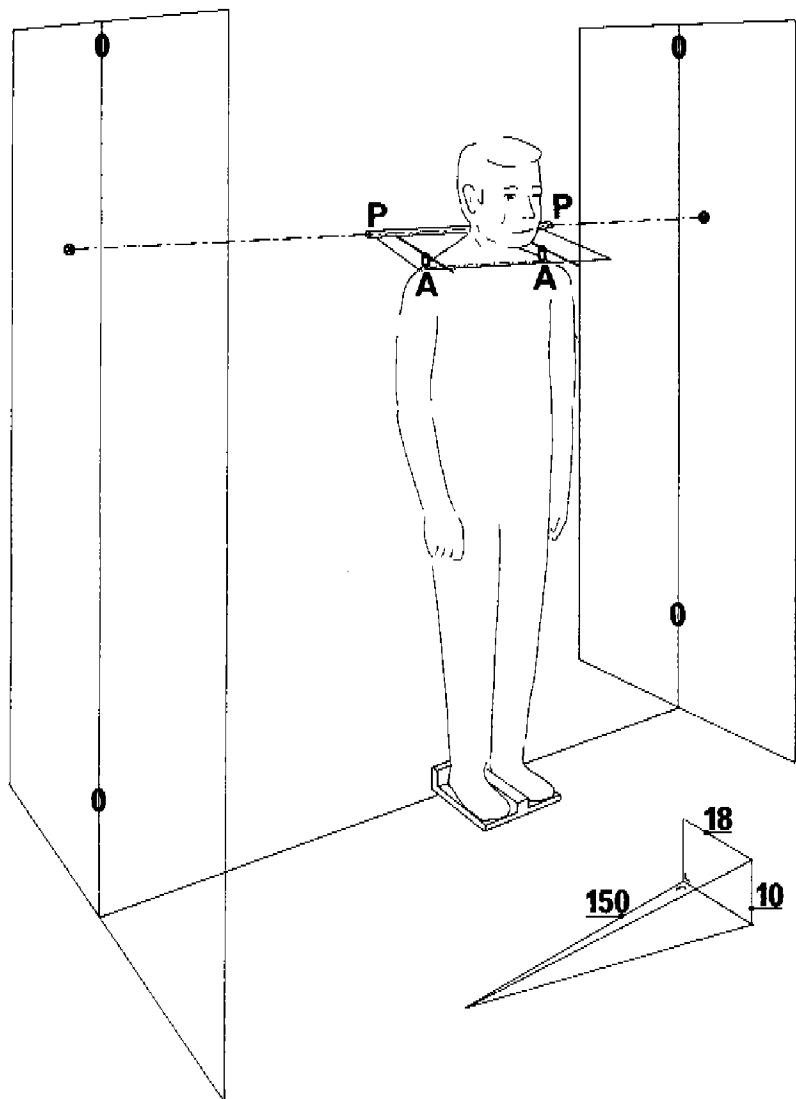


Fig. 2.5. *Measuring shoulder rotation*

The plastic pegs A each with one spherical extremity rest on the shoulders on the spot of the acromion. The distance between points A is adjustable in accordance with the width of the shoulders. By means of a rigid but at the same time light frame the line A-A runs parallel with the centre line of pipe P-P. At the extremities of the straight pipe reticles are fitted. In the middle of the pipe a bulb is burning, radiating light beams that produce an image of the reticles on the two boards put up on either side of the person. Assume that the reproduction of the reticle on the left-hand board is at 8 cm from the middle of the board (line O) in backward direction, and the one on the right-hand board 10 cm from the middle in forward direction. At a distance between the boards of 150 cm, the angle to be measured in the horizontal plane is given by

$$\tan \varphi = \frac{8 + 10}{150} = 0.12. \text{ Consequently, } \varphi \text{ is } 6^{\circ}51'.$$

Let us assume next that the difference in height of the position of the reproduction of the reticles is 10 cm, then the oblique posture of the shoulders will be found from

$$\tan \Psi = \frac{10 \cos \varphi}{150} = 0.0662, \text{ which yields } \Psi = 3^{\circ}47'.$$

The most important advantage of this indirect measurement is that the posture of the person is not influenced since only a light frame has to be carried on the shoulders.

## Mathematical backgrounds with respect to the description of the three-dimensional form of the human thoracolumbar spine

### 3.1 A formula with a comparatively great number of parameters

The formula manipulated and chosen arbitrarily in view of the description of the lateral X-ray pictures as discussed in Part I - 3.1. is:

$$y = \frac{1}{3} C_1 z^3 + Az^2 + C_2 z + B \sin \frac{\pi z}{L} + D \cos \frac{\pi z}{L} - D \quad (3.1.1.)$$

$$\text{with } C_1 = \frac{m - 2A - D \left(\frac{\pi}{L}\right)^2}{2L}$$

$$C_2 = \frac{R + D \left(2 + \frac{\pi}{6}\right)^2 - \frac{mL^2}{6} - \frac{2AL^2}{3}}{L}$$

$R$  is the  $y$ -coordinate of the bottommost point,  $L$  is the  $z$ -coordinate of this point and  $m$  is the second derivative of  $y$  with respect to  $z$  at that point.

After filling in in (3.1.1.) the coordinates of the geometrical centres of the vertebral bodies measured, with the help of the method of least squares, such values of the parameters are determined that produce a curve showing the optimum correspondence with the centres measured.

Expression (3.1.1.) is also used for the A-P taken X-ray pictures, substituting  $x$  for  $y$  (coordinate system Part I - Fig. 3.3.). In all total X-ray pictures examined by us the differences between the calculated and measured values of  $x$  and  $y$  respectively, did not exceed the measuring errors.

### 3.2 Top-view of the human spine

Fig. 3.1. illustrates the constructional way in which a perspective drawing of the spatial form of the vertebral column, shown in Part I - Fig. 3.1. and 3.2., is obtained.

In the coordinate system Part I - Fig. 3.3., the spatial curve has been completely determined by:



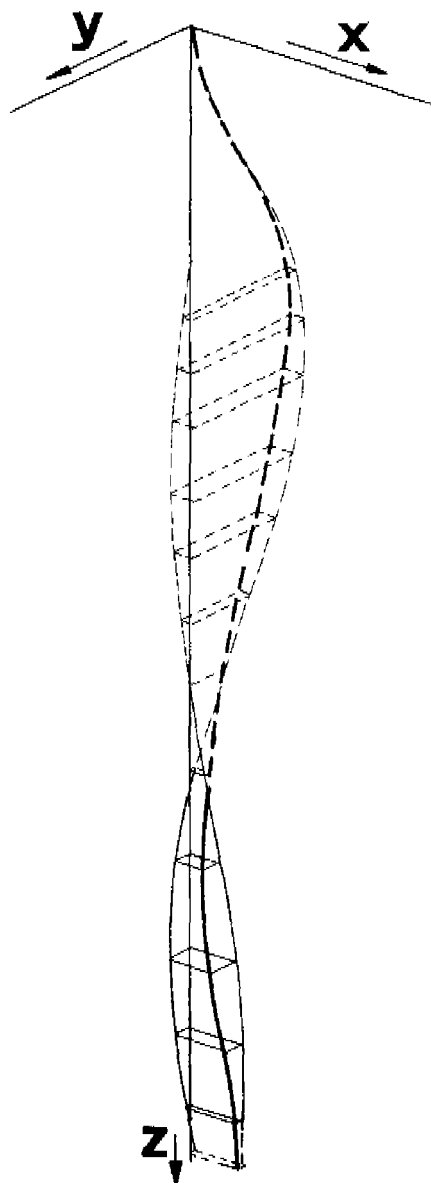


Fig. 3.1 *Spatial curve*

$$\begin{aligned}x &= x(t) \\y &= y(t) \\z &= t \quad \text{with } t \text{ as a parameter}\end{aligned}$$

The projection of this curve on the  $x - y$  plane is found by calculating the values of  $x$  and  $y$ , relative to the successive values of  $t$ .

### 3.3. Calculation of axial rotations

As to the symbols and mathematical expressions manipulated in 3.3. and 3.4. we refer to (41).

It is known that axial rotations occur in the spine when the Anterior - Posterior projection of the spine is no longer straight. The spine is then spatially curved.

It was our aim, starting from the spatial curve determined mathematically, to find a mathematical measure of the rotations perceptible in the vertebral column.

We kept in view that this measure had to meet the following criteria:

- (1) No axial rotations occur when the spine is perfectly straight in A-P projection.
- (2) In spite of the spine being (partially) straight in lateral projection, axial rotations do occur in case of bending in the frontal plane.
- (3) The axial rotations will increase in proportion as the curvatures in the spatial curve are increasing.
- (4) With a given magnitude of the curvature in the spatial curve it is accompanied by a greater axial rotation in proportion as its direction is lying closer in the direction of the frontal plane.

It is now obvious that on the ground of (3) the mathematical measure to be determined should in any case be related to the curvatures in the spatial curve.

In Fig. 3.2.  $\underline{k}$  is the curvature vector taken in an arbitrary point of the spatial curve.

Through this vector arbitrarily positioned in space, a plane can be placed that (a) runs parallel with the  $x$ -axis or (b) runs parallel with the  $y$ -axis.

In both cases the intersections with the  $x - z$  plane and with the  $y - z$  plane are perpendicular to each other.

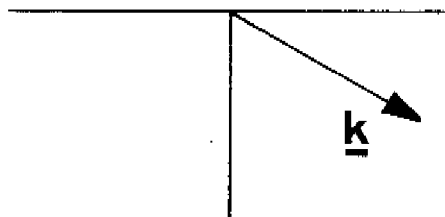


Fig. 3.2. *Curvature vector*

Let  $\underline{k}$  be equal to  $ae_1 + be_2 + ce_3$  (Fig. 3.3.)  
 or  $\underline{k} = (a, b, c)$

The component of  $\underline{k}$  lying in the  $x - z$  plane and in the plane mentioned under (a) is  $(a, 0, 0)$ .

The component of  $\underline{k}$  lying in the  $x - z$  plane and in the plane mentioned under (b) is  $(a, 0, c)$ .

Both components meet the criteria posited.

It has been determined experimentally that the component  $(a, 0, 0)$  of  $\underline{k}$  satisfies best as a mathematical measure of the axial rotations in the vertebral column.

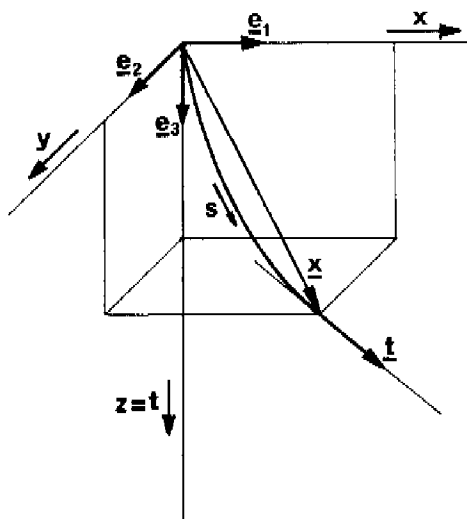


Fig. 3.3. *Symbols for differential geometry*

Elaboration:

The curvature  $\underline{k}$  in a point of the spatial curve (Fig. 3.3.) is given by:

$$\underline{k} = \frac{d\underline{t}}{ds} = \frac{\frac{d\underline{t}}{dt}}{\left| \frac{d\underline{x}}{dt} \right|} \quad (3.3.1.)$$

in which  $\underline{t}$  is the tangent vector and  $\underline{x}$  is the positional vector.

Calculation  $\left| \frac{d\underline{x}}{dt} \right|$ :

$$\underline{x} = x\underline{e}_1 + y\underline{e}_2 + t\underline{e}_3$$

$$\frac{d\underline{x}}{dt} = \frac{dx}{dt}\underline{e}_1 + \frac{dy}{dt}\underline{e}_2 + \underline{e}_3$$

$$\left| \frac{d\underline{x}}{dt} \right| = \sqrt{\left(\frac{dx}{dt}\right)^2 + \left(\frac{dy}{dt}\right)^2 + 1} = \beta \quad (3.3.2.)$$

Calculation  $\frac{d\underline{t}}{dt}$ :

Unit tangent vector  $\underline{t}$  is:

$$\underline{t} = \frac{d\underline{x}}{ds} = \frac{\frac{d\underline{x}}{dt}}{\left| \frac{d\underline{x}}{dt} \right|} = \frac{dx}{\beta} \cdot \underline{e}_1 + \frac{dy}{\beta} \cdot \underline{e}_2 + \frac{1}{\beta} \cdot \underline{e}_3$$

$$\frac{d\underline{t}}{dt} = \frac{d^2x}{dt^2} \cdot \frac{1}{\beta^2} \cdot \frac{dx}{dt} \cdot \frac{d\beta}{dt} \cdot \underline{e}_1 + \frac{d^2y}{dt^2} \cdot \frac{1}{\beta^2} \cdot \frac{dy}{dt} \cdot \frac{d\beta}{dt} \cdot \underline{e}_2 + \frac{d\beta}{dt} \cdot \frac{1}{\beta^3} \cdot \underline{e}_3 \quad (3.3.3.)$$

$$\text{with } \frac{d\beta}{dt} = \frac{\frac{dx}{dt} \cdot \frac{d^2x}{dt^2} + \frac{dy}{dt} \cdot \frac{d^2y}{dt^2}}{\beta}$$

Calculation of  $\underline{k}$  by substituting (3.3.2.) and (3.3.3.) in (3.3.1.):

$$\underline{k} = \frac{\frac{d^2x}{dt^2} \cdot \frac{1}{\beta^3} \cdot \frac{dx}{dt} \cdot \frac{d\beta}{dt}}{\beta^3} \cdot \underline{e}_1 + \frac{\frac{d^2y}{dt^2} \cdot \frac{1}{\beta^3} \cdot \frac{dy}{dt} \cdot \frac{d\beta}{dt}}{\beta^3} \cdot \underline{e}_2 + \frac{\frac{d\beta}{dt}}{\beta^3} \cdot \underline{e}_3 \quad (3.3.4.)$$

or:  $\underline{k} = a.\underline{e}_1 + b.\underline{e}_2 + c.\underline{e}_3$

which yields:

$$a = \frac{\frac{d^2 x}{dt^2} \cdot \beta - \frac{dx}{dt} \cdot \frac{d\beta}{dt}}{\beta^3} \quad (3.3.5.)$$

From the measuring results it not only appeared that the measure  $a$  in (3.3.5.) gives a good impression of the trend of the axial rotations in the spines examined by us, but also that a fair linear connection between  $a$  and axial rotations may be assumed, so that the real axial rotations are given by:

$$\varphi = \lambda.a \quad (3.3.6.)$$

in which  $\lambda$  is a multiplying factor to be determined for each individual separately.

### 3.4. Relation between force-phenomena and spatial curve

In the following approximation we imagine first the spatial curve as the form of an infinitesimally thin rod with infinitely great rigidity in which, as a result of loads imposed on it, intrinsic forces are active to establish equilibrium. This experimental thought is necessary because in an infinitesimally thin rod the direction of the cross-section and the position of the principal axis of second moment of area may be neglected.

By assuming infinite rigidity, we may confine ourselves to the form given and we need have no conception of material properties and of the form in unloaded condition.

The only thing that does interest us here is the component in tangential direction of the intrinsic bending moments present in the rod.

*Determination of the line of moments of torsion:*

- (a) Torsion resulting from a force  $F$  in the  $z$ -direction exerted on the upper extremity of the rod.

Equilibrium of moments gives:

$$\underline{M}_{bx} = y.F.\underline{e}_1$$

$$\underline{M}_{by} = -x.F.\underline{e}_2$$

The component of  $\underline{M}_{bx}$  on the tangent is the moment of torsion

$\underline{M}_{w1}$  at  $(x(t), y(t), t)$ .

$$\underline{M}_{w1} = \frac{(\underline{M}_{bx} \cdot \underline{t})\underline{t}}{|\underline{t}|^2} \text{ with } |\underline{t}| = 1$$

This leads to

$$M_{w1} = (\underline{M}_{bx} \cdot \underline{t}) = \frac{y.F. \frac{dx}{dt}}{\sqrt{\left(\frac{dx}{dt}\right)^2 + \left(\frac{dy}{dt}\right)^2 + 1}}$$

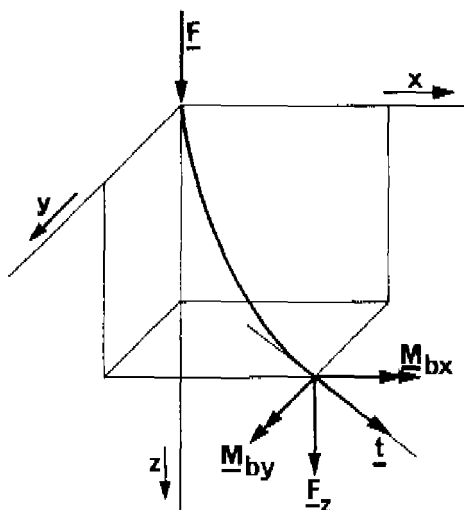


Fig. 3.4. Equilibrium with a force  $F$

Analogously, the projection of  $\underline{M}_{by}$  on the tangent becomes:

$$M_{w2} = (\underline{M}_{by} \cdot \underline{l}) = \frac{-x \cdot F \cdot \frac{dy}{dt}}{\sqrt{\left(\frac{dx}{dt}\right)^2 + \left(\frac{dy}{dt}\right)^2 + 1}}$$

With  $M_{wF} = M_{w1} + M_{w2}$

we obtain

$$M_{wF} = \frac{y \cdot F \cdot \frac{dx}{dt} - x \cdot F \cdot \frac{dy}{dt}}{\sqrt{\left(\frac{dx}{dt}\right)^2 + \left(\frac{dy}{dt}\right)^2 + 1}} \quad (3.3.7.)$$

- (b) Torsion resulting from a moment of torsion  $M_w$  in the  $z$ -direction exerted on the upper extremity of the rod. (Fig. 3.5)

$$\underline{M}_{wz} = -M_w \cdot \underline{e}_3$$

The projection of  $\underline{M}_{wz}$  on the tangent is  $\underline{M}_{wT}$ :

$$\underline{M}_{wT} = \frac{(\underline{M}_{wz} \cdot \underline{l}) \underline{l}}{|\underline{l}|^2} \quad \text{with } |\underline{l}|^2 = 1$$

this leads to

$$M_{wT} = (\underline{M}_{wz} \cdot \underline{l}) = \frac{-M_w}{\sqrt{\left(\frac{dx}{dt}\right)^2 + \left(\frac{dy}{dt}\right)^2 + 1}} \quad (3.3.8.)$$

- (c) Torsion resulting from a bending moment in the  $x$  and  $y$ -directions  $M_x$  and  $M_y$  exerted on the upper extremity of the rod. (Fig. 3.6)

$$\underline{M}_{bx} = -M_x \cdot \underline{e}_1$$

$$\underline{M}_{by} = -M_y \cdot \underline{e}_2$$

In the same way as in the case of (a) the component of  $\underline{M}_{bx}$  in the tangential direction,  $M_{wbx}$ , becomes:

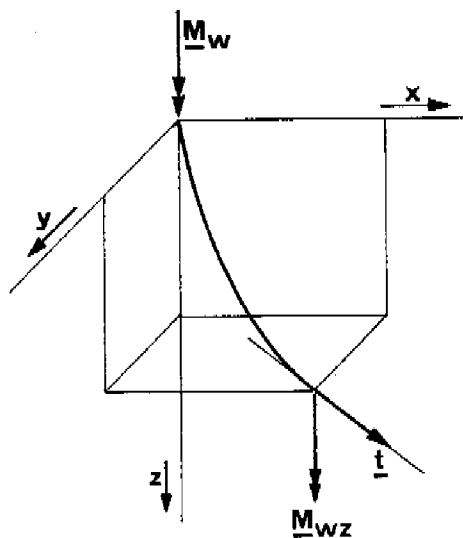


Fig. 3.5

Equilibrium with a moment of torsion  $M_w$

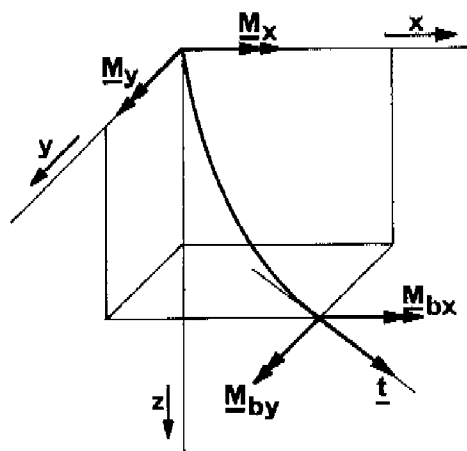


Fig. 3.6.

Equilibrium with the bending moments  $M_x$  and  $M_y$

$$M_{wbx} = \frac{-M_x \cdot \frac{dx}{dt}}{\sqrt{\left(\frac{dx}{dt}\right)^2 + \left(\frac{dy}{dt}\right)^2 + 1}} \quad (3.3.9.)$$



and in the same way the component of  $\underline{M}_{by}$  in the tangential direction,  $M_{wby}$ , becomes:

$$M_{wby} = \frac{-M_y \frac{dy}{dt}}{\sqrt{\left(\frac{dx}{dt}\right)^2 + \left(\frac{dy}{dt}\right)^2 + 1}} \quad (3.3.10.)$$

- (d) Torsion resulting from a uniformly distributed load exerted along the axis of the rod.

In point  $\underline{x} = (x_1, y_1, t_1)$  bending moments  $dM_{bx}$  and  $dM_{by}$  balance the moments caused by the force  $q \cdot ds$ , to which applies  $dM_{bx} = q \cdot ds (y_1 - y(t))$  and  $dM_{by} = -q \cdot ds (x_1 - x(t))$ . For the component of the resultant of these moments in the direction of the tangent,  $dM_{wq}$ , we can use equation (3.3.7.) which yields:

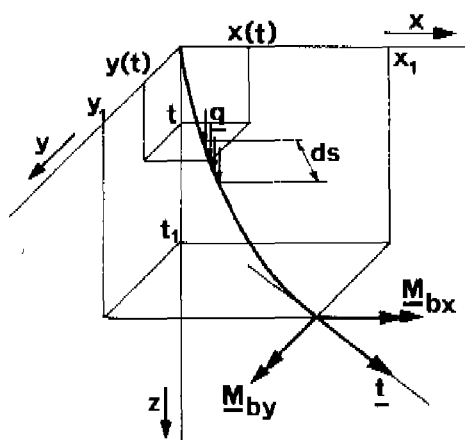


Fig. 3.7. *Equilibrium with a uniform distributed load  $q$ .*

$$dM_{wq} = \frac{q \cdot ds (y_1 - y(t)) \cdot \left(\frac{dx}{dt}\right)_1 - q \cdot ds (x_1 - x(t)) \cdot \left(\frac{dy}{dt}\right)_1}{\sqrt{\left(\frac{dx}{dt}\right)_1^2 + \left(\frac{dy}{dt}\right)_1^2 + 1}} \quad (3.3.11.)$$

The length of the rod from  $(0, 0, 0)$  down to  $(x_1, y_1, t_1)$  is:

$$s = \int_0^{t_1} \left| \frac{dx}{dt} \right| dt \quad (3.3.12.)$$

$$\text{and } ds = \left| \frac{dx}{dt} \right| dt \quad (3.3.13.)$$

Substitution of (3.3.13.) in (3.3.11.) followed by integration from 0 to  $t_1$  produces the total moment of torsion effected by  $q$ :

$$M_{wq} = q \int_0^{t_1} \left| \frac{dx}{dt} \right| \cdot \frac{(y_1 - y(t)) \left(\frac{dx}{dt}\right)_1 - (x_1 - x(t)) \left(\frac{dy}{dt}\right)_1}{\sqrt{\left(\frac{dx}{dt}\right)_1^2 + \left(\frac{dy}{dt}\right)_1^2 + 1}} dt \quad (3.3.14)$$

- (e) Torsion resulting from a load  $g$  linearly increasing with the coordinate  $s$ :  $g = q + X.s$

For calculating the moment of torsion  $M_{wg}$  effected by a load linearly increasing with the coordinate  $s$  we use equation (3.3.14.).

If we write in it

$$\frac{(y_1 - y(t)) \left(\frac{dx}{dt}\right)_1 - (x_1 - x(t)) \left(\frac{dy}{dt}\right)_1}{\sqrt{\left(\frac{dx}{dt}\right)_1^2 + \left(\frac{dy}{dt}\right)_1^2 + 1}} = \gamma$$

$M_{wg}$  becomes:

$$\begin{aligned} M_{wg} &= \int_0^{t_1} g \cdot \left| \frac{dx}{dt} \right| \cdot \gamma \cdot dt \\ &= q \int_0^{t_1} \left| \frac{dx}{dt} \right| \cdot \gamma \cdot dt + \int_0^{t_1} X.s \cdot \left| \frac{dx}{dt} \right| \cdot \gamma \cdot dt \end{aligned}$$

By using equation (3.3.12.) we obtain:

$$M_{wg} = q \int_0^{t_1} \left| \frac{dx}{dt} \right| \cdot \gamma \cdot dt + X \int_0^{t_1} \left| \frac{dx}{dt} \right| \cdot \gamma \cdot \left\{ \int_0^t \left| \frac{dx}{d\tau} \right| d\tau \right\} \cdot dt \quad (3.3.15.)$$

The contribution of each force phenomenon to the moment of torsion can now be calculated. If they are taken as a unit, they yield Fig. 3.12 in Part I.

This figure is based on the spatial curve of the person mentioned in Part I - Fig. 3.1. With other individuals in the nature of things other figures are to be found.

Fig. 3.12 in Part I does not comprise the contribution of the load  $g$  (for gravitation). In the preceding has been indicated in what a way such a load could be inserted into the calculations. Because these calculations have not yet procured satisfying results, we enter more closely into this matter at the end of this chapter, we have confined ourselves in the following to calculations based exclusively on  $F$ ,  $M_x$ ,  $M_y$  and  $M_z$ .

#### *Moment of torsion coupled to axial rotations existing in the scoliotic spine*

According to White, it may be assumed that in the spine there is a linear connection between moment of torsion  $M_T$  and axial rotation  $\varphi$ .

Assuming furthermore that with  $M_T = 0$  also  $\varphi = 0$ , we can note down:

$$\frac{d\varphi}{ds} = \frac{M_T}{GI_p} \quad (3.3.16.)$$

in which  $GI_p$  is a measure of the torsional rigidity (in  $\text{Nmm}^2$ ). We found that  $\lambda a$  in expression (3.3.6.) is a good measure of the axial rotations  $\varphi$  existing in the spine. With (3.3.16.) we then obtain:

$$M_T = GI_p \lambda \cdot \frac{da}{ds} \quad (3.3.17.)$$

As a first approach we posit that this intrinsic moment of torsion is the sum of the moments of torsion originating from the force phenomena applied:

$$M_T = F \cdot M'_{wF} + M_w \cdot M'_{wT} + M_x \cdot M'_{wbx} + M_y \cdot M'_{wby} \quad (3.3.18.)$$

in which  $M'_{wF}$  is the moment of torsion resulting from a unit force  $F$ , etc.

With (3.3.17.) and (3.3.18.) we next obtain:

$$\frac{da}{ds} = \alpha M'_{wF} + \mu M'_{wT} + \delta M'_{wbx} + \epsilon M'_{wby} \quad (3.3.19.)$$

$$\text{with } \alpha = \frac{F}{GI_p \lambda}, \quad \mu = \frac{M_w}{GI_p \lambda}, \quad \delta = \frac{M_x}{GI_p \lambda}, \quad \epsilon = \frac{M_y}{GI_p \lambda}$$

$$\frac{da}{ds} = \frac{da}{dt} \cdot \frac{dt}{ds} = \frac{dt}{ds} = \left| \frac{dx}{dt} \right|$$

with (3.3.2.) and (3.3.5.) we obtain:

$$\frac{da}{ds} = \frac{\frac{da}{dt}}{\left| \frac{dx}{dt} \right|} = \frac{\frac{d^3 x}{dt^3} \cdot \beta - \frac{dx}{dt} \frac{d^2 \beta}{dt^2}}{\beta^4} - 3 \cdot \frac{\frac{d\beta}{dt} \left( \frac{d^2 x}{dt^2} \cdot \beta - \frac{dx}{dt} \frac{d\beta}{dt} \right)}{\beta^5} \quad (3.3.20.)$$

$$\text{with } \frac{d\beta}{dt} = \frac{\frac{dx}{dt} \cdot \frac{d^2 x}{dt^2} + \frac{dy}{dt} \cdot \frac{d^2 y}{dt^2}}{\beta}$$

$$\text{and } \frac{d^2 \beta}{dt^2} = \frac{\left( \frac{d^2 x}{dt^2} \right)^2 + \left( \frac{d^2 y}{dt^2} \right)^2 + \frac{dx}{dt} \cdot \frac{d^3 x}{dt^3} + \frac{dy}{dt} \cdot \frac{d^3 y}{dt^3} - \left( \frac{d\beta}{dt} \right)^2}{\beta}$$

By using the method of least squares, the values of  $\alpha$ ,  $\mu$ ,  $\delta$  and  $\epsilon$  were defined, which substituted in the right hand side of equation (3.3.19.), furnished the best adaptation to the values of  $\frac{da}{ds}$  at the various levels of the spine.

When handling equation (3.3.19.), it was taken into account that the intrinsic moment of torsion  $M_T$  is active in the direction of the axial rotation in the spine, which is taken positive in the positive sense of rotation of the system of coordinates.

From Fig. 3.12 in Part I it becomes evident that for adaptation of  $M_T$  to  $\frac{da}{ds}$  the computer disposes of a reasonable number of possibilities. The adaptations carried out according to the method of least squares appeared to be as has been illustrated in Part I - Fig. 3.13. for the case of Fig. 3.12 in Part I.

A better adaptation of  $M_T$  to  $\frac{da}{ds}$  can be obtained by introducing into the calculation more load factors. However, it became evident that the introduction of a load, such as  $g = q + \chi s$ , is not possible in the actual stage of our knowledge. The calculations carried out with  $g$ , while maintaining  $F$  because on the ground of the literature an approximation could be made of the true magnitude of  $F$ , led to ampler adaptation possibilities for the computer and consequently to a bigger chance for a wrong sign of one of the by now six multiplying factors. In none of the five cases, elaborated in this way, sensible results have been obtained. Applying a further refinement to the calculations will be possible no sooner than after having at our disposal the knowledge of the division of the load along the spine emerging from the force of gravitation, together with the knowledge of the (irregular) division of the torsional rigidity along the spine. That even then uncertainties remain is indicated in Part I - Chapter 3.

## Mathematical backgrounds with respect to hypotheses about two wear-and-tear phenomena that manifest themselves in case of angular rotation of two successive vertebrae

### 4.1. Determination of the straight part in the spatial curve

In order to calculate the magnitude of the curvatures in the spatial curve we start from equation (3.3.4.), in which the curvature vector  $\underline{k}$  is given. The magnitude  $|\underline{k}|$  of this vector is:

$$|\underline{k}| = \sqrt{\left(\frac{d^2x}{dt^2}\beta - \frac{dx}{dt} \cdot \frac{d\beta}{dt}\right)^2 + \left(\frac{d^2y}{dt^2}\beta - \frac{dy}{dt} \cdot \frac{d\beta}{dt}\right)^2 + \left(\frac{d\beta}{dt}\right)^2} \quad (4.1.1.).$$

With  $\beta$  given in (3.3.2).

The curvatures of the curves in the planes of the lateral and the A-P projections have a direction that changes its sign suddenly in an inflection point. The curvature vector  $\underline{k}$  in (3.3.4.), which is related to the spatial curve, does not show this phenomenon, so that we have to base the determination of the spot where the spatial curve is straightest, on the smallest numerical value of the curvature found with (4.1.1).

### 4.2. Wear and tear of the annulus fibrosus

By displacing vertebral body 2 (Fig. 4.1) from its original position (dotted line) to an arbitrarily chosen position (solid line), this can be reached by a translation along the way  $y$ , by a translation along the way  $x$  and finally by a rotation over the angle  $\psi$ . We start from the following three assumptions:

- (1) The fibres 1 and 2 are straight in the original position and remain straight after displacement.
- (2) The elongation of the fibres per unit of length is equal from place to place. This means that the fibres are supposed

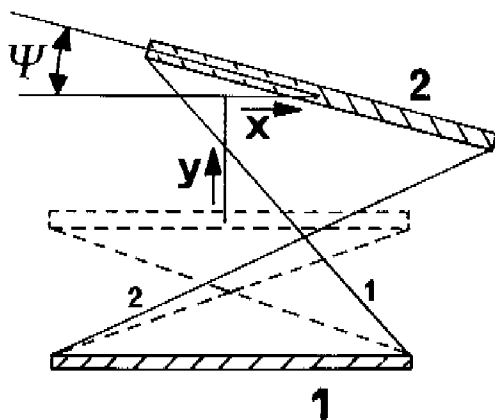


Fig. 4.1. *Arbitrarily angular rotation*

to be equally thick and that the material properties in longitudinal direction are equal throughout.

(3) The vertebral bodies are rigid.

After translation in direction  $y$  (Fig. 4.2.) points A and B keep together, taking into account the elongation of the fibres. Also in case of a translation in the horizontal direction (Fig. 4.3.) A and B keep together.

Thus the diverging of the points A and B is exclusively a consequence of angular rotation.

Consequently Fig. 4.4. will suffice for the determination of the magnitude of the divergency between A and B.

Symbols: In the original position:

length of the fibres	$= L$
height of the disc	$= h$
distance $GA =$ distance $HB$	$= R$
distance $OQ =$ distance $OT$	$= S \left( 0 < S < \frac{h}{\tan \omega} \right)$
angle between the fibres and the cartilaginous plate	$= \omega$

In the rotated position:

angular rotation	$= \psi$
------------------	----------

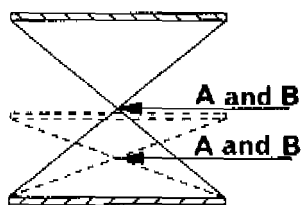


Fig. 4.2. Translation in direction  $y$

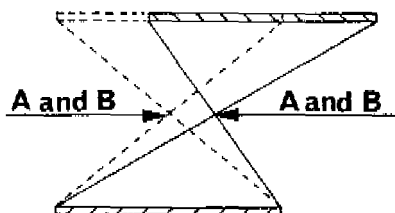


Fig. 4.3. Translation in direction  $x$

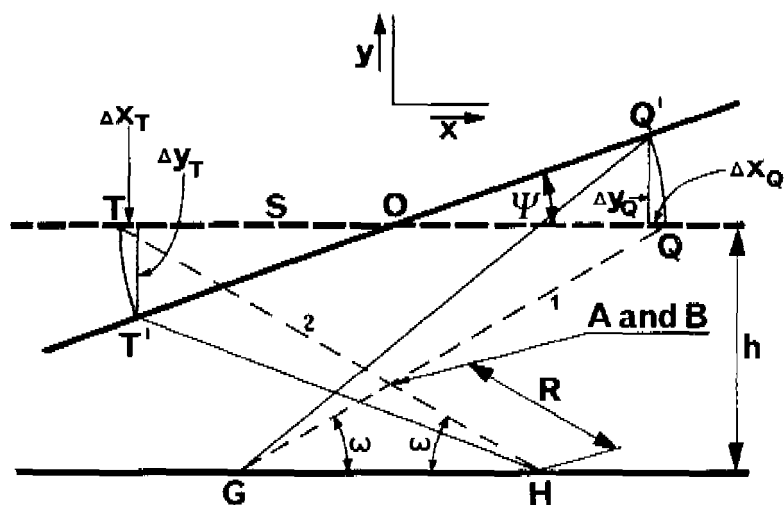


Fig. 4.4 Angular rotation.



To be determined: the magnitude of the distance between A and B after angular rotation. This is called the Divergency ( $D$ ).

Deduction:	Displacement of Q towards Q':	Displacement of T towards T':
	$\Delta x_Q = -S(1 - \cos\psi)$	$\Delta x_T = S(1 - \cos\psi)$
	$\Delta y_Q = S \sin\psi$	$\Delta y_T = -S \sin\psi$

Displacement of A (on fibre 1) with respect to the state of rest (fibre 1 becomes longer):	Displacement of B (on fibre 2) with respect to the state of rest (fibre 2 becomes shorter):
--	---

$$\Delta x_A = -\frac{R}{L} S(1 - \cos\psi) \qquad \Delta x_B = \frac{R}{L} S(1 - \cos\psi)$$

$$\Delta y_A = \frac{R}{L} S \sin\psi \qquad \Delta y_B = -\frac{R}{L} S \sin\psi$$

The distance between the new positions of A and B ( $A'$  and  $B'$ ) is the Divergency,

This is illustrated in Fig. 4.5.

$$\begin{aligned} D = A'A + B'B &= \sqrt{(\Delta x_A)^2 + (\Delta y_A)^2} + \sqrt{(\Delta x_B)^2 + (\Delta y_B)^2} \\ &= 2 \frac{R}{L} S \sqrt{(1 - \cos\psi)^2 + \sin^2\psi} \\ &= 4 \frac{R}{L} S \sin \frac{1}{2} \psi \end{aligned}$$

$$\text{with } S = \frac{h}{\tan\omega} - R \cos\omega$$

So the Divergency becomes:

$$D = \frac{4 \sin \frac{1}{2} \psi}{L} \left( \frac{Rh}{\tan\omega} - R^2 \cos\omega \right) \qquad (4.2.1.)$$

In order to define at what magnitude of  $R$  the Divergency is maximum, the derivative of  $D$  with respect to  $R$  is taken zero:

$\frac{\partial D}{\partial R} = 0$  leads to

$$\frac{4 \sin \frac{1}{2} \psi}{L} \left( \frac{h}{\tan \omega} - 2 R \cos \omega \right) = 0$$

This is complied with by:

$$R = \frac{1}{2} \frac{h}{\sin \omega} = \frac{1}{2} L \quad (4.2.2.)$$

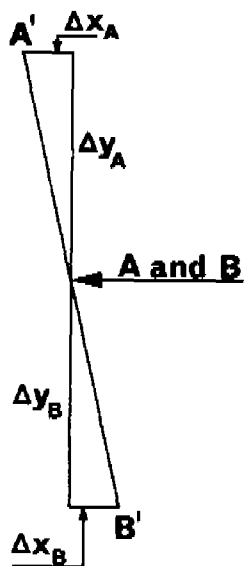


Fig. 4.5. Divergency of A and B

Thus  $D$  is maximum for the points of intersection situated half-way the distance between the vertebral bodies. Substitution of (4.2.2.) in (4.2.1.) produces the magnitude of  $D$  with respect to the spots in the middle of the distance between the vertebral bodies.

$$D_{\text{middle}} = \frac{h \cdot \sin \frac{1}{2} \psi}{\tan \omega} \quad (4.2.3.)$$

To get an impression of the order of magnitude of  $D$  we calculate  $D$  with  $\omega = 28^\circ$  (18),  $\psi = 6^\circ$  and  $h = 10$  mm:

$$D_{\text{middle}} = \frac{10 \cdot 0.0523}{0.5317} \approx 1 \text{ millimetre}$$

## References

### Part I.

- 1 Åkerblom, B. : Standing and sitting posture. Thesis. AB Nordiska Bokhandeln, Stockholm, 1948.
- 2 Appleton A.B. : Posture practitioner, 1946, 156, 48-55.
- 3 Basmajian J.V. : Electromyography of postural muscles. Chapter 6 in: Evans F., Gaynor, Biomechanical studies of the musculo skeletal system. Springfield Illinois, 1961.
- 4 Broek A., van den : Leerboek der beschrijvende ontleedkunde Boeke J. en Barge J. van de mens. Deel I. Utrecht, 1954.
- 5 Bonne A.J. : De ziekte van Scheuermann. Thesis. Groningen, 1955.
- 6 Bonne A.J. : On the shape of the human vertebral column. Acta Orthopaedica Belgica, 1969.35.
- 7 Brown I., Hansen R.J. and Yorra A.J. : Some mechanical tests on the lumbosacral spine with particular reference to the intervertebral discs. J. of Bone and Joint Surgery, Vol 39-A, 1957, p. 1135-1164.
- 8 Buytendijk F.J.J. : Algemene theorie der menselijke beweging. Het Spectrum (Utrecht) 1948.
- 9 Cailliet R. : Low back pain syndrome. Oxford, 1962.
- 10 Charrière L. : La kinésithérapie dans le traitement des algies vertébrales. Masson editeurs, Paris, 1965.
- 11 Cramer A. : Funktionelle Merkmale von Störungen der Wirbelsäulenstatik. Die Wirbelsäule in Forschung und Praxis. Band 5.

- 12 Davis P.R. : The medial inclination of the human thoracic intervertebral articular facets. *J. Anat.* 93:68, 1959.
- 13 Galante J.O. : Tensile properties of the human lumbar annulus fibrosus. Thesis. *Acta Orthop. Scand. Suppl.* 100, 1967.
- 14 Gregerson G.G. and Lucas D.B. : An in vivo study of the axial rotation of the human thoracolumbar spine. *J of Bone and Joint Surgery*, Vol 49-A, No 2, march 1967.
- 15 Güntz E. : Die Kyphose im Jugendalter. Die Wirbelsäule in Forschung und Praxis, Band 2.
- 16 Gutmann G. : Zur Frage der konstruktionsgerechten Beanspruchung von Lendenwirbelsäule und Becken beim Menschen. *Asklepios*, Vol 6, Nr 9, 1965.
- 17 Hicks J.H. : The three weight bearing mechanisms of the foot. *Biomechanical Studies of the musculoskeletal system.* Edited by Evans G.F. Publisher: Charles C. Thomas, Springfield, Illinois, U.S.A. 1961.
- 18 Horton W.G. : Biologische und biochemische Beobachtungen an der menschlichen Zwischenwirbelscheibe. Die Wirbelsäule in Forschung und Praxis Band 15.
- 19 Karaharju : Deformation of vertebrae in experimental scoliosis. *Acta Orth. Scand. Suppl.* 105, 1967.
- 20 Leger W. : Die Form der Wirbelsäule mit Untersuchungen über ihre Beziehung zum Becken und die Statik der aufrechten Haltung. Ferdinand Enke Verlag Stuttgart, 1959.
- 21 Lucas D.B., Bresler B. : Stability of the ligamentous spine. Intern report biomechanics laboratory of the

University of California. San Francisco - Berkeley, 1961.

- 22 Meyer H. von : Die Statik und Mechanik des menschlichen Knochengerustes. Leipzig, 1873.
- 23 Nachemson, A. : Lumbar intradiscal pressure. Acta Orth. Scand. Suppl. 42, 1960.
- 24 Novogrodsky M. : Die Bewegungsmöglichkeit in der menschlichen Wirbelsäule. Bern, 1911.
- 25 Raşch P.J. and Burke R.K. : Kinesiology and applied anatomy. Lea and Febiger, Philadelphia 1967.
- 26 Rathke F.W. : Die Juvenilen Rückgratverkrümmungen. Georg Thieme Verlag. Stuttgart, 1961.
- 27 Reese W.O. : Structural mechanics: an etiological factor in idiopathic scoliosis. Proceedings of the 8th ICMBE, Chicago 1969.
- 28 Rolander S.D. : Motion of the lumbar spine with special reference to stabilizing effect of posterior fusion. Thesis. Acta Orth. Scand. Suppl. 90, 1966.
- 29 Rüdinger R. : The perpendicular in relation to walking casts. J of Bone and Joint Surgery. Vol 38-A, 1956, pp 1379-1381.
- 30 Sheldon W.H. : Atlas of Men, New York, 1954.
- 31 Snijders C.J. : On the form of the human spine and some aspects of its mechanical behaviour. Acta Orth. Belgica. 1969, 35. and: Proceedings of the 8th International Conference on Medical and Biological Engineering. Chicago, 1969.
- 32 Sonnerup L. : Mechanical analysis of the human intervertebral disc. Proceedings of the 8th ICMBE. Chicago, 1969.
- 33 Staffel F. : Die menschlichen Haltungstypen und ihre

- Beziehungen zu den Rückgratsverkrümmungen. Wiesbaden, 1889.
- 34 Strasser H. : Lehrbuch der Muskel- und Gelenkmechanik Band II, Springer, Berlin, 1913.
- 35 Ubbens R. : Over de röntgendiagnostiek van de lumbale hernia nuclei pulposi, thesis, Groningen, 1960.
- 36 White A.A. : Analysis of the mechanics of the thoracic spine in man. Acta Orth. Scand. Suppl. 127, 1969.
- 37 Williams M. and Lissner H.R. : Biomechanics of human motion. Saunders Company, London 1962.

#### References Part II

- 38 Alblas J.B. : Syllabus van de colleges Mechanica II. Technische Hogeschool Eindhoven 1963.
- 39 Born M. : Stabilität der elastischen Linie in Ebene und Raum unter verschiedenen Grenzbedingungen. Göttingen 1906.
- 40 Haantjes : Inleiding tot de differentiaal-meetkunde. Noordhoff, Groningen, 1954.
- 41 Lipschutz M.M. : Differential Geometry. Mc Graw-Hill Book Company, New York 1969.
- 42 Saalschütz L. : Der belastete Stab unter einwirkung einer seitlichen Kraft auf Grundlage des strengen Ausdrucks für den Krümmungsradius. Leipzig 1880.
- 43 Snijders C.J. : Metalen Veren. Polytechnisch Tijdschrift, Werktuigbouw. Vol 25, (1970) no. 4, p. 158-162. Vol 25, no. 5, p. 191-198. Vol 25, no. 6, p. 258-262. Vol 25, no. 7, p. 291-296.

- 44 Timoshenko S.P.  
and Gere J.M. : Theory of Elastic Stability.  
Mc Graw-Hill Book Company, New York,  
1961.
- 45 Votta F.A. : The theory and design of long-deflection  
constant force spring elements.  
Trans. ASME 74(1952) p. 439-450.



# List of symbols

Quantities and Units. ISO recommendation R31.

Quantity	Symbol of quantity	Name of unit	International symbolic abbreviation for unit	Dimension	Conversion factors
length	<i>l</i>	metre inch	m	[L]	1 in. = 0.0254 m = 25.4 mm
mass	<i>m</i>	kilogramme pound (avoirdupois)	kg	[M]	1 lb. = 0.45359237 kg
time	<i>t</i>	second	s	[T]	
force	<i>F</i>	newton kilogramme-force pound-force	N	[MLT <sup>-2</sup> ]	(1N = 1 kg × 1 ms <sup>-2</sup> ) 1 kgf = 9.80665 N 1 lbf = 4.44822 N

Symbol	unit	name
<i>a</i>	mm <sup>-1</sup>	component of curvature in <i>x</i> -direction (Part I - Fig. 3.3.)
<i>b</i>	mm <sup>-1</sup>	component of curvature in <i>y</i> -direction (Part I - Fig. 3.3.)
<i>c</i>	mm <sup>-1</sup>	component of curvature in <i>z</i> -direction (Part I - Fig. 3.3.)
<i>d</i>	mm	distance; diameter
<i>d<sub>a</sub></i>	mm	average width of vertebral bodies in the sagittal projection
<i>e</i>	mm	eccentricity of processus spinosus with respect to the vertebral body in the A-P projection
<i>ε</i>		unit vector along coordinate axis (Part II - Fig. 3.3)

$g$	N	downward linearly increasing load exerted on the spine by gravitation
$h$	mm	height of disc
$\frac{k}{m}$	mm <sup>-1</sup>	curvature vector measure of the curvature at the bottommost point of the thoracolumbar spine (second derivative of $y$ with respect to $x$ at that point in formula Part I - 1.2.1).
$p$	Nmm <sup>-2</sup>	pressure
$q$	N	uniformly distributed load exerted on the spine
$s$		parameter on spatial curve
$t$		parameter
$\frac{t}{x}$		unit tangent vector
$x$		coordinate
$y$		coordinate
$z$		coordinate
$A$		coefficient
$B$		coefficient
$C$		coefficient
$D$		coefficient
$E$	Nmm <sup>-2</sup>	modulus of elasticity
$EI$	Nmm <sup>2</sup>	flexural rigidity
$F$	N	force
$G$	Nmm <sup>-2</sup>	shear modulus
$GI_p$	Nmm <sup>2</sup>	torsional rigidity
$I$	mm <sup>4</sup>	second moment of area about an axis - in the case of bending
$I_p$	mm <sup>4</sup>	second polar moment of area - in the case of torsion
$K$	mm <sup>-1</sup>	curvature of a plane curve
$L$		vertical coordinate of the bottommost point of the thoracolumbar spine
$M$	Nmm	bending moment
$M_x$	Nmm	bending moment in $x$ -direction exerted at point Th1 (Part I - Fig. 3.11)
$M_y$	Nmm	bending moment in $y$ -direction exerted at point Th1 (Part I - Fig. 3.11)
$M_w$	Nmm	bending moment in $z$ -direction exerted at point Th1 (Part I - Fig. 3.11)
$M_{bx}$	Nmm	intrinsic moment in $x$ -direction
$M_{by}$	Nmm	intrinsic moment in $y$ -direction
$M_{wz}$	Nmm	intrinsic moment in $z$ -direction

$M_T$	Nmm	total intrinsic torsion moment in the spine (in tangential direction)
$M_{wF}$	Nmm	part of $M_T$ resulting from a force $F$ exerted at point Th1
$M_{wq}$	Nmm	part of $M_T$ resulting from a uniformly distributed load exerted on the spine
$M_{wg}$	Nmm	part of $M_T$ resulting from a downward linearly increasing load exerted on the spine by gravitation
$M_{wbx}$	Nmm	part of $M_T$ as a result of a bending moment $M_x$ exerted at point Th1
$M_{wby}$	Nmm	part of $M_T$ as a result of a bending moment $M_y$ exerted at point Th1
$M_{wT}$	Nmm	part of $M_T$ as a result of a torsion moment $M_w$ exerted at point Th1
N		newton; unit of force, see table above
P	N	transverse force; force in horizontal direction
R		horizontal coordinate of the bottommost point of the thoracolumbar spine
$\alpha$		multiplication factor
$\beta$		see equation Part II - 3.3.2
$\gamma$		see equation Part II - 3.3.15
$\delta$		multiplication factor
$\epsilon$		multiplication factor
$\eta$	rad mm <sup>-1</sup>	axial rotation per unit of spine length
$\lambda$		multiplication factor for the mathematical measure of axial rotations
$\mu$		multiplication factor
$\pi$		$\pi = 3.14159265$
$\sigma$		standard deviation; $\sigma = \sqrt{\frac{\sum (x_i - x_m)^2}{n - 1}}$ with $x_i =$ one of the values measured, $x_m =$ average of the values measured, and $n =$ number of repeated measurements
$\tau$		parameter
$\varphi$	rad, degree	axial rotation
$\chi$		multiplication factor
$\psi$	rad, degree	angular rotation
$\omega$	rad, degree	angle between annulus fibre and cartilaginous plate

## Abbreviations

A-P	Anterior-Posterior
L3	third lumbar vertebra
M8	metric screw thread with outer diameter 8 mm
Th1	first thoracal vertebra

## Terminology

acromion	top of shoulders
annulus fibrosus	part of the intervertebral disc; fibrous ring enclosing the nucleus pulposus
articulus talocruralis	uppermost hock
bending point	inflection point; straight part in a curve
cartilaginous plate	transition of vertebral body to intervertebral disc
centre line	form of the spine
coxarthrosis	affection of the hip-joint not attributed to inflammation
curvature	a curve can be approximated by an arc of a circle at any arbitrary point; the curvature is the reciprocal of the radius of such a circle. A circle with a short radius has a relatively large curvature
dorsal contour	the dorsal contour of the spine is the fluent line passing through the points on the skin considered to represent the most dorsal points of the processus spinosi
ectomorphic type	build of body approximately leptosome (slim body with peaky face and sharp nose) with predominant development of the ecto- derm (skin, nervous system) (Sheldon)
endomorphie type	build of body approximately pyknic (squat figure) with predominant development of the endoderm (alimentary canal) (Sheldon)
flexural rigidity	resistance against bending; bending stiffness
form of the spine	the fluent line passing through the geome-

frontal plane	the $x-z$ plane in Part I - Fig. 3.3.
kyphose-sacrum area	part of the spine from the most dorsal point of the kyphosis down to the bottom-most intervertebral disc
kyphosis	(thoracal) part of the spine, which seen from the ventral side is concave
ligamentum longitudinalis anterior and posterior	vertical band of fibrous tissue that runs along the whole length of the spine
lordosis	part of the spine which seen from the ventral side is convex
mesomorphic type	build of body approximately athletic with predominant development of the mesoderm (bones, muscles) (Sheldon)
M.ilio-psoas	see Part I - Fig. 1.5
motion segment	part of the spine composed of two vertebrae and one intervertebral disc
M. triceps surae	calf muscles ending in the Achilles tendon
nucleus pulposus	gelatinous central portion of an intervertebral disc
plantar aponeurosis	tendinous layer covering the muscles of the footsole
processus spinosus	process of the vertebra directed backward
sacrum (os)	bone composed of connated caudal vertebrae
sagittal plane	the $y-z$ plane in Part I - Fig. 3.3
sclerosis	induration (osteosclerosis)
scoliosis	laterally crooked spine
spondylolisthesis	shifting of vertebrae
spondylolysis	separation of the solid connection between front and back half of a vertebral arc by a layer of connective tissue
spondylosis deformans	affection of the intervertebral disc manifesting itself by abnormal growth of bone tissue near the fastening of the annulus fibrosus to the vertebral body (Randwulstbildung) (Parrot mouth)
standard deviation	see $\sigma$ in list of symbols
thoracolumbar spine	part of the spine from the level of the shoulders down to the sacrum composed of 12 thoracal and 5 lumbar vertebrae
torsional rigidity	resistance against torque; torsional stiffness
ventral side	in all illustrations dealing with lateral

vertebral body

aspects of the spine the ventral side is at the right  
solid part of a vertebra being virtually rectangular in lateral aspect

## Summary

In the thesis the form of the spine of persons in natural erect posture is the centre of attention. Geometrical data of the spine measured in X-ray pictures or on the dorsal contour are fed into a digital computer. By calculating numerical values of a number of parameters in mathematical formulae the form of any spine can be numerically defined. This method opens the way to statistical research of form, and moreover, the length of the bent spine and curvatures can be calculated in this way. By combining a lateral and an Anterior-Posterior X-ray picture the spatial form of the spine can be defined mathematically. This description of form is applied in cases of scoliosis where especially the top view of the spine is of interest. A mathematical measure is introduced to calculate, starting from the spatial curve, the axial rotations in the spine. With this mathematical measure the position of the axis of axial rotation at the various levels in the spine is calculated. Starting from the mathematically fixed form, defined for standing as well as for sitting postures, conclusions are made as to the loading of the spine.

Attention is paid to the mechanical phenomena in intervertebral discs, which play an important part in the mechanical behaviour of the entire spine. Hypotheses are given about two wear-and-tear mechanisms in the intervertebral discs that may result from frequent bending of the spine. A number of theoretical considerations are supported by experiments on autopsy specimens.

The work is presented in two parts: Part I is especially intended for the medical science, Part II gives the mathematical and technical backgrounds of Part I, as well as descriptions of the apparatus especially developed for the research.

## Curriculum vitae

De auteur werd op 4 november 1941 te Malang geboren. In 1950 verliet hij Indonesië. Na de Lagere School bezocht hij de Rijks H.B.S. te Roermond en de Lorentz H.B.S. te Arnhem, waar hij in 1958 het eindexamen H.B.S.-B aflegde. Hij studeerde werktuigbouwkunde aan de Technische Hogeschool Eindhoven.

Een langdurig verblijf in een ziekenhuis richtte reeds tijdens zijn studietijd zijn belangstelling op de toepassingsmogelijkheden van werktuigkundige kennis in de geneeskunde. Naar aanleiding hiervan werd een afstudeeronderwerp gekozen uit het gebied van de adaptatie-instrumenten ten behoeve van lichamelijk gehandicapten. Zijn afstudeerhoogleraar was Prof. ir. A. Horowitz. Het ingenieursdiploma werd hem uitgereikt in februari 1966, waarna hij wetenschappelijk medewerker werd in de groep "Landbouw- en Kleine Werktuigen" aan de Technische Hogeschool Eindhoven. Naast zijn onderwijstaak was hij betrokken bij de ontwikkeling en constructie van apparaten bestemd voor gebruik in ziekenhuizen en de huisartsenpraktijk en apparatuur ten behoeve van lichamelijk gehandicapten; tevens verrichtte hij fundamenteel onderzoek met betrekking tot mechanische verschijnselen in de menselijke wervelkolom.

Een aantal van zijn werkzaamheden vond plaats in het kader van zijn lidmaatschap van: de werkgroep adaptatie-instrumenten van de Stichting Technische Voorlichting ten behoeve van Lichamelijk Gehandicapten (V.L.G.) te 's-Gravenhage; een adviescommissie voor het Bio-Revalidatiecentrum te Arnhem en de Afdeling Research van de Stichting Manuele Therapie te Eindhoven.

In 1969 maakte hij een studiereis door Schotland, de Verenigde Staten en Canada.

Van zijn hand verschenen publicaties in medische en technische tijdschriften in binnen- en buitenland.



## STELLINGEN

1. De uitspraak van Galante, als zouden de meer naar het midden van de intervertebrale discus gelegen vezels van de annulus fibrosus een rangschikking hebben zoals deze voorkomt bij de draden van textiel, is onjuist.  
J.O. Galante: Tensile properties of the human lumbar annulus fibrosus. Acta Orthopaedica Scandinavica Supplementum 100, 1967.
2. Het vaststellen van de buigstijfheid van de menselijke wervelkolom bij ventro-flexie door middel van belastingsproeven op een autopsy specimen, bestaande uit slechts twee vertebrae en één intervertebrale discus, is niet juist.
3. Het is waarschijnlijk dat een in ongedwongen staande houding ten opzichte van de heupgewrichten meer naar voren gedragen romp evenwichtsmechanismen om de assen van deze gewrichten oproept, welke gepaard gaan met beweging in het Ilio-Sacrale gewricht.  
C.J. Snijders: Die Reproduzierbarkeit der Stellung des menschlichen Beckens beim Stehen (niet gepubliceerd) (Onderzoek uitgevoerd in samenwerking met Dr. G. Gutmann, voorzitter van de "Forschungsgemeinschaft für Arthrologie und Chirotherapie").
4. Bij de huidige stand van de techniek verdient het aanbeveling dat de trombosediensten voor het bepalen van stollingstijden van bloed gebruik maken van een pipet, waarvan de eigenschappen tenminste gelijkwaardig zijn aan die van de Sanzpipet.
5. De door modeverschijnselen ingegeven veronachtzaming van de betekenis van de "rechtlijn van Von Meyer" heeft geleid tot schoenen die in vorm gelijkenis vertonen met een sarcophaag en die een grafkist zijn voor de goede functie van de voet.
6. Bij het dimensioneren van in massa te vervaardigen veren, welke een geringe doch zeer nauwkeurige kracht moeten leveren, verdient het aanbeveling een grote verende lengte te kiezen.  
C.J. Snijders: Metalen veren, Enige aspecten van de berekening, de fabricage en de toepassing.  
Polytechnisch Tijdschrift Werktuigbouw.  
Jaargang 25 (1970) nr. 4, p. 158 - 162, nr. 5, p. 191 - 198,  
nr. 6, p. 258 - 262, nr. 7, p. 291 - 296.
7. Zolang men uitgaat van een bestaande belangstelling voor samenwerking in wetenschappelijk onderzoek tussen medici en technici, dient men bezwaar aan te tekenen tegen de belemmering van deze samenwerking zoals die in de hand wordt gewerkt door de geografische scheiding van de Medische Faculteiten en Academische Ziekenhuizen enerzijds, en de Technische Hogescholen anderzijds en door het ontbreken van geïnstitutionaliseerd onderwijs over en weer. Vergelijking met andere landen leert dat mede als gevolg van genoemde belemmering, naast voordelen voor de volksgezondheid, goede kansen voor de Nederlandse economie worden gemist.  
C.J. Snijders: Verslag van een studiereis door Schotland, de Verenigde Staten en Canada.  
Intern Rapport, Technische Hogeschool Eindhoven, 1969.

8. In Nederland bestaat behoefte aan een Nationaal Centrum voor het ontwerpen, het ontwikkelen en het construeren van apparatuur ten behoeve van lichamelijke gehandicapten.
9. Het is om ethische en praktische redenen zinvol om niet-medici, die in het kader van hun medisch-technisch wetenschappelijk onderzoek in contact kunnen komen met patienten, voor te bereiden op en te onderwerpen aan een eed in de geest van de Eed van Hippocrates.
10. Dat op een aanzienlijk aantal weggedeelten het aantal overtredingen van het verbod tot overschrijden van aangegeven maximum snelheden - dit verbod is vastgelegd in artikel 51 van het Reglement Verkeersregels en Verkeerstekens - vermoedelijk minstens een factor tienduizend groter is dan het aantal bekeuringen dat op grond van genoemd artikel wordt uitgedeeld, is mogelijk enerzijds gevolg van onvoldoende controle en onvoldoende sancties en anderzijds gevolg van onvoldoende aan verkeerssituaties aangepaste maximum snelheden.
11. Door zich te houden aan aangegeven maximum snelheden past men regelmatig zijn snelheid niet aan aan die van het overige verkeer, waardoor het ontstaan van voor het overige verkeer gevaarlijke situaties in de hand wordt gewerkt, hetgeen strafbaar is gesteld in artikel 25 van de wegenverkeerswet.
12. Dat in verhouding slechts weinigen in hun auto gebruik maken van veiligheidsriemen en achterhoofdsteunen staat mogelijk mede in verband met het niet algemeen bekend zijn van de werkelijke functie van beiden.  
Tj. Meyer, arts, en C.J. Snijders: Verslag van een bezoek aan General Motors Safety Research and Development Laboratory.  
Intern rapport, Stichting Manuele Therapie, Eindhoven 1969.
13. De loyaliteit ten opzichte van het bestaande, het in-zich-goede, kan in de verhoudingen in de samenleving gemakkelijk ten kwade werken wanneer geen oog bestaat voor nieuwe inzichten en ontstane andere verbanden.  
Prof. Mr. B.V.A. Röling: De Wetenschap van Oorlog en Vrede (p. 26).  
Scripta Academica Groningana  
Uitg.: J.B. Wolters, Groningen 1961.

Eindhoven, 22 december 1970.

C.J. Snijders.